UNIVERSITÀ
DEGLI STUDI
DI PADOVA

Università degli Studi di Padova

Dipartimento di Biologia

SCUOLA DI DOTTORATO DI RICERCA IN: BIOSCIENZE E BIOTECNOLOGIE
INDIRIZZO: BIOCHIMICA E BIOFISICA
CICLO XXVI

INVOLVEMENT OF BIOGENIC ACTIVE AMINES IN MITOCHONDRIAL MEMBRANE PERMEABILIZATION AND PRO-APOPTOTIC FACTORS RELEASE

Direttore della Scuola: Ch.mo Prof. Giuseppe Zanotti
Coordinatore d'indirizzo: Ch.mo Prof. Fabio Di Lisa
Supervisore: Ch.ma Prof.ssa Maria Catia Sorgato
Co-Supervisore: Ch.mo Prof. Antonio Toninello

Dottoranda: Pamela Martinis

Table of contents

Abstract 1

Sommario 3

Abbreviations 5

Introduction 7

Mitochondria 7

Mitochondria and Ca^{2+} 8

Mitochondrial ROS production 9

Mitochondria and apoptosis 9

Mitochondrial permeability transition and controversies 10

Pro-apoptotic factors 11

Mitochondrial outer membrane permeabilization 12

Biologically active amines 13

Polyamines 13

Polyamines and diseases 14

Cellular transport of polyamines 14

Polyamines and mitochondria 14

Agmatine 15

Agmatine and diseases 16

Cellular transport of agmatine 16

Agmatine and mitochondria 16

Materials and Methods 19

Mitochondria isolation 19

Protein content determination 20

Standard medium for mitochondrial incubation 21

Transmembrane potential measurement with ionoselective electrode 22

Mitochondrial swelling determination 26

Assay for evaluating the release of cyt c, SMAC/DIABLO and AIF 26
Assay for evaluating the presence/activation of Bax 28
Fluorimetric assay to hydrogen peroxide determination 28
Uptake of agmatine in mitochondria 28
Thermodynamic analyses of ligand-receptor interactions 29
Part I Agmatine action on the permeabilization of mitochondrial membranes 31
Bivalent effect of agmatine on the MPT 31
Results 33
Effect of agmatine on pro-apoptotic factors release 33
MPT-independence 37
Possible involvement of Bax 39
Possible involvement of the Voltage-Dependent Anion Channel 41
Discussion 43
Part II Analyzing agmatine action by using its analog α-methyl-agmatine 47
ROS production by agmatine 47
α-methyl-agmatine 47
Results 49
α-methyl-agmatine uptake by RLM 49
Production of hydrogen peroxide by α-methyl-agmatine 52
Effect of α-methyl-agmatine on pro-apoptotic factors release 53
MPT-independence 56
Possible involvement of the Voltage-Dependent Anion Channel 58
Discussion 61
Part III Polyamines action on the permeabilization of mitochondrial membranes 63
Effect of polyamines on the MPT 63
Results 65
Effect of polyamines on pro-apoptotic factors release 65
MPT-independence 69

Possible involvement of the Voltage-Dependent Anion Channel 71

Discussion 73

Part IV Polyamines efflux from mitochondria 75

Polyamines cycling in mitochondria 75

Results 77

Spermine efflux 77

Membrane potential-independence 78

Correlation with adenine nucleotide translocator 80

Discussion 83

Conclusions 85

References 87

Abstract

Activation of the intrinsic pathway of apoptosis is related to the permeabilization of mitochondrial membranes. This complex process is far away from being completely understood but, generally, could be divided into two steps that, depending on the experimental conditions, can be linked or independent: the permeabilization of the mitochondrial outer membrane and the opening of the mitochondrial permeability transition pore. Both processes are tightly regulated by different components that attract increasing interest as promising targets for several diseases treatment, in particular cancer. A large number of mitochondrial permeability transition pore-targeting agents, indeed, are under studies because the mitochondrial apoptotic machinery in cancer cells is structurally and functionally different from that of normal cells. Thus, mitochondrial-targeting agents are expected to have a tumor selectivity.

In this scenario, a family of compounds known as biologically active amines acquires increasing importance. These amines, among which the most-known spermine, spermidine, putrescine and agmatine, are polycationic molecules at physiological pH, naturally present in almost all living species where they exert an essential role for cell growth and differentiation. It is to note that the polyamine biosynthetic pathway is very active in cancer cells and that high polyamines concentrations are often present in rapidly dividing tumor cells and growing tissues. Moreover the deregulation of polyamine metabolism may induce apoptosis. Thus, their primary role in regulating proliferation and cell death led scientists to investigate their role at a mitochondrial level. The main target of these amines seems to be the mitochondrial permeability transition: spermine, spermidine and putrescine share an inhibitory action whereas agmatine acts (in liver) as an inducer or an inhibitor, depending on the concentrations used. Furthermore in mitochondria two specific mitochondrial transporters have been detected: one for spermine, spermidine, and putrescine and one for agmatine.

The aim of this work is to study the action of biologically active amines as regulators of mitochondrial membrane permeabilization and pro-apoptotic factors release in isolated rat liver mitochondria. In particular their interaction with specific membrane structures is analyzed, trying to elucidate their mechanism of action.

The first part of the work evidences the agmatine double effect on the permeability transition process. In particular the attention is focused on agmatine inhibiting action. Despite its protective effect on the mitochondrial permeability transition, the amine is able to induce the release of some pro-apoptotic factors. A possible explanation relates to the induction of the mitochondrial outer membrane permeabilization.

A further confirmation of this proposal is obtained in the second part, by a comparison between agmatine and its analogue alpha-methyl-agmatine, a more powerful inhibitor of the mitochondrial permeability transition. The use of this compound allows to exclude that the production of hydrogen peroxide exhibited

by agmatine is one of the main causes of the mitochondrial outer membrane permeabilization observed.

In the third part, the effect of the polyamines (in particular spermine and spermidine) on the permeabilization on mitochondrial membranes and on the release of pro-apoptotic factors is reported. Despite their well-known protective action against the opening of the pore, spermine and spermidine share with agmatine a similar behavior in inducing the release of some pro-apoptotic factors, even through different pathways. Thus, their mechanism of action is investigated, trying to evidence the specific membrane components involved.

Finally, in the fourth part, an investigation about the mechanism of efflux of spermine is shown, focusing on the possibility that it could be linked with the efflux of ATP and phosphate, most likely in an electroneutral fashion. This observation is supported by the use of specific inhibitors of the adenine nucleotide translocator and phosphate carrier.

In conclusion, the results obtained in this study first of all support the hypothesis that the permeabilization of the inner and outer membranes could be viewed as two distinct processes, even if often linked between them. Furthermore it is possible to state that the mitochondrial outer membrane permeabilization could be a contact point between intrinsic and extrinsic apoptosis, being induced both by intra- and extra-mitochondrial signals. It is already reported that the release of cytochrome c from mitochondria does not always result in apoptosis induction. In particular the redox state of the protein is crucial for the subsequent cascade of events: only oxidated cytochrome c is able to trigger apoptosis. For this reason, it is reasonable to think that the release of cytochrome c induced by biologically active amines could represent a starting point, but not a point of no return. In this context polyamines represent a useful tool to study both the mitochondrial outer membrane permeabilization and the mitochondrial permeability transition, trying to delineate structural and functional features. Moreover, in living cells polyamines are able to prevent or induce apoptosis, and the latter effect is caused by their metabolization by amine oxidases, with the production of cytotoxic metabolites. This dichotomic action depends on polyamines concentration, that is modulated, as supported by our data, also by mitochondrial polyamine cycling. More study is required to detect all structural mechanism involved in their cycling but, at least for spermine, a possible pathway of efflux is detected.

Sommario

L'attivazione dell'apoptosi intrinseca è correlata alla permeabilizzazione delle membrane mitocondriali. Questo complicato processo, sebbene non sia stato ancora completamente compreso, può essere generalmente suddiviso in due fasi: la permeabilizzazione della membrana mitocondriale esterna e l'apertura del poro di transizione di permeabilità mitocondriale. In base alle condizioni sperimentali tali fasi possono essere collegate o indipendenti. Diversi componenti che regolano i suddetti processi sono attualmente in fase di studio, poiché si sono rivelati bersagli promettenti per il trattamento di numerose malattie, tra le quali in particolare il cancro. Infatti, il macchinario apoptotico mitocondriale nelle cellule tumorali è strutturalmente e funzionalmente diverso da quello delle cellule normali e quindi un gran numero di composti che hanno come target la transizione di permeabilità potrebbe per tale motivo esibire una selettività tumorale.

In questo contesto, una famiglia di composti noti come amine biologicamente attive acquista un'importanza crescente. Queste amine, tra cui le più note sono spermina, spermidina, putrescina e agmatina, sono molecole policationiche a pH fisiologico, naturalmente presenti in quasi tutte le specie viventi, in cui esercitano un ruolo essenziale per la crescita e la differenziazione cellulare. È da notare che la via biosintetica delle poliamine è molto attiva nelle cellule tumorali e che concentrazioni elevate di poliamine sono spesso presenti in cellule tumorali in divisione ed in tessuti in proliferazione. Inoltre, la de-regolazione del metabolismo delle poliamine può indurre l'apoptosi. Per questi motivi, il loro ruolo primario nella regolazione della proliferazione e della morte cellulare ha portato gli scienziati a studiarne il ruolo a livello mitocondriale. Il target principale delle amine biologicamente attive sembra essere la transizione di permeabilità mitocondriale: spermina, spermidina e putrescina esibiscono un'azione inibitoria mentre l'agmatina (nel fegato) si comporta da induttore o inibitore, a seconda delle concentrazioni usate. Inoltre nei mitocondri è stata dimostrata l'esistenza di due trasportatori specifici: uno per spermina, spermidina e putrescina ed uno per l'agmatina.

Lo scopo di questo lavoro è quello di studiare l'azione delle amine biologicamente attive quali regolatrici della permeabilizzazione della membrana mitocondriale esterna e del rilascio dei fattori pro-apoptotici in mitocondri isolati da fegato di ratto. In particolare viene analizzata la loro interazione specifica con le strutture di membrana, allo scopo di chiarire il loro meccanismo di azione.

La prima parte del lavoro evidenzia il duplice effetto dell'agmatina sul processo di transizione di permeabilità. In particolare l'attenzione è focalizzata sull'effetto inibitorio dell'amina nei confronti dell'apertura del poro di transizione mitocondriale. Infatti, nonostante il suo effetto protettivo sulla transizione di permeabilità, l'amina è in grado di indurre il rilascio di alcuni fattori pro-apoptotici. Una possibile spiegazione considera l'induzione della permeabilizzazione della membrana mitocondriale esterna.

Un'ulteriore conferma di questa ipotesi è trattata nella seconda parte della tesi, per mezzo del confronto tra gli effetti mostrati dall'agmatina e dal suo analogo alfa-metil-agmatina, un più potente inibitore della transizione di permeabilità mitocondriale. L'utilizzo di tale analogo permette di escludere che la produzione di perossido di idrogeno osservata in presenza di agmatina sia una delle cause principali della permeabilizzazione della membrana esterna.

Nella terza parte, è riportato l'effetto delle poliamine (in particolare della spermina e della spermidina) sulla permeabilizzazione delle membrane mitocondriali e sul rilascio dei fattori pro-apoptotici. Nonostante la ben nota azione protettiva di questi composti nei confronti dell'apertura del poro, spermina e spermidina condividono con l'agmatina un comportamento simile nell'indurre il rilascio di alcuni fattori pro-apoptotici, sebbene attraverso meccanismi diversi. Il loro meccanismo d'azione è perciò indagato, cercando di mettere in evidenza le specifiche componenti di membrana coinvolte.

Infine, nella quarta parte, viene mostrato uno studio sul meccanismo di efflusso della spermina, indagandone il possibile collegamento con l'efflusso di ATP e fosfato, molto probabilmente in modo elettricamente neutro. Questa osservazione è supportata dall'uso di inibitori specifici della traslocasi degli adenin nucleotidi e del fosfato.

In conclusione, i risultati ottenuti in questo studio innanzitutto sostengono l'ipotesi che la permeabilizzazione delle membrane interna ed esterna possa essere vista come due distinti processi, anche se spesso legati tra loro. Inoltre è possibile affermare che la permeabilizzazione della membrana mitocondriale esterna potrebbe essere un punto di contatto tra apoptosi intrinseca ed estrinseca, essendo indotta sia da segnali intra- che extra-mitocondriali. E' da considerare che il rilascio di citocromo c dai mitocondri non porta in ogni caso all'induzione dell'apoptosi. In particolare lo stato redox della proteina è cruciale per la successiva cascata di eventi: solo il citocromo c ossidato, infatti, è in grado di innescare l'apoptosi. Per questo motivo, è ragionevole pensare che il rilascio di citocromo c indotto dalle amine biologicamente attive possa rappresentare un punto di partenza, ma non un punto di non ritorno. In questo contesto, le poliamine rappresentano uno strumento utile per studiare sia la permeabilizzazione della membrana esterna mitocondriale che la transizione di permeabilità mitocondriale, cercando di delinearne le caratteristiche strutturali e funzionali. Inoltre, a livello cellulare, le poliamine sono in grado di prevenire o indurre l'apoptosi e quest'ultimo effetto è causato dal loro metabolizzazione da parte delle amine ossidasi, con la produzione di composti citotossici. Questa azione dicotomica dipende dalla concentrazione delle poliamine, che è modulata, come dimostrato dai nostri dati, anche attraverso il loro ciclaggio all'interno dei mitocondri. Nonostante siano chiaramente necessari ulteriori studi per individuare tutti i meccanismi strutturali coinvolti nel loro ciclaggio, almeno per la spermina, viene individuata una possibile via di efflusso.

Abbreviations

αMeAGM	alpha-methyl-agmatine
ADC	arginine decarboxylase
AdNT	adenine nucleotide translocase
AGM	agmatine
AIF	apoptosis inducing factors
Bak	Bcl-2 agonist or killer
Bax	Bcl-2 associated X protein
Bcl-2	B cell lymphoma 2
BKA	bongkrekic acid
CsA	cyclosporin A
CypD	cyclophylin D
Cyt. *c*	cytochrome c
HRP	horseradish peroxidase
I_2	imidazoline receptor type 2
IAPs	inhibitor of apoptosis proteins
IM	inner membrane
MAO	monoamine oxidase
MOMP	mitochondrial outer membrane permeabilization
MPT	mitochondrial permeability transition
MPTP	mitochondrial permeability transition pore
OM	outer membrane
PUT	putrescine
RLM	rat liver mitochondria
ROS	reactive oxygen species
RR	ruthenium red
SDS	sodium dodecyl sulfate

Smac/DIABLO	Second mitochondria-derived activator of caspase/ Direct IAP binding protein with low pI
SPD	spermidine
SPM	spermine
TPP^+	tetraphenylphosphonium
VDAC	voltage-dependent anion channel
ΔE	electrode potential variation
ΔpH	chemical gradient
$\Delta\Psi$	mitochondrial electric membrane potential
$\Delta\mu_H^+$	electrochemical gradient

Introduction

Mitochondria

Mitochondria, also termed as the cell "powerhouses" for their ability to convert redox energy in ATP, are small double-membrane organelles implicated in the regulation of the life and death of eukaryotic cells. Indeed, they are implicated in the modulation of several metabolic processes culminating in the synthesis of ATP, but also in phospholipids and heme synthesis. Moreover, besides regulating the levels of intracellular signaling molecules (*e.g.*, Ca^{2+} and reactive oxygen species (ROS)), they are also activators of the "intrinsic" apoptotic pathway [Osellame *et al*., 2012; Tait and Green, 2012].

Mitochondrial bioenergetic activity is strongly dependent on the integrity of mitochondrial membranes (particularly the inner one), given that its insulating properties are fundamental for the correct electron flux along the respiratory complexes and consequently for the establishment of the electrochemical gradient ($\Delta\mu_{H+}$), characteristic of these energy transducing membranes. As it is well-known, $\Delta\mu_{H+}$ is given by the sum of the electrical transmembrane potential ($\Delta\Psi$) and the chemical gradient (ΔpH), expressed in mV.

The organelle morphology differs among cell types: from solitary organelles in hepatocytes to an intricate network in many epithelial cells [Scorrano, 2013]. In hepatocytes and fibroblasts they are typically characterized by a length of 3-4 μm and a diameter of 1 μm, resembling approximately small bacteria in size and shape. The number of mitochondria per cell is also variable from cell type to cell type. According to the classic model of Palade [Palade, 1952], mitochondria have an outer membrane (OM) and an inner membrane (IM), the latter being characteristically invaginated and forming sheet-like structures called *cristae*. As showed in Fig. 1, this organization was hypothesized to generate an intermembrane space (enclosed by the OM and the IM) and a matrix (enclosed by the IM) [Scheffler, 2001].

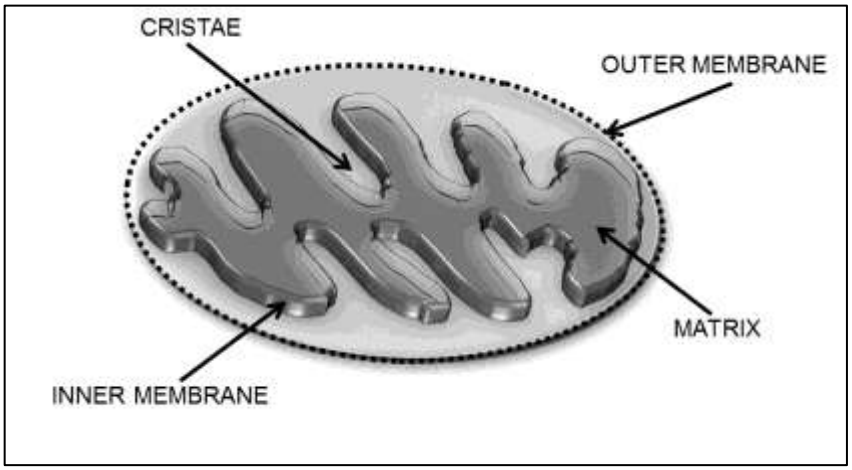

Fig. 1 The classical morphological model of mitochondria.

However more recent studies exploiting the technique of electron tomography, have modified this view, whereby additional subdivision of the IM lead to the formation of the inner boundary membrane and the *cristae,* which are identified as separated compartments. Their continuity with the inner boundary membrane is achieved by narrow tube-like structures called *cristae* junctions (Fig. 2) [Scheffler, 2001; Scorrano, 2013].

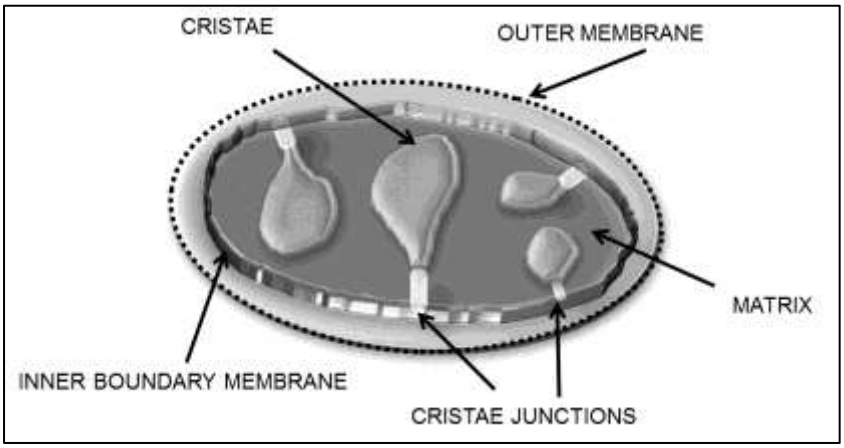

Fig. 2 The new morphological model of mitochondria.

Mitochondria and Ca^{2+}

Ca^{2+} is an important signaling molecule not only in cells, but also in mitochondria that maintain a large Ca^{2+} gradient across their IM, achieved through an extensively studied mechanism of accumulation. The direct demonstration of this process in isolated mitochondria was published in 1961, when the work of DeLuca and Engstrom demonstrated the ability of kidney mitochondria to accumulate large quantities of Ca^{2+} with a mechanism requiring ATP, Mg^{2+} and inorganic phosphate. Only recently the electrophoretic uniporter responsible for Ca^{2+} uptake has been identified as a 40 kDa protein of the IM [De Stefani *et al.*, 2011]. On the other hand, the efflux mechanism is regulated through a Na^{+}/Ca^{2+} exchanger, whose activity was identified by Carafoli and collaborators [1974], and an H^{+}/Ca^{2+} antiporter described in some mitochondrial types [Fiskum *et al.*, 1979]. Several mitochondrial enzymes are regulated by Ca^{2+}, thus justifying the necessity of a bidirectional flux or, as proposed by several authors, a Ca^{2+} cycling mechanism. Moreover, the accumulation of high Ca^{2+} concentrations in the presence of phosphate, as demonstrated by Lötscher and collaborators [1980], may lead to complete and irreversible depolarization of the organelle. These conditions cause an alteration of the IM permeability termed mitochondrial permeability transition (MPT), (see pag. 10). As Grijalba and collaborators [1999] demonstrated, Ca^{2+} alters the lipid organization of the IM, by its interaction with the anionic head of the phospholipid cardiolipin (IM). These alterations in membrane organization may compromise the conformation and subsequently the functionality of membrane components (including coenzyme Q), thus affecting respiratory chain function. As a result, the generation of cytotoxic ROS is favored. [Vercesi *et al*., 1997]

Mitochondrial ROS production

Mitochondrial clearly play a crucial role in regulating the redox state of the cell. Indeed, the respiratory chain is the primary putative source of ROS, mainly produced during the flow of electrons through complexes I, II and III [Murphy, 2009; Moreno-Sánchez *et al*., 2013]. Normally, the generated ROS are in a sufficient small amount to be removed by the scavenging systems of the organelle, which include superoxide dismutase, catalase, glutathione and thioredoxin reductase. However, when ROS production overcomes the ROS scavenging capacity (*e.g.*, in the presence of exceeding amounts of Ca^{2+} and phosphate, as described in the precedent section, and/or when scavenging pathways are inactivated), accumulated high ROS can cause several damages in both mitochondria and the rest of the cell [Kowaltowski *et al*., 2001; Murphy, 2009].

In mitochondria, the above mentioned oxidative damage can cause alterations of the redox state of both membrane and matrix components (glutathione, thiols, electron transport chain complexes) and DNA, all of which clearly hamper mitochondrial functions. In these conditions, mitochondria are clearly not able to perform their metabolic functions. Indeed, mitochondrial oxidative stress have been demonstrated to be a fundamental step in the induction of apoptosis in RLM [Halestrap *et al*., 1993], (but not in brain mitochondria [Grancara *et al*., 2011]).

Mitochondria and apoptosis

Cell death can be classified as apoptotic (programmed) or necrotic (accidental), even if the boundaries between these two forms are not always clearly defined [Osellame *et al.*, 2012].

Apoptosis is an active and coordinated process that requires energy to occur and is fundamental for the development of the organisms, removing exceeding, damaged or aged cells. It can occur through two signaling pathways: the extrinsic pathway, which involves cell surface receptors and culminates with the activation of caspase 8, and the intrinsic pathway, which requires mitochondrial permeabilization.

Conversely, necrosis is the result of a metabolic failure that leads to the cell “energy collapse”, leading to the breakdown of ion gradients, cell swelling, and structural disorganization.

According to Osellame and collaborators [2012], the rupture of mitochondrial membranes is crucial for both apoptotic and necrotic processes, although they claim that, while the activation of the MPT is one of the major mechanism driving necrosis, the mitochondrial outer membrane permeabilization (MOMP) is characteristic of the intrinsic apoptotic process. Halestrap [2005], instead, distinguishes between the induction of transient MPT (in which ATP production is

maintained) leading to apoptotic cell death, and permanent MPT induction, (in which ATP content is depleted) leading to necrotic cell death. Clearly, in both hypotheses the permeabilization of mitochondrial membranes appears crucial to the cell death machinery.

Mitochondrial permeability transition and controversies

Under normal physiological conditions, the mitochondrial IM is permeable only to a few, selected metabolites and ions. However, in response to noxious stimuli (*e.g.*, Ca^{2+} overloading, oxidative stress, cytotoxic agents), a non-specific pore, the so-called mitochondrial permeability transition pore (MPTP), opens in the contact sites between the IM and OM, allowing the passage of molecules with molecular masses up to 1.5 kDa. It is to underline that, even though both membranes seem to be eventually involved, the MPT is essentially a process of the IM, given that experiments using mitoplasts (*i.e.*, mitochondria deprived of the OM) showed all the same a typical MPT [Dalla Via *et al*., 2014; Siemen and Ziemer, 2013], with disrupted permeability of the IM and passage of solutes across it. The free passage of protons then causes the uncoupling of oxidative phosphorylation and hydrolysis of ATP. As a consequence, retention of proteins in the matrix (due to the pore dimensions) ensues a colloid-osmotic pressure allowing the entry of water into the matrix, mitochondrial swelling, c*ristae* unfolding, matrix expansion, all of which finally disrupt the OM with the release of mitochondrial proteins including cytochrome c (cyt. *c*), Second mitochondria-derived activator of caspase/Direct IAP binding protein with low pI (Smac/DIABLO), Apoptosis Inducing Factor (AIF) [Halestrap, 2005; Brenner and Moulin, 2012].

Several studies have addressed the issue of MPTP as a dynamic multiprotein complex and the proposed composition involved different interacting proteins: the adenine nucleotide translocator (AdNT), the matrix peptidyl-prolyl isomerase cyclophillin D (CypD), the phosphate carrier, but also the OM protein voltage-dependent anion channel (VDAC), and the cytosolic and intermembrane space hexokinase and creatine kinase, respectively. Since the mid-1990s, several MPTP candidates have been knocked out in mice, but these genetic studies have failed to support their implication in the pore. In particular, they suggest a regulatory function for AdNT and CypD and exclude an essential role for VDAC [Brenner and Moulin, 2012]. Conversely, a recently proposed hypothesis suggests that MPTP is composed by dimers of F_0F_1-ATP synthase that, when incorporated into lipid bilayers, are able to form Ca^{2+}-activated channels, with features in common to the MPTP studied *in situ* [Giorgio *et al.,* 2013].

Further studies are clearly required to clarify the MPTP composition, which remains an extremely important scientific issue, in view of the possible involvement of the MPTP in mitochondria-associated dysfunctions that warrants development of mitochondria-targeting drugs.

Pro-apoptotic factors

The release of pro-apoptotic proteins from mitochondria is a well-known crucial process to activate the cell death machinery. Among them, this work has focused primarily on cyt. *c*, Smac/DIABLO and AIF.

Cyt. *c* is a 12.5 kDa soluble metalloprotein located to the side of the IM facing the intermembrane space; which shuttles electrons from Complex III (cytochrome c reductase) to Complex IV (cytochrome c oxidase) of the respiratory chain [van Gurp *et al.*, 2003]. The presence of different pools of cyt. *c* has been proved: loosely bound pools are mainly bound to membrane phospholipids (especially cardiolipin) by electrostatic interactions whereas tightly bound pools are partially embedded into the IM due to hydrophobic interactions [Ott *et al.*, 2001]. In response to several pro-apoptotic stimuli, leading to the OM permeabilization, cyt. *c* is released into the cytosol where it binds dATP and Adaptor molecule apoptosis-Protease Activating Factor I, initiating the formation of the apoptosome. This complex, in turn, starts the activation of the caspase cascade, leading to chromatin condensation, DNA fragmentation and cell death [Dalla Via *et al*., 2014].

Smac/DIABLO is a 23 kDa protein present in the intermembrane space that, upon the OM permeabilization, is released into the cytosol [Maly, 2007]. The physiologic function of Smac/DIABLO is still unknown, although it has been reported that it enhances apoptosis by binding to members of the inhibitor of apoptosis proteins (IAPs) family. Smac/DIABLO competes with the caspases for the (inhibitory) binding to IAPs, because this factor has regions structurally similar to those that in caspases bind IAPs. Thus, IAPs inhibitory effect is removed by Smac/DIABLO and caspases are able to act in apoptosis [van Gurp *et al.*, 2003; Dalla Via *et al*., 2014].

AIF is a type-I IM protein (62 kDa), whose N-terminal portion is exposed to the matrix and the C-terminus protrudes into the intermembrane space [Otera et al., 2005]. In physiological conditions AIF exhibits antioxidant activity and is required for the correct assembly and maintenance of Complex I of the respiratory chain [Vahsen et al., 2004]. The release of AIF into the cytoplasm is caused by its cleavage to a 57 kDa protein in response to apoptotic signals. The released AIF induces nuclear apoptosis in a caspase-independent manner by translocating to the nucleus and inducing DNA fragmentation and chromatin condensation [Dalla Via *et al*., 2014].

Mitochondrial outer membrane permeabilization

As emphasized, there are two main models that account for the release of pro-apoptotic factors during mitochondria-mediated apoptosis [Green and Reed, 1998]. In one model, the permeabilization of mitochondrial membranes occurs through MPTP formation, involving both the mitochondrial membranes, whereas the other one conceives the main involvement of MOMP. The latter process is characterized by the formation of channels in the OM (taking place independently of mitochondrial swelling), and can be induced by stimuli such as hypotonicity, hydrogen peroxide, and pro-apoptotic B cell lymphoma 2 (Bcl-2) family proteins [Arnoult *et al*., 2002; Gogvadze *et al*., 2006].

According to the function, Bcl-2 proteins can be divided into anti-apoptotic and pro-apoptotic members. This latter group is further divided into two subfamilies based on the presence of specific Bcl-2 homology domains (BH1, BH2 and BH3): Bcl-2 associated X protein (Bax) and Bcl-2 agonist or killer (Bak), sharing BH1-BH3 domains, are the effectors of MOMP; while BH3-only proteins can interact with Bax and Bak, or with the other anti-apoptotic members [Green and Kroemer, 2004]. These proteins share structural similarity with bacterial pore forming toxins, suggesting that they can act similarly in the OM [Tait and Green, 2010]. According to Bleicken and collaborators [2013], after the translocation of Bax to the OM, Bax and Bak changes of conformation occur, leading to their oligomerization and to the formation of pores. However, the exact mechanism by which Bcl-2 proteins regulate this process is still a matter of debate.

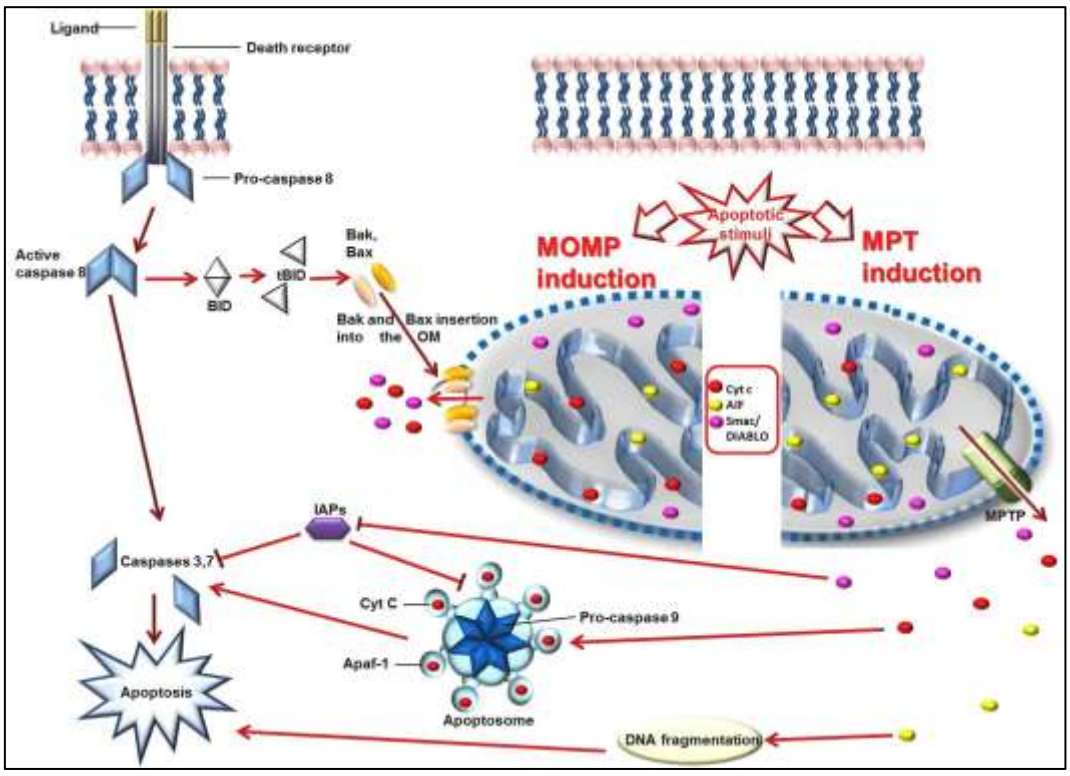

Fig. 3 Intrinsic and extrinsic pathways of apoptosis.

Biologically active amines

Biologically active amines represent a class of compounds physiologically synthesized in living organisms. According to a classification proposed by COST actions 917 and 922 (research programs financed by the Commission of the European Communities DG/XIIB), active amines are distinguished in polyamines (putrescine, spermidine and spermine) and biogenic amines (agmatine, serotonin, tyramine, histamine, phenylethylamine, tryptamine and cathecolamines) [Toninello *et al.*, 2004].

Polyamines

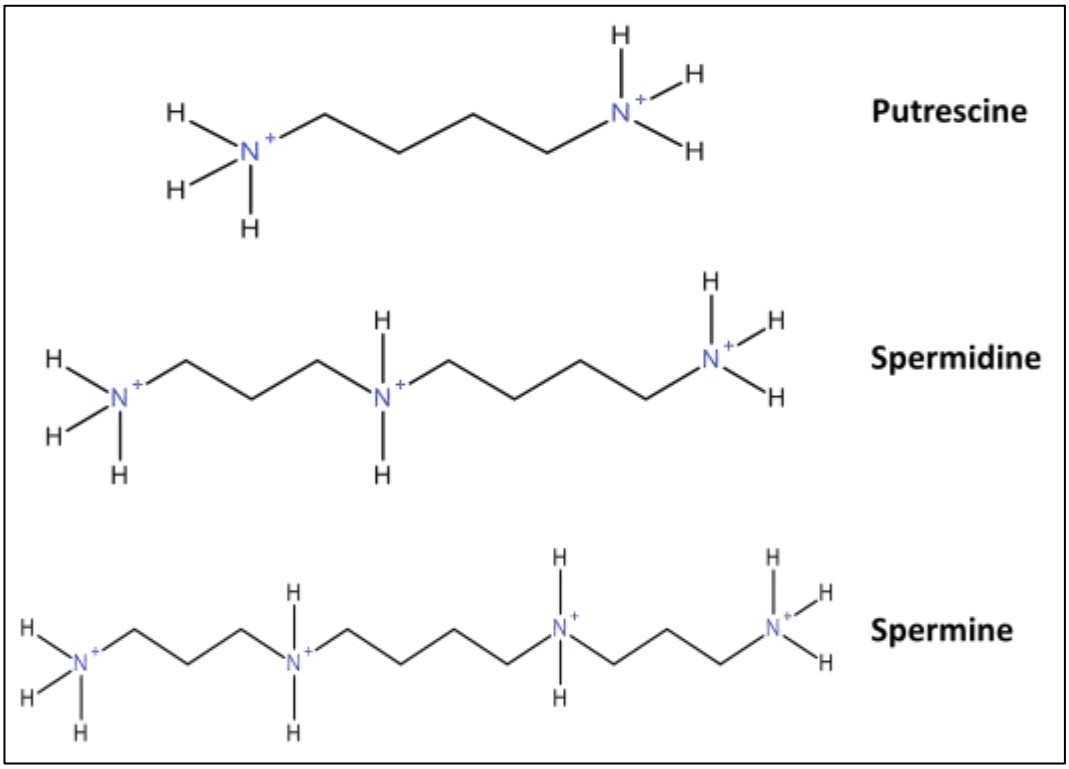

Fig. 4 Polyamines.

Putrescine (PUT), spermidine (SPD) and spermine (SPM) are decarboxylation products of ornithine and S-adenosyl-methionine metabolism in nearly all eukaryotic cells. Under physiological conditions, these molecules are fully protonated (poly)cations [Agostinelli *et al.*, 2010]. Polyamines total intracellular concentration is in the mM range, although the majority is bound to various anions in the cell, such as DNA, RNA, proteins, and phospholipids [Casero and Marton, 2007]. These amines share a multitude of functions affecting cell growth and proliferation, *e.g.*, regulation of gene transcription, posttranscriptional processes, ion channels, and protein kinases activity; modulation of membrane structures/functions, structure and stability of nucleic acids; and progress of the cell cycle [Pegg and Casero, 2011].

Polyamines and diseases

The interest in polyamine research has increased since the realization that polyamines and their metabolites may play critical roles in human diseases. Indeed, alterations of polyamine levels and metabolism have been detected in many diseases (*e.g.*, chronic renal failure, liver cirrhosis, cystic fibrosis, Alzheimer's and Parkinson's Diseases, Duchenne muscular dystrophy and cancer). With regard to cancer, increased polyamines concentrations have been found in many solid tumors, and similar increases in urinary and serum polyamine content are common features of malignancy. Moreover, the polyamine biosynthetic pathway is more active in tumor tissues, making it an attractive target for the design of chemotherapeutic drugs [Wallace and Fraser, 2004].

Cellular transport of polyamines

The cellular content of polyamines, which plays, as above mentioned, important roles in cell proliferation and differentiation, is highly regulated by their biosynthesis, degradation, and transport processes. With regard to their transport in mammalian cells, a specific transporter has not been yet identified, although it was found that polyamine accumulation is energy-dependent and selective. It has been proposed that polyamines are imported first by a plasma membrane carrier and then sequestered into preexisting vesicles [Hoshino *et al*., 2005]. Very recent advances in the field described by Nowotarski and collaborators [2013] suggest two other mechanisms for polyamines import: the first supports the binding of SPM on heparan sulfate groups of glypican 1 on the cell surface, with the subsequent internalization of the amine. SPM is then freed by a nitric oxide-oxidation-mediated process. The other proposition suggests a caveolin-1-dependent internalization. The subsequent release of the internalized compounds has been described only for PUT through the solute carrier family 3 member 2 exporter, while a nitric oxide synthase 2-dependent reaction is thought to destabilize the SPM-receptor complexes.

Polyamines and mitochondria

Mitochondria apparently lack a polyamine biosynthetic pathway, although substantial quantities of SPM and SPD have been detected in heart, liver and brain mitochondria, as a consequence of a transport system present in the membranes of these organelles [Toninello, 2001]. The first demonstration of a polyamine transport system in the mitochondrial membranes was published by Toninello and collaborators in 1985, by evidencing that SPM internalization in mitochondria occurs through an energy-dependent mechanism. Further investigations [Dalla Via *et al.*, 1996; 1999; Toninello *et al.*, 1992a; 1992b] identified two binding sites for SPM and SPD, both with mono-coordination, low affinity and high binding capacity, whereas only one binding site was evidenced for PUT. This site was correspondent to one of the binding sites for SPM and SPD. The polyamines were demonstrated to be mutually competitive inhibitors, indicating a common transport system.

The structure of these amines allows their specific interaction with mitochondrial membranes and it is probably responsible for the variety of effects ascribable to these molecules (*e.g.*, activation of the mitochondrial uptake of hexokinase and protein kinases CKI and II, stimulation of the activity of pyruvate dehydrogenase, and inhibition of ATP hydrolysis, by the F_1-ATPase [for a review see Toninello *et al.*, 2004]). The main target of polyamines seems to be the MPT and Toninello and collaborators reported for the first time in 1984 the ability of SPM to prevent Ca^{2+}-induced MPT in RLM. Several subsequent studies confirmed its inhibitory effect not only in liver [Tassani *et al.*, 1995], but also in other organs (*e.g.*, heart [Toninello *et al.*, 1990], intestine [Anup *et al.*, 1999]). The protective effect of polyamines on MPT induction is not completely understood and several mechanism have been investigated in order to elucidate their activity [Toninello *et al.*, 2004]. Besides the stabilization of mitochondrial membranes due to their charged molecule [Lapidus and Sokolove, 1993], one of the main actions of polyamines, in particular of SPM, resides in their antioxidant properties [Sava *et al.*, 2006]. SPM is able to exhibit a scavenging action by reacting with the hydroxyl radical ($OH\cdot^{-}$) and resulting in the production of SPM dialdehyde (1,12-bis-1,12-dioxo-4,9-diazododecane). Taking into account that MPT opening is linked with the so-called redox catastrophe [Susin *et al.*, 1998], the above described effect is undoubtedly fundamental in explaining SPM inhibition of MPT.

Despite this effect, and thus the anti-apoptotic potential of polyamines, Stefanelli and collaborators [2000] reported also a CsA-insensitive release of cyt. *c* induced by these molecules in rat heart mitochondria. This effect was demonstrated to be independent from mitochondrial damage and probably the pool of cyt. *c* released was not part of the electron transport chain, a possibility supported by the evidence of the presence of different cyt. *c* pools in mitochondria [Ott *et al.*, 2001].

Agmatine

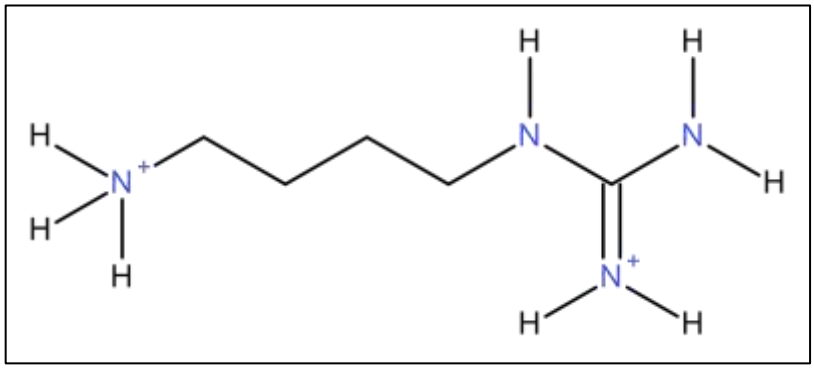

Fig. 5 Agmatine.

Discovered in 1910 by the Nobel Laureate Albrecht Kossel [Kossel, 1910], agmatine (AGM) [1-(4-Aminobutyl)guanidine] is an ubiquitous biogenic amine

with two positive charges at physiologic pH. In mammals, it is synthesized from arginine by the enzyme arginine decarboxylase (ADC) (mainly in brain), although a great deal of AGM may be absorbed from the diet [Salvi *et al*., 2006]. Burgeoning research shows that AGM is implicated in multiple biological functions as: ligand of α-adrenergic and imidazoline receptors type 2 (I_2); neuromodulator and co-transmitter; modulator of some arginine metabolic pathways; inductor of nitric oxide synthesis, and modulator of polyamine metabolism [for a review on AGM see Piletz *et al.*, 2013].

Agmatine and diseases

After the discovery of the first neuroprotective effects of AGM in 1995, the research involving this amine increased rapidly on several areas such as neuro-, nephron- and cardioprotection [Piletz *et al.,* 2013]. This resulted in reports showing that, from the first human clinical trials, oral AGM is safe and effective in alleviating neuropathic pain [Keynan *et al.*, 2010]. Intriguingly, depending on the cell type and its stage of proliferation, it has also been shown that AGM exhibits antiproliferative effects in rat hepatoma cells [Gardini *et al*., 2003] and in leukemia cells [Haenisch *et al.*, 2011], but it can also induce intrinsic apoptosis in non-proliferative hepatic cells [Gardini *et al*., 2001] and counteracts tumor necrosis factor-α in retinal ganglion cells [Hong *et al.*, 2009]. In conclusion, the complexity of AGM actions is summarized by the following statement by Piletz and collaborators [2013]: “AGM is now considered to be capable of exerting modulatory actions simultaneously at multiple target sites, thus fitting the therapeutic profile of a ‘magic shotgun’ for complex disorders”.

Cellular transport of agmatine

As previously mentioned, AGM may also come from the diet. After being absorbed by the stomach, AGM is taken up by several organs, in particular by the liver. Being (di-)protonated, to pass across the membranes, AGM needs a transport that, in hepatocytes [Cabella *et al*. 2001], endothelial [Babál et al., 2000], and kidney cells [Del Valle *et al*., 2001] is likely the same mechanism exploited by polyamines (see above). However in glyomal cells [Molderings *et al*., 2001] and in a cell line derived from human embryonic kidney, AGM may use a different means. In particular, in the latter case, the involvement of the extraneuronal monoamine transporter and the organic cation transporter 2 may be also suggested [Gründemann *et al*., 2003].

Agmatine and mitochondria

AGM is transported in mitochondria, where also its metabolic enzymes ADC and agmatinase are present, as well as the I_2, a 60 kDa protein that localizes to the OM and constitutes a monoamine oxidase (MAO) domain [Raddatz *et al.,* 2000].

Previous data, on AGM activity in isolated RLM, have demonstrated that AGM may have different effects on mitochondrial bioenergetics that depend on the concentrations used: at low concentrations (10-100 μM) it may act as a typical amplifier of the Ca^{2+} (plus phosphate) induction of MPT, while at high

concentrations (1 mM) it inhibits this phenomenon [Battaglia *et al*., 2007]. It is necessary to point out that the discrimination between low and high concentrations is not arbitrary, but it is based on previous published data demonstrating that AGM concentration in hepatocyte cytosol is about 0.5 mM [Gardini *et al*., 2001]. In this respect, it is necessary to remind that AGM permeates both the mitochondrial membranes (presumably at OM/IM contact sites) using a specific electrophoretic transporter, a channel or a single-binding centre-gated pore, which was identified in RLM [Salvi *et al*., 2006]. Analyses, applying a thermodynamic approach developed by Di Noto and collaborators [1996, 2002], have demonstrated the presence of two binding sites (S_1 and S_2) for AGM on mitochondrial membranes, both with mono-coordination [Martinis *et al.*, 2012]. S_1 is probably localized on the I_2 that, as previously mentioned, is itself a MAO domain. Because AGM can inhibit MAO activity, its binding to S_2 further underlines the importance of the molecule. Finally, the work proposes a hypothesis concerning AGM binding sites: S_1 sensing AGM concentration (outside mitochondria) eventually modifies the properties of S_2, the transport site.

AGM induction of the MPT, at low concentrations, is triggered by the oxidation of AGM, probably catalyzed by a copper-dependent amine oxidase present in RLM [Cardillo *et al.*, 2009]. This enzyme can be responsible for the large amount of H_2O_2 detected in presence of AGM (both in the presence or the absence of Ca^{2+}). The ROS produced results in the bioenergetics collapse of the organelle and in the activation of the intrinsic pro-apoptotic pathway. On the contrary, a completely different scenario is observable at higher concentrations: AGM is able to inhibit the MPT induced by Ca^{2+} (plus phosphate), probably due to its antioxidant properties. In fact, in these conditions, the amine is able to generate an oxidative stress, but the amount of still unreacted molecules may act as a scavenger, thus exhibiting self-protection. This scavenger mechanism exhibited by AGM is applicable when the targeted ROS is the $OH\cdot^-$: unprotonated AGM reacts with $OH\cdot^-$ to form dihydroxyaminobutyl-guanidine and, subsequently, guanidobutyric aldehyde by the spontaneous dehydration and hydrolysis, with a reaction already proposed for SPM [Sava *et al*., 2006].

Materials and methods

Mitochondria isolation

Mitochondrial preparation from rat liver was performed by using the modified method of Schneider and Hogeboom [1950] by conventional differential centrifugation. All operations were carried out at a temperature of 4°C, maintaining the equipment in melting ice.

The liver was taken from Wistar rats of (200-300 g), after 16 hours fasting, minced and washed in an isolation medium with 250 mM sucrose, 5 mM Hepes and 2 mM EGTA (pH 7.4). After washing out the blood, the minced organ was homogenized using a Potter homogenizer with a Teflon pestle. The homogenate was centrifuged in a Beckman J2-21 centrifuge, with Ja-17 rotor, cooled at 0-5°C. The first low-speed centrifugation, at 2300 rpm (755 g) for 10 min, is used to remove nuclei and intact cells. The supernatant, containing mitochondria, microsomes, and cytosol, was subjected to a second centrifuge at 9000 rpm (10800 g) for 10 min. This centrifugation allows the separation of mitochondria (pellet fraction) from microsomes and cytosol (supernatant). From the walls of the test tubes deposited fat was removed with tissue paper and then the pallet was washed with a medium without EGTA to remove additional fat residues. The pellet was resuspended in 20-30 ml of medium and homogenized by hand in a test tube Potter. The obtained suspension was washed in a final centrifuge at 11000 rpm (15900 g) for 5 minutes. The supernatant was removed and the pellet was washed gently to remove the surface film, consisting of broken or damaged mitochondria. The pellet was then resuspended in 2 ml of medium and it was homogenized by hand in a small test tube Potter. The content was then stored in a test tube immersed in melting ice.

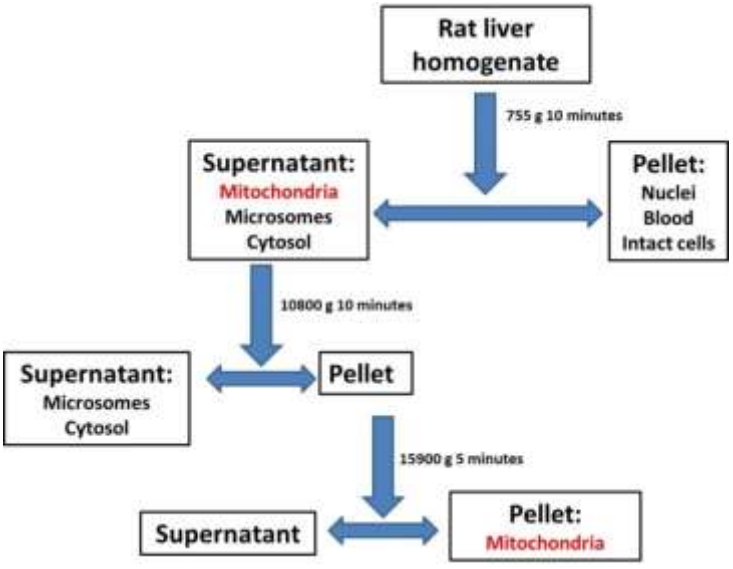

Fig. 6 Schematic summary of the preparation of rat liver mitochondria.

Protein content determination

The protein content of the mitochondrial suspension, was measured by the biuret method with bovine serum albumin as standard [Gornall *et al*., 1949]. The method uses the formation of a violet complex between rameic ion and amidic nitrogen of proteins (biuret reaction).

The Gornall solution contains:

- Rameic sulphate (CuSO4 • 5 H2O) 1.5 g/l
- Sodium and potassium tartrate (NaKC4H4O6 • 4 H2O) 6 g/l
- Sodium hydroxide (NaOH) 30 g/l

Preparation of Gornall reagent:

1.5 g of rameic sulfate and 6 g of sodium and potassium tartrate are placed in 500 ml of bidistilled water. Under constant stirring 300 ml of NaOH 10% (w/v) are added and made up to volume with bidistilled water up to reach a final liter.

The reagent thus prepared should be stored in the dark, due to its sensitivity to light.

Procedure

Five test tubes are prepared (one blank, two samples, two serum albumin standards) according to the scheme reported in Table 1.

	Blank	**Sample1**	**Sample2**	**Standard 1** **1 mg/3 mL**	**Standard 2** **2 mg/3 mL**
H_2O	0.500	0.475	0.475	0.250	-
Deoxycholate 3%	1.000	1.000	1.000	1.000	1.000
Isolated mitochondria	-	0.025	0.025	-	-
Albumin (4 mg/mL)	-	-	-	0.250	0.500
Gornall Reagent	1.500	1.500	1.500	1.500	1.500

Table 1. Outline of the protein assay according to the method of Gornall. All amounts are expressed in ml.

The standard is used for the construction of the calibration line. To verify the correct preparation of the reagent of Gornall is considered that 1 mg of albumin with reagent gives an absorbance of 0.090 in a spectrophotometer at a wavelength of 540 nm.

The reagent of Gornall acts by complexing the proteins according to the reaction of biuret, and produces a violet color whose absorbance maximum is at 540 nm. The reaction takes place at 30°C for 10 minutes.

The blank is used to calibrate the spectrophotometer and to make sure that the absorbance of the samples are due only to the mitochondrial proteins present.

The absorbance of the two samples are measured at 540 nm in an UV/VIS KONTRON UVIKON 922 spectrophotometer.

The formula, derived from the calibration line, by which we are able to calculate the volume in which is present a milligram of mitochondrial proteins is :

$$V = \frac{1}{\overline{A}_{\max} \times 44.44} \times 100$$

and it is derived from the composition of two proportions:

$$x{:}25\mu l = 1mg{:}V(\mu l \rightarrow ?)$$

$$1 \text{ mg prot} : 0.090 = x : \overline{A}_{media}$$

Standard medium for mitochondrial incubation

Mitochondria (1 mg/ml) were incubated in the following medium:

component	concentration
Sucrose	200 mM
Hepes	10 mM
Succinate	5 mM
Rotenon	1.25 μM
Phosphate	1 mM

Table 2. Composition of the standard medium of incubation.

The medium was at pH 7.4 and 20°C. All variations or additions at this medium will be reported in the appropriate captions in the result section.

Transmembrane potential measurement with ionoselective electrode

The transmembrane electric potential ($\Delta\Psi$) was measured using a specific electrode on the basis of distribution of the lipid-soluble cation tetraphenylphosphonium (TPP^+) [Affolter and Sigel, 1979; Kamo *et al*., 1979].

The electrode is a complex semipile formed by an anion reversible electrode, at Cl^- (inner reference electrode), inserted in a case containing a TPP^+Cl^- solution at known concentration, at contact with a TPP^+ permeoselective membrane. This semipile exhibits an electric potential that changes with logarithm of TPP^+ activity in the sample. It is coupled with an electrode at constant potential (outer reference electrode) and formed a pile, with an electroengine force/power that results linear function of activity logarithm of the ion to measure.

The membrane separates two solution at different concentration of the same electrolyte (TPP^+Cl^-): TPP^+ is the counterion and Cl^- is the coordinate ion of the membrane, because their charges are respectively opposite and equal to the charge in the membrane structure, given by tetraphenylborate (TPB^-). The membrane is a cationic membrane, because is permeable to TPP^+.

The pile exhibits a potential variation (ΔE), that is measure of the proceed of the process of counterions transfer from high concentration solution c'' (fixed) to lower concentration solution c' (unknown), with c''>c'.

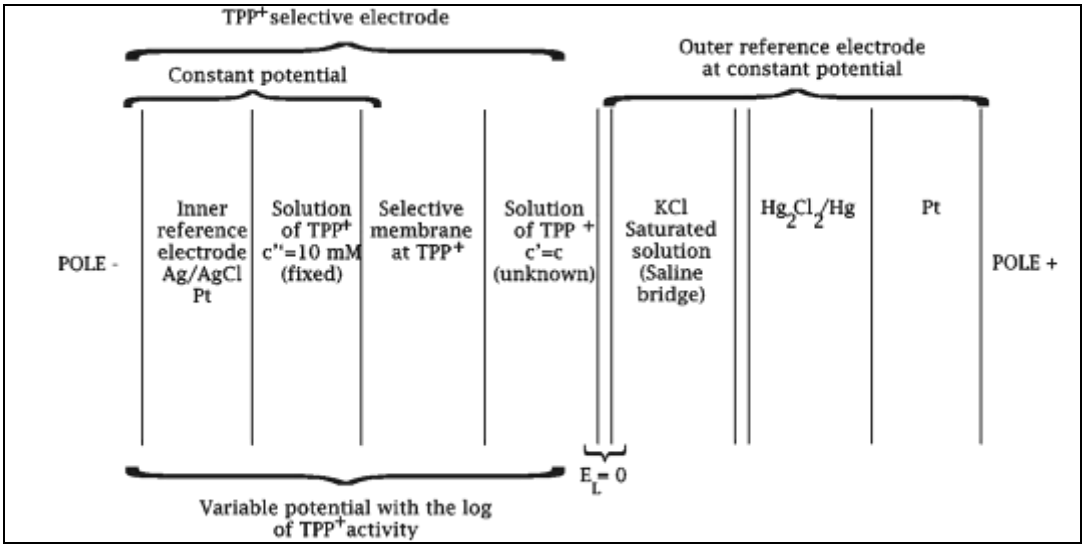

Fig. 7. TPP^+ selective electrode.

The inner and outer electrode potentials are constant, and the potential difference of the pile is determined only by membrane potential (function of the ratio between unknown and known concentration of the counterion TPP^+) and interliquide potential (E_L), minimized by KCl saturated saline bridge.

The ΔE results:

$$\Delta E = E_1 - E_2$$

$$E_1 = E_{k'} + \Delta E_X$$

$$E_2 = E_{k''} + E_L$$

Where:

E_1 = ionoselective electrode potential

E_2 = outer reference electrode potential + interliquide junction potential

$E_{k'}$ = inner reference electrode potential

ΔE_x = ionoselective membrane potential difference

$E_{k''}$ = outer reference electrode potential

E_L = interliquide junction potential ≈0

$$\Delta E = E_{k'} + \Delta E_X - E_{k''} - E_L$$

$$\Delta E = E_{k'} - E_{k''} + \Delta E_X$$

Setting: $E_{k'} - E_{k''} = z$ (constant)

Then:

$$\Delta E_X = E_0 + \frac{2.3RT}{nF}\log c'' - E_0 - \frac{2.3RT}{nF}\log c'$$

Setting: $E_0 + \frac{2.3RT}{nF}\log c'' = U$ (constant)

The ionoselective membrane potential difference (ΔE_x) becomes:

$$\Delta E_X = U - \frac{2.3RT}{nF}\log c'$$

And pile ΔE results:

$$\Delta E = z + U - E_0 - \frac{2.3RT}{nF}\log c'$$

Finally, setting: $z + U - E_0 = K$, it is obtained:

$$\Delta E = K - \frac{2.3RT}{nF} \log c' \qquad [1]$$

Where:

K = constant resulting from the algebraic sum of all the constant potentials in the electrode

F = 96485 coulombs mol^{-1} = 23.06 Kcal $volt^{-1}$ mol^{-1}

R = 8.341 Joule mol^{-1} K^{-1}

T = 20°C

The electrode response is linear with the logarithm of TPP^+ concentration, with an increase of about 58 mV every ten unit of variation in the TPP^+ concentration, until the concentration decreases to 10^{-7} M, according to Nernst's equation.

The $\Delta\Psi$ is determined measuring the TPP^+ distribution across the mitochondrial membrane with the electrode. The mitochondrial membrane is permeable to TPP^+, that distributes according to Nernst's equation:

$$\Delta\psi = \frac{2.3RT}{nF} \log \frac{[TPP^+]_{out}}{[TPP^+]_{in}} = 58 \log \frac{[TPP^+]_{out}}{[TPP^+]_{in}} \qquad [2]$$

Where:

$[TPP^+]_{out}$ = outer TPP^+ concentration

$[TPP^+]_{in}$ = inner TPP^+ concentration

determining the variation of electrode ΔE.

Considering the law of mass conservation:

$$V[TPP^+]_{out} + v[TPP^+]_{in} = V[TPP^+]_0 \qquad [3]$$

Where:

V = medium volume containing 1 mg of mitochondrial proteins (1 ml in our system)

v = volume of inner mitochondrial space corresponding to 1 mg of mitochondrial proteins (≈ 1 μl)

$[TPP^+]_0$ = TPP^+ concentration before mitochondrial addition

Equation [3] is inserted in [2] and ΔE is correlated to $[TPP^+]_{out}$, with some mathematic passages, it is obtained:

$$\Delta\psi = 58\log\frac{v}{V} - 58\log\left(10^{\left(\frac{\Delta E-\Delta E_0}{58}\right)} - 1\right) \qquad [4]$$

Where:

ΔE_0 = electrode potential difference before mitochondrial addition

In order to calculate correctly the $\Delta\Psi$ it is necessary to know the v/V ratio, that is the v value. If mitochondrial volume does not vary during experiment, the 58 log v/V remains constant.

The v value was calculated using the [^{14}C]sucrose distribution [Palmieri and Klingenberg, 1979], and it corresponds to 1 μl/mg of mitochondrial proteins. Jensen *et al*. [1986], comparing the $\Delta\Psi$ value obtained measuring the ^{86}Rb and that measuring with electrode, propose to correct with the subsequent equation:

$$\Delta\psi_{Rb} = \frac{(\Delta\psi_{el} - 66.16mV)}{0.92} \qquad [5]$$

In which $\Delta\Psi_{el}$ is the value obtained in [4].

Before to proceed in $\Delta\Psi$ measure, it is performed the electrode calibration, to determine experimentally the ratio $\frac{2.3RT}{nF}$

The ratio corresponds to the slope of the line:

$$\Delta E = K - \frac{2.3RT}{nF}\log c'$$

The calibration was performed in the incubation condition, without mitochondria, adding TPP^+ and measuring the electrode variation. The final concentration of TPP^+ should not exceed 1-2 μM, because an excessive amount of TPP^+ can later depolarize the mitochondrial membrane.

The slope calculation was derived graphically: the measured ΔE values are carried in function of log[TPP^+]. The ΔE corresponding to an increase in TPP^+ concentration of ten times is extrapolate. The theoretical value, according to Nernst, corresponds to 58 mV.

After calibration, mitochondria were added to incubation medium, TPP^+ enters across mitochondrial membrane and distributes between medium and matrix, according to Nernst's equation. A potential difference at the electrode was originated respect to the value reached after calibration, named ΔE-ΔE_0, and registered by the recorder as a deflection (decrease of TPP^+) concentration in the medium. The fitting of this potential difference variation in the [4] allow to obtain the $\Delta\Psi$ value.

Mitochondrial swelling determination

Mitochondrial swelling occurs when solute enters in high quantity in mitochondrial matrix, *e.g.,* when mitochondrial permeability transition happens, causing an increase in the osmotic pressure. Mitochondria, in fact, have the ability to behave like osmometers and, therefore, can swell or contract through accumulation or expulsion of water, according to the tonicity of the medium in which they are suspended.

This phenomenon can be detected by using the technique of "light-scattering" that consists in the ray of light dispersion when it crosses the mitochondrial suspension. If matrix volume is increased, it can be observed a decrease of dispersion and, consequently, a decrease also of absorbance.

RLM (1mg/ml) were incubated in standard medium for about 15 minutes in the different experimental conditions. Swelling was monitored using an UV/VIS KONTRON UVIKON 922 spectrophotometer, at 540 nm of wavelength.

Assay for evaluating the release of cyt. *c*, Smac/DIABLO and AIF

Samples (1mg prot/ml) were incubated in the various experimental conditions, in standard medium, for about 15 minutes at 20°C and were then centrifuged at 14000 rpm for 2 minutes with Centrifuge 5415C. The supernatant fraction (containing the pro-apoptotic factors) was concentrated with the PAGEprep^{TM} Protein Clean-Up and Enrichment Kit (PIERCE). Concentrated samples were then incubated at 100°C for 4 minutes and loaded on SDS-page gel.

SDS-polyacrilamide gel electrophoresis (SDS-Page) is one of the main methods used for the qualitative analysis of protein mixtures and it is based on the separation of proteins according to size. Sodium dodecil sulfate (SDS) is an anionic detergent that, binding to proteins, provokes their denaturation. Thus, each protein is fully denatured and carries on a series of negatively charged SDS molecules along the polypeptide chain because, on overage, each SDS molecule binds to every two amino acids residues. During the electrophoretic process SDS-protein complexes migrate, under the effect of the electric field, towards the anode.

SDS-polyacrylamide gels were prepared following the method of Laemmli [1970]. In every experiment presented, in order to determine the molecular weight of the proteins and also to identify the proteins of interest, molecular weight standards were used.

The electrophoretic plate is composed of two types of gel:

1. Stacking gel (pH 6.8) has the function to concentrate protein samples
2. Running gel (pH 8.8) in which the real separation of protein takes place

Polyacrilamide gels are usually defined in terms of the total percentage of acrylamide present. For cyt. *c* and Smac/DIABLO determination, a gel of 15% acrylamide has been used while for AIF detection a gel of 10% acrylamide has been chosen.

The electrophoretic plate (8x10cm) was fixed in a dedicated device (Mighty Small SE 250, Hoefer Scientific Instruments). The electrophoresis duration was approximately 1.5 hours with an electrical current of 35 mA/gel.

At the end of the electrophoretic process, the pattern of separated protein has to be transferred or blotted from the gel to a sheet of nitrocellulose paper. The transfer is achieved using a proper buffer (25 mM Tris, 192 mM glycine and 20% methanol, pH 8) and applying a current of 100 mA for 2 hours (for cyt. *c* and Smac/DIABLO) and 350 mA for 50 minutes (for AIF).

After blotting, membrane was saturated for 30 minutes, under constant shaking, with a saturation buffer containing TBS 1X and 3% BSA. TBS 1X was diluted from an initial buffer (TBS 20X) composed as follows: 1 M Tris/HCl and 3 M NaCl (pH 7.5).

The membrane was then incubated over-night at 4°C with an appropriate antibody diluted in a buffer containing TBS 1X and 0.1% Tween.

Mouse monoclonal antibody anti-cytochrome c was purchased from Pharmingen, rabbit polyclonal antibody anti-Smac/DIABLO and rabbit polyclonal antibody anti-AIF from Millipore.

After the binding between the first antibody and the protein of interest, three washes of about 10 minutes each were performed, at room temperature, with the washing buffer (TBS 1X and 0.1% Tween). Then the membrane was incubated, under constant shaking, with the second antibody (PerkinElmer), obtained against the animal species immunized for the first antibody and diluted in the washing buffer. Again three washes of 10 minutes each were performed and then the membrane was ready for antibody detection. The system adopted was enhanced chemiluminescence (ECL) where the reagents, in contact with the membrane, give rise to a reaction of chemiluminescence in correspondence to the position of antigene-antibody complexes, detected by autoradiography.

In this study the Amersham ECL Prime Western Blotting Detection Reagent kit was adopted.

Densitometry was performed on scanned Western Blot images using the ImageJ gel analysis tool [Abramoff *et al*., 2004]. The gel analysis tool was settled in order to consider the mean gray value, the min and max gray value and the area of each experimental band. The overall brightness and contrast of every whole image was optimized for the densitometric analysis, without modifying the information present in it, according to Rossner and Yamada [2004]. Results were expressed are percentages and normalized against the background.

Assay for evaluating the presence/activation of Bax

RLM (5mg/ml) were incubated in standard medium, in the various experimental conditions, for about 15 minutes at 20°C. This mitochondrial concentration was chosen in order to compare these results with the other Western Blot reported in which, as previously described, the supernatant was concentrated with a specific kit. After incubation and centrifugation (14000 rpm for 2 minutes with Centrifuge 5415C), mitochondrial pellets (P) and supernatants (S), derived from different mitochondrial preparations (1^{st}, 2^{nd}, 3^{rd}, 4^{th}), were analyzed by SDS-Page and Western Blot, as described in the previous section for cyt. *c* and Smac/DIABLO. To detect Bax presence and Bax activation, a rabbit polyclonal antibody anti-Bax (N-terminous) and a mouse monoclonal antibody anti-Bax (6A7), respectively, from Santa Crutz, were used.

Fluorimetric assay to hydrogen peroxide determination

The H_2O_2 produced by mitochondria was measured by scopoletin (6-metoxy-7-idroxy-1,2-benzopirone) method [Loschen *et al.*, 1971]. Mitochondria (0,5 mg/ml) were incubated in the standard medium in presence of 2 μM scopoletin and 10 μM horseradish peroxidase (HRP), at 20°C.

The HRP, in presence of H_2O_2, oxidizes scopoletin that loses its fluorescence, with the following reaction:

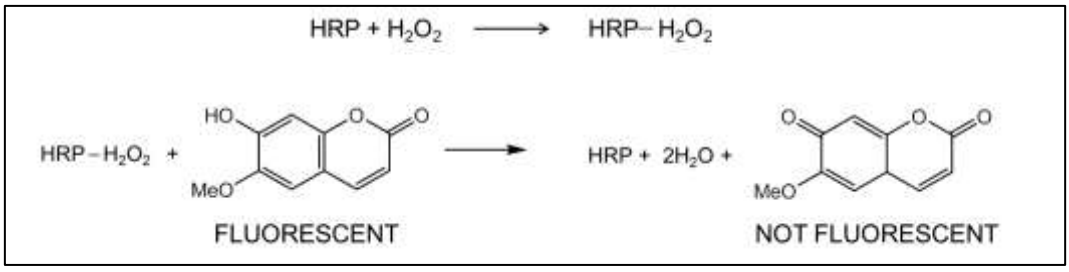

The fluorescence was measured utilizing a SHIMADZU RF-5000 spectrofluorimeter, with 350 nm of excitation wavelength and 460 nm of emission wavelength.

The amount of H_2O_2 produced by mitochondria wass calculated, from the values obtained, by using a calibration curve obtained with H_2O_2.

Uptake of agmatine in mitochondria

Mitochondria (1mg/ml) were incubated in the standard medium in presence of radio-labeled agmatine (50 μCi/mmol), at 20°C. AGM accumulation by RLM was determined with the centrifugation-filtration method on gradient, as previously described [Toninello *et al.*, 1985], with the utilization of plastic test tubes for

micro-centrifuge Eppendorf 5414. In the test tubes 0.15 ml of saccarose 12.5% (w/v) with ρ= 1.08 were added and, upper, 0.40 ml of a silicon oil mixture with ρ=1.05 (AR 100/AR 150 (2:1) Walker-Chemie Gmbh, Munich). At different times 0.5 ml of each sample were collected, placed in the tubes on the layer of silicon oil, and centrifuged at 14000 *g* for 1 minute.

During centrifugation, mitochondria crossed the layer of silicon oil and leaved sediment in sucrose. Supernatant was drawn and tube walls were washed two times with bidistilled water. Then, the layer of silicon oil was also drawn, leaving only the sucrose layer. Tubes were shaken with vortex in order to detach the mitochondrial pellet from the walls and 0.85 ml of solubilizing buffer (1 mM EDTA, 0.1% NaCl, 0.9% Sodium deoxycholate) were added.

Finally, the solubilized pellet was transferred in mini Poly-Q vials were 3 ml of scintillation liquid (Ultima Gold) were added and radioactivity was determined by using a Beckman counter LS-1800.

Thermodynamic analyses of ligand-receptor interactions

Binding parameters were obtained by applying thermodynamic treatment of ligand-receptor interactions [Di Noto *et al*., 1996; 2002]. For the simulation of agmatine binding (B) as a function of the free agmatine amount in solution (F), it was applyed the following equation, characteristic of a system with two binding sites:

$$[B] = [B_{\max 1}] \cdot \left(\frac{[F] \cdot \frac{1}{K_{1,1}}}{1 + \frac{[F]}{K_{1,1}}} \right) + [B_{\max 2}] \cdot \left(\frac{[F] \cdot \frac{1}{K_{2,1}}}{1 + \frac{[F]}{K_{2,1}}} \right) \qquad [6]$$

The binding constants and the consequent energies of interaction were determined using Eq [6] for Scatchard analyses and Eq [7] for Hill analyses. These equations were both obtained from the same general equation [Di Noto *et al*., 1996; 2002] and their rationale considers receptors with different groups of binding sites (s) where each one could have multiple coordination (n_i). The subsequent algebric elaborations were previously developed [Dalla Via *et al*., 1996].

$$\frac{[B]}{[F]} = \sum_{i=1}^{s} \left\{ \left[B_{max,i} \right] - [B_i] \right\} \cdot \left[\frac{1}{K_{i,1}(t)} + \varepsilon_i(F) \right] \qquad [7]$$

$$\ln \left\{ \frac{[B]}{\left[B_{max,i} \right] - [B]} \right\} = \ln \left\{ \sum_{i=1}^{s} x_i(F) \left[\frac{1}{k_{i,1}(t)} + \varepsilon_i(F) \right] \right\} + \ln[F] \qquad [8]$$

where

$$\varepsilon_i(F) = \sum_{k=2}^{n_i} \frac{[F]^{k-1}}{\prod_{j=1}^{k} k_{i,j}(t)}$$

represents the appropriate measure of the extent of multiple coordination on the *i*-th sites. [$B_{max,i}$] is the maximum concentration of ligand that may be bound to the *i*-th sites, [B_i] is the concentration of ligand bound to the *i*-th sites, [B_{max}] is the maximum receptor-bound ligand concentration and [B] is the concentration bound to the receptor. [F] is the free ligand concentration, $K_{i,j}(t)$ is the affinity constant of the ligand for the *i*-th site, *j* is the occupancy number, and *t* is the time. Fitting was performed using a home written package of Igor procedures working in the Igor Pro ver. 6.0.4.0 of WaveMetrix Inc. (Oregon, USA, 2007). The fits were performed by using the Igor minimization subroutines which are called from the main package.

The distribution of total bound agmatine on its binding sites was calculated by the parameter $X_i(F)$. This parameter is the mole fraction of the *i*-th site that may bound to the receptor and has been calculated by means of Eq. [8].

$$X_i(F) = \left(\left[B_{max,i}\right] - [B_i]\right)/([B_{max}] - [B])$$

$$= 1/(1 + \beta_i[F]) \qquad [9]$$

where β_i is a parameter that describes the influence of the parallel filling of the other k-th sites in comparison to filling of the i-th site.

AGM binding energy and the Hill factor were calculated substituting *s*=2 and n_i=1 in Eqs. [6] and [7] and by considering *t*=0, thus obtaining the following equations:

$$\frac{[B]}{[F]} = ([B_{max}] - [B]) \cdot \left[\frac{\Delta K}{1+\beta_1[F]} + \frac{1}{K_{2,1}}\right] \qquad [10]$$

where

$$\Delta K = \left({}^{1}/_{K_{1,1}}\right) - \left({}^{1}/_{K_{2,1}}\right)$$

$$\ln\left\{\frac{[B]}{[B_{max}]-[B]}\right\} = \ln\left\{\frac{\Delta K}{1+\beta_1[F]} + \frac{1}{K_{2,1}}\right\} + \ln[F] \qquad [11]$$

Part I

Agmatine action on the permeabilization of mitochondrial membranes

Bivalent effect of agmatine on the MPT

It has been shown that AGM exerts several effects on (isolated) mitochondria, revealing close relationships between this amine and the organelle functions [for a review see Agostinelli *et al*., 2010]. As detailed in the Introduction, AGM shows opposite effects, acting as an amplifier or an inhibitor of the MPT, depending on the concentration: at low concentrations (10-100 μM) AGM produces H_2O_2 and induces the MPTP opening by oxidative stress; at high concentrations (1 mM), although it still generates large amounts of H_2O_2, AGM self-scavenging effect prevents alterations of the redox state and other bioenergetics parameters of mitochondria [Battaglia *et al*., 2007].

This dichotomic effect has been the issue of the first part of the thesis. Due to the strong correlation between MPT and the release of pro-apoptotic factors, it was studied whether the above opposite effects could be further confirmed by the release/retention of the main pro-apoptotic proteins.

Results

Effect of agmatine on pro-apoptotic factors release

Mitochondria incubated in standard medium and in presence of high Ca^{2+} concentrations, undergo the induction of MPT that, as above emphasized, is evidenced by the colloid-osmotic swelling of the organelles. This phenomenon is evaluated by monitoring the decrease of apparent absorbance of the mitochondrial suspension at 540 nm.

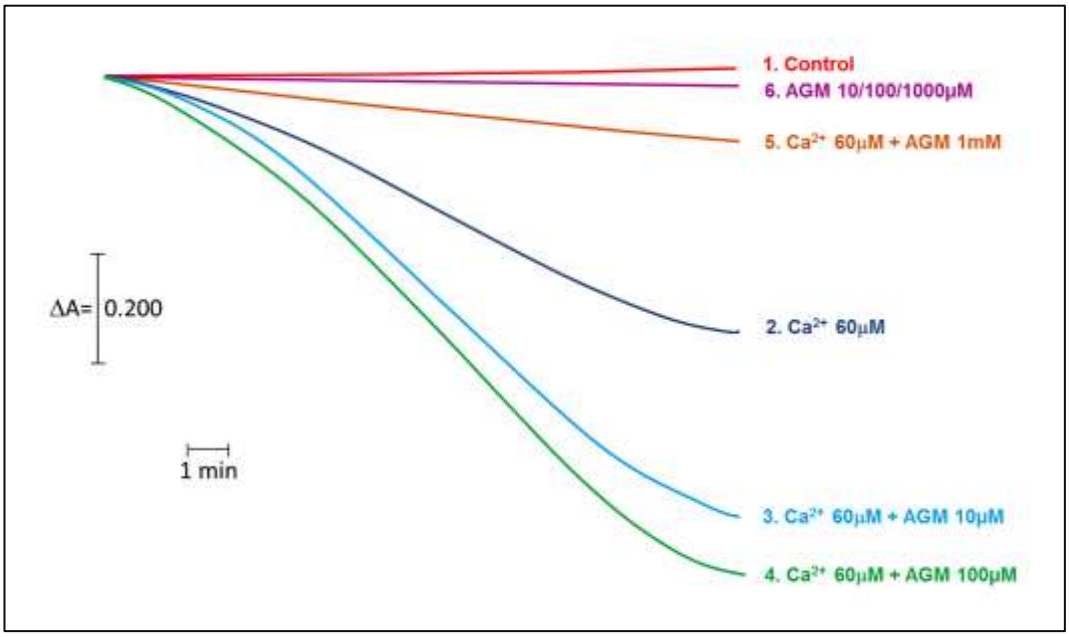

Fig. 8 Effect of agmatine on mitochondrial swelling induced by Ca^{2+}.
RLM (1mg/ml) were incubated in standard medium, as described in Materials and methods section. Where present: Ca^{2+} and AGM at the concentrations indicated at side of the traces. Downward deflections indicate mitochondrial swelling. Assays performed five times gave almost identical results.

Fig. 8 shows the above mentioned bivalent effect of different concentrations of AGM on mitochondrial swelling induced by Ca^{2+}. In particular, it is well evidenced the double effect: 10 µM and 100 µM AGM (traces 3 and 4, respectively) are able to amplify the effect of Ca^{2+} alone (trace 2), whereas 1mM AGM (trace 5) shows an inhibitory activity. AGM alone (trace 6), at all the concentrations tested, is comparable to the control (trace 1). These results clearly demonstrate a protective effect of 1mM AGM on the mitochondrial swelling and an inductive effect at low concentrations.

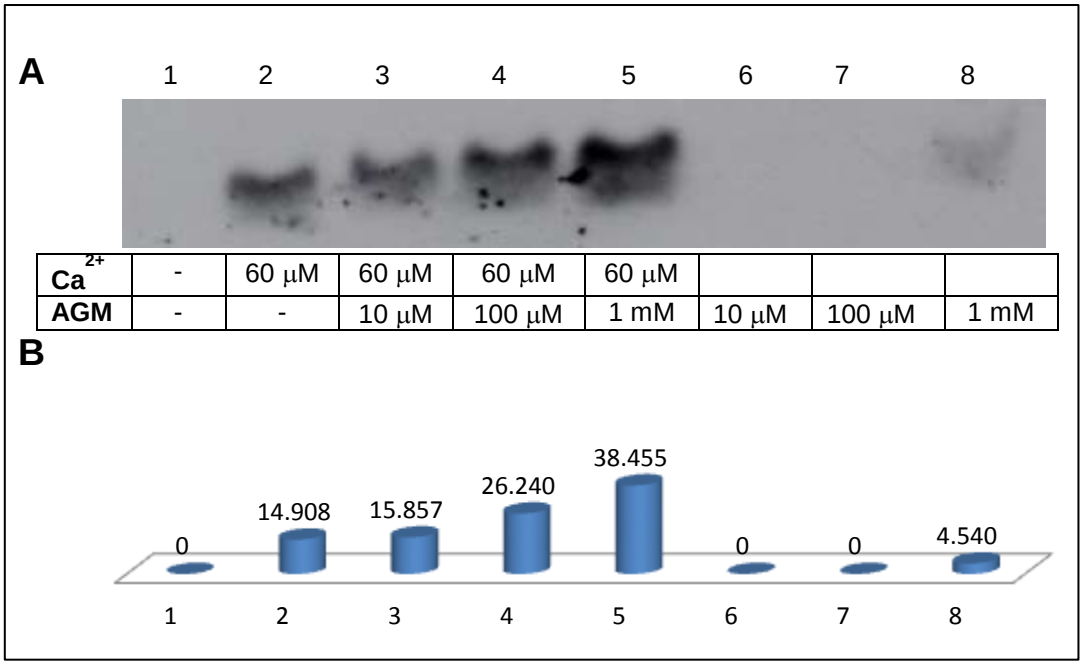

Fig. 9 Release of cytochrome c induced by agmatine in presence of Ca^{2+} (A) and densitometric analysis (B). RLM (1mg/ml) were incubated in standard medium under the same conditions as in Fig. 8 and the supernatant fraction was analyzed by SDS-Page and Western Blot, as described in Material and methods section. Assays performed four times gave almost identical results. The values reported in Fig. 9B are expressed as percentage.

Fig. 9A reports the result of the Western Blot conducted on the mitochondrial supernatant fractions, showing the release of cyt. *c*. In Fig. 9B a densitometric output is shown. It is clear that 10 and 100 μM AGM, in the presence of Ca^{2+} (lanes 3 and 4, respectively), causes a considerable loss of the protein, about 16% and 26% higher if compared to the control (lane 1), thus confirming the pro-apoptotic effect of the amine. A similar output, although with a lesser extent, is observable also with Ca^{2+} alone (lane 2, 15%), observation in agreement with Ca^{2+} induction of MPT. Taking into account the MPT-inhibitory effect of 1 mM AGM shown in Fig. 8, the result reported in lane 5 is unexpected. As observable, the pattern of release present in lane 5 (38%) is higher than that present in lanes 2, 3 and 4 (15%, 16%, and 26%, respectively). Thus, cyt. *c* seems to be released also through a different process, probably MPT-independent.

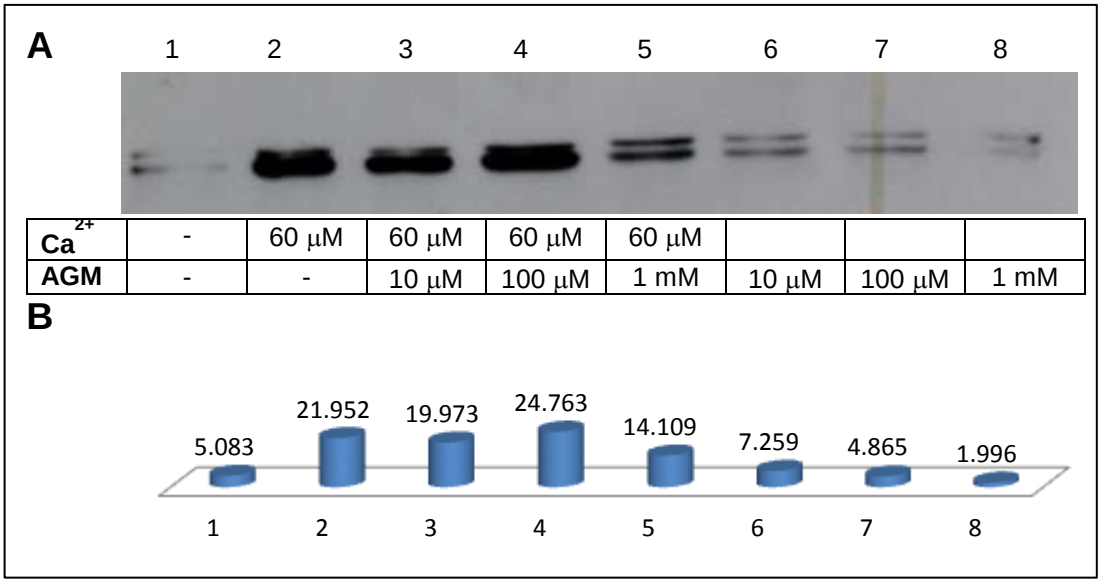

Fig. 10 Release of AIF induced by agmatine in presence of Ca^{2+} (A) and densitometric analysis (B). RLM (1mg/ml) were incubated in standard medium under the same conditions as in Fig. 8 and the supernatant fraction was analyzed by SDS-Page and Western Blot, as described in Material and methods section. Assays performed four times gave almost identical results. The values reported in Fig. 10B are expressed as percentage.

A different scenario is observable analyzing the release of AIF (showed in Fig. 10A), which is induced only by Ca^{2+} alone (lane 2, 22%) or in the presence of low AGM concentrations (lanes 3 and 4, 20% and 25%, respectively). The release of AIF in the presence of Ca^{2+} and 1mM AGM is considerably lower (lane 5, about 14%). The same consideration can be made if the effects of AGM alone at all the concentrations (lanes 6-8, 7%, 5% and 2%, respectively) are compared to the control (lane 1, 5%). This result is in agreement with the induction of mitochondrial swelling showed in Fig. 8.

As described in the Introduction, the intra-mitochondrial localization of these proteins is different: while cyt. *c* is an intermembrane space protein, AIF is a transmembrane protein of the IM. Thus, in order to evaluate if the localization of the proteins is important for explaining the obtained results, a third pro-apoptotic factor was analyzed, Smac/DIABLO, which is present in the intermembrane space.

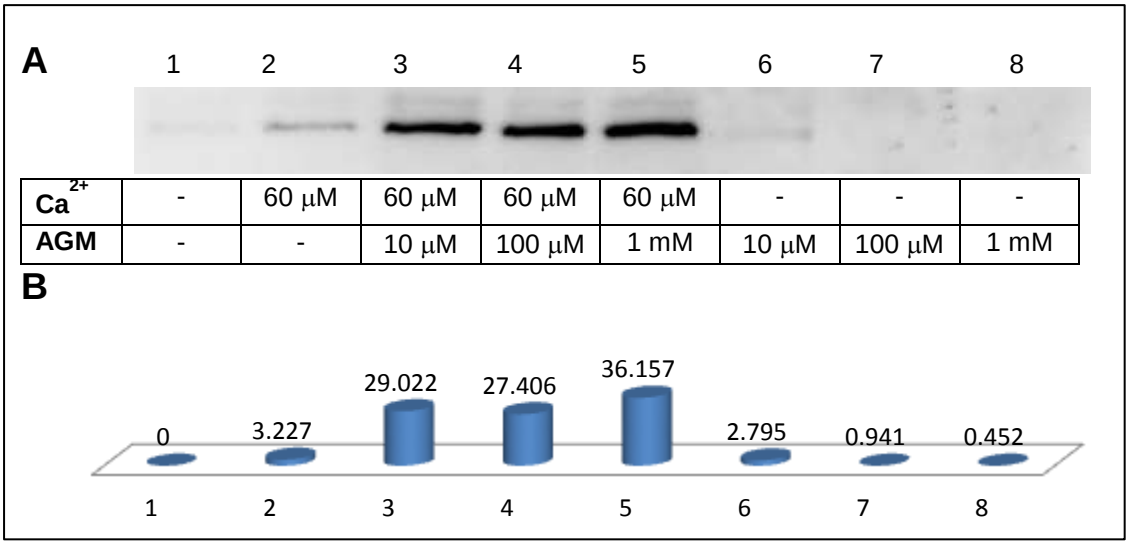

Fig. 11 Release of Smac/DIABLO induced by agmatine in presence of Ca^{2+} (A) and densitometric analysis (B). RLM (1mg/ml) were incubated in standard medium under the same conditions as in Fig. 8 and the supernatant fraction was analyzed by SDS-Page and Western Blot, as described in Material and methods section. Assays performed four times gave almost identical results. The values reported in Fig. 11B are expressed as percentage.

The output shown in Fig. 11 resembles the release of cyt. *c* (Fig. 9A): 10 and 100 μM AGM, in the presence of Ca^{2+} (lanes 3 and 4), cause a considerable loss of the protein (29% and 27%, respectively), about thirty times higher if compared to the control (lane 1, 0%) and to Ca^{2+} alone (lane 2, 3%), and the presence of 1mM AGM further enhances its release (lane 5, 36%). This output indicates that Smac/DIABLO and cyt. *c* (both intermembrane space proteins) could exit from mitochondria utilizing the same pathway, suggesting also that the mitochondrial localization of the factors is important in AGM-induced release. Moreover, the observed release of cyt. *c* and Smac/DIABLO happens without mitochondrial swelling, as demonstrated by the experiment reported in Fig 8, thus in the absence of MPT induction.

MPT-independence

The MPT phenomenon has been widely studied over the past years and several inductors and inhibitors have been identified. One of the most well-known inhibitors is the immuno-suppressive drug cyclosporin A (CsA). This compound binds to CypD, which is one of the candidate components for the MPTP complex. In fact, as reported by Leung and Halestrap [2008], MPTP opening involves a conformational change in a membrane protein that is facilitated by the binding of CypD. This modification can occur also in the absence of CypD, but higher Ca^{2+} concentrations are needed, supporting at least a MPT-regulatory action for CypD. Thus, CsA binding to CypD results in MPT prevention [Halestrap *et al*., 1997; Halestrap, 2009].

In order to evaluate the possible MPT-independence of the differential release of pro-apoptotic factors induced by AGM, experiments with CsA were performed, as observable in Figs. 12-13.

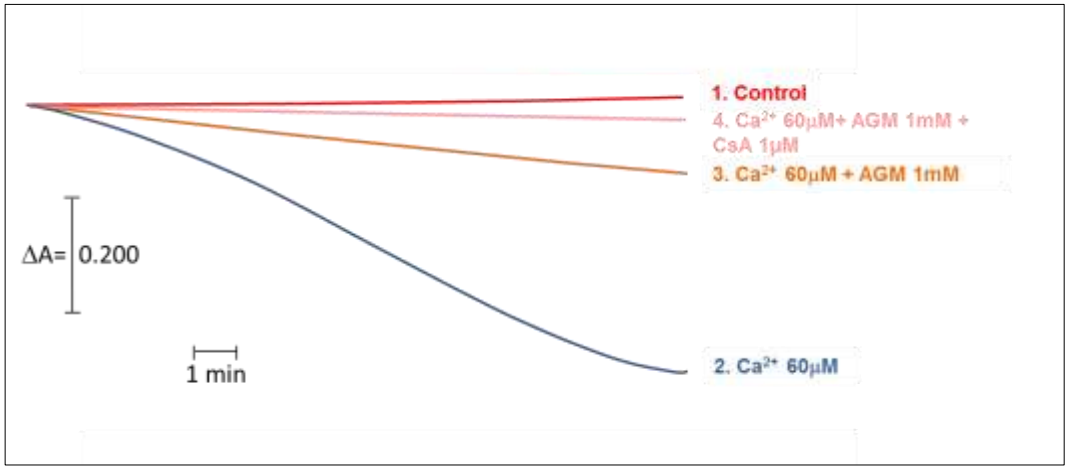

Fig. 12 Effect of agmatine and cyclosporin A on mitochondrial swelling induced by Ca^{2+}.

RLM (1mg/ml) were incubated in standard medium, as described in Materials and methods section. When present: Ca^{2+}, AGM and CsA are at the concentrations indicated at side of the traces. Downward deflections indicate mitochondrial swelling. Assays performed five times gave almost identical results.

In Fig. 12 it is reported the protecting effect exhibited by 1 mM AGM (trace 3) against the swelling induced by Ca^{2+} (trace 2). The addition of CsA (trace 4), as expected, further enhances AGM action.

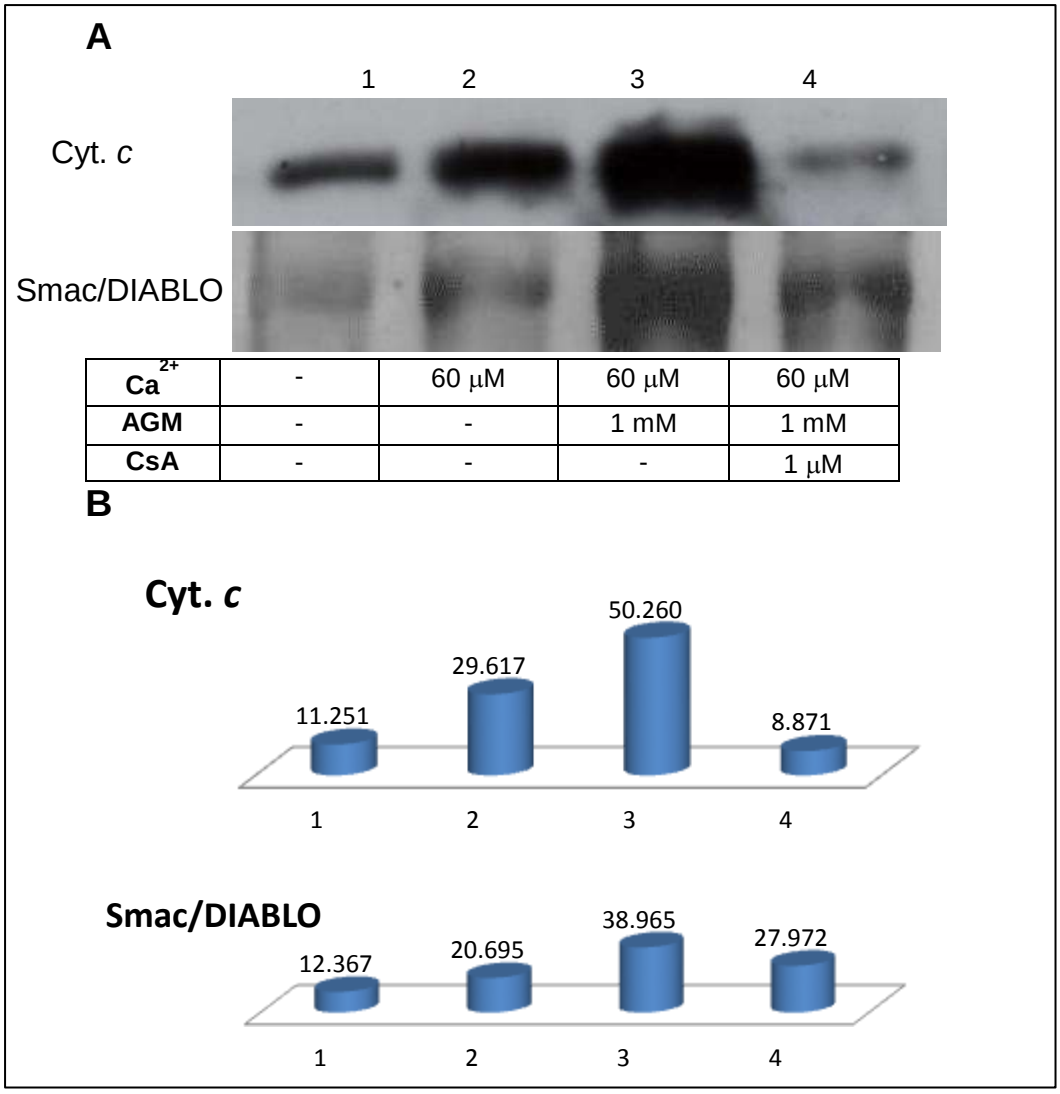

Fig. 13 Release of cytochrome c and Smac/DIABLO induced by agmatine in presence of Ca^{2+} and cyclosporin A (A) and densitometric analysis (B).

RLM (1mg/ml) were incubated in standard medium under the same conditions as in Fig. 12 and the supernatant fraction was analyzed by SDS-Page and Western Blot, as described in Material and methods section. Assays performed four times gave almost identical results. The values reported in Fig. 13B are expressed as percentage.

The correspondent Western Blot conducted on the mitochondrial supernatant fractions is shown in Fig. 13A. With regard to the release of cyt. *c*, it is clear the almost total prevention exhibited by CsA (lane 4, 9%) with respect to the effect of AGM plus Ca^{2+} (lane 3, 50%). A similar output is evidenced also for the release of Smac/DIABLO. CsA, even if with less extent, exhibits a partial prevention (lane 4, 28%) on the synergic effect shown by AGM plus Ca^{2+} (lane 3, 39%).

With regard to these results, some considerations can be made: first of all, the release of the above mentioned factors occurs in the absence of swelling and thus without MPT induction. Also, the MPT inhibitor CsA does exhibit a partial prevention, suggesting that its effect could have another explanation.

Possible involvement of Bax

In healthy cells, Bax is mostly cytosolic, although small pools have been localized in mitochondria, loosely attached to the OM or even membrane-inserted [Renault and Manon, 2011; Westphal *et al*., 2011]. The translocation of this pro-apoptotic protein, as described above, is one of the initial steps to induce MOMP, but it is not sufficient itself. Thus, a subsequent signal is required for the activation (oligomerization and pore formation) of Bax. Moreover, Costantini and collaborators [2000] reported that Bax-induced membrane permeabilization is inhibited by CsA.

These previous observations raised the interest to assess whether Bax is involved in AGM-induced permeabilization. For this purpose, first of all, an experiment was performed in order to detect the presence of the protein in the mitochondrial preparations.

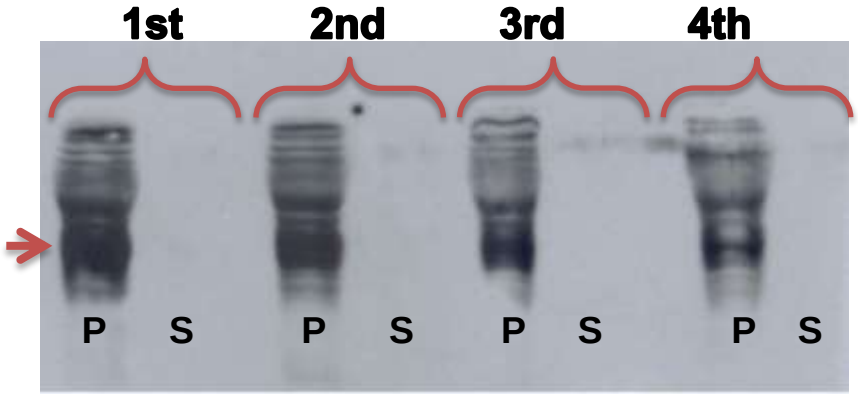

Fig 14. Bax presence in the mitochondrial pellet and supernatant fractions.
RLM (5mg/ml) were incubated in standard medium, as described in Material and methods section. Mitochondrial pellets (P) and supernatants (S), derived from different mitochondrial preparations (1^{st}, 2^{nd}, 3^{rd}, 4^{th}), were analyzed by SDS-Page and Western Blot. Assays performed four times gave almost identical results.

The presence of Bax in different mitochondrial preparations is evidenced in Fig. 14. A 20 kDa band is evident, indicating that the protein is clearly localized in every pellet portion (P), whereas the supernatant fraction does not show any signal. Mitochondria have not been treated with MPT/MOMP inducers and thus it is reasonable to think that the protein could be anchored to the OM, but probably not active (pro-apoptotic).

During apoptosis both Bax and Bak undergo conformational changes and the use of an anti-Bax conformation-specific antibody (6A7) allows to detect the presence of the protein, upon an apoptotic signal [Westphal *et al*., 2011].

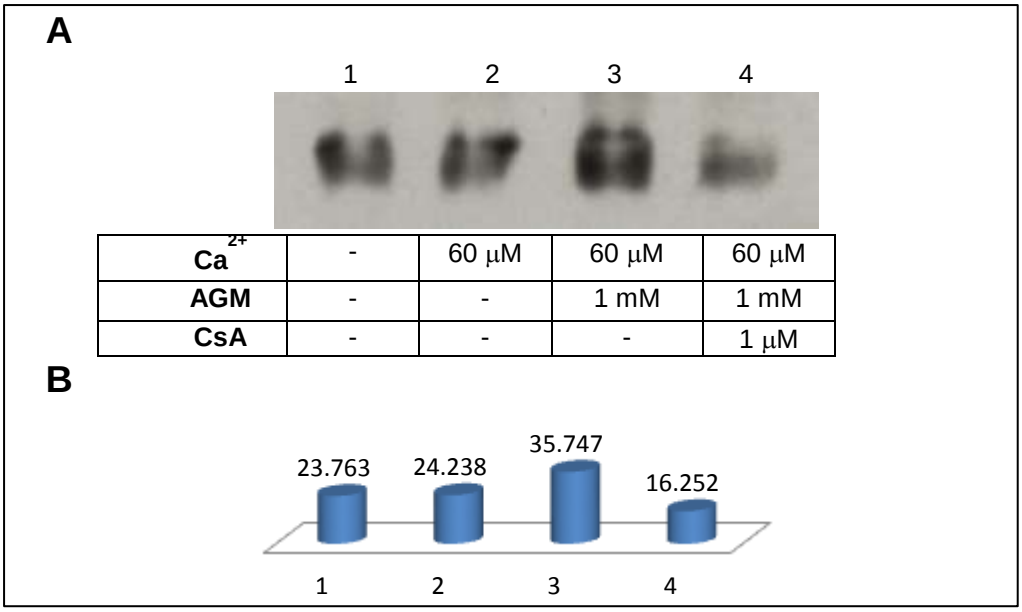

Ca^{2+}	-	60 μM	60 μM	60 μM
AGM	-	-	1 mM	1 mM
CsA	-	-	-	1 μM

Fig. 15 Presence of activated Bax in the mitochondrial pellet fraction (A) and densitometric analysis (B).

RLM (5mg/ml) were incubated in standard medium and analyzed by SDS-Page and Western Blot, as described in Material and methods section. Assays performed four times gave almost identical results. The values reported in Fig. 15B are expressed as percentage.

In Fig. 15A it is represented the result of the Western Blot conducted on the mitochondrial pellet fraction: a stronger activation of the protein in the presence of Ca^{2+} plus AGM is evidenced (lane 3, 36%), comparing with that in the presence of Ca^{2+} alone (lane 2, 24%). The addition of CsA considerably decreases the signal (lane 4, 16%). These data support the involvement of Bax in AGM action.

Possible involvement of the Voltage-Dependent Anion Channel

VDAC, besides being one of the most abundant proteins of the OM, exhibits a preponderant role in regulating metabolite fluxes across this membrane. As concerning the MOMP model, the involvement of different proteins is under study and several models demonstrate that Bax could directly interact with VDAC, resulting in pore openings formation. Moreover, VDAC alone is indispensable for ROS-induced cyt. *c* release in a MPT-independent pathway [Kumarswamy and Chandna, 2009]. Taking into account these observations, the effect of a powerful VDAC inhibitor, Ruthenium Red (RR) [Israelson *et al*., 2008], was tested, as reported in Figs. 16-17.

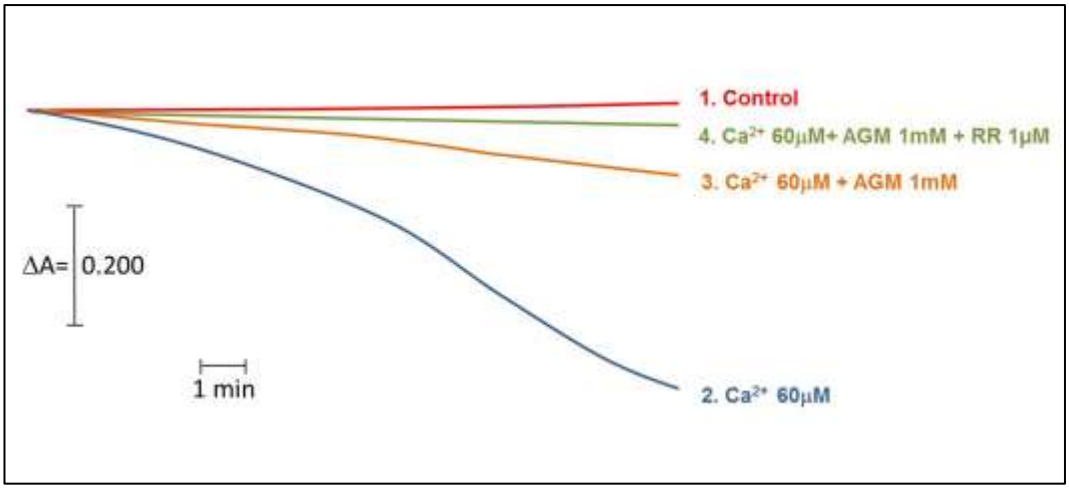

Fig. 16 Effect of agmatine and Ruthenium Red on mitochondrial swelling induced by Ca^{2+}.

RLM (1mg/ml) were incubated in standard medium, as described in Materials and methods section. When present: Ca^{2+}, AGM and RR at the concentrations indicated at side of the traces. Downward deflections indicate mitochondrial swelling. Assays performed five times gave almost identical results.

Fig. 16 shows that the swelling induced by Ca^{2+} (trace 2) is prevented by the addition of 1mM AGM (trace 3). The presence of RR (trace 4) further enhances the above mentioned inhibition.

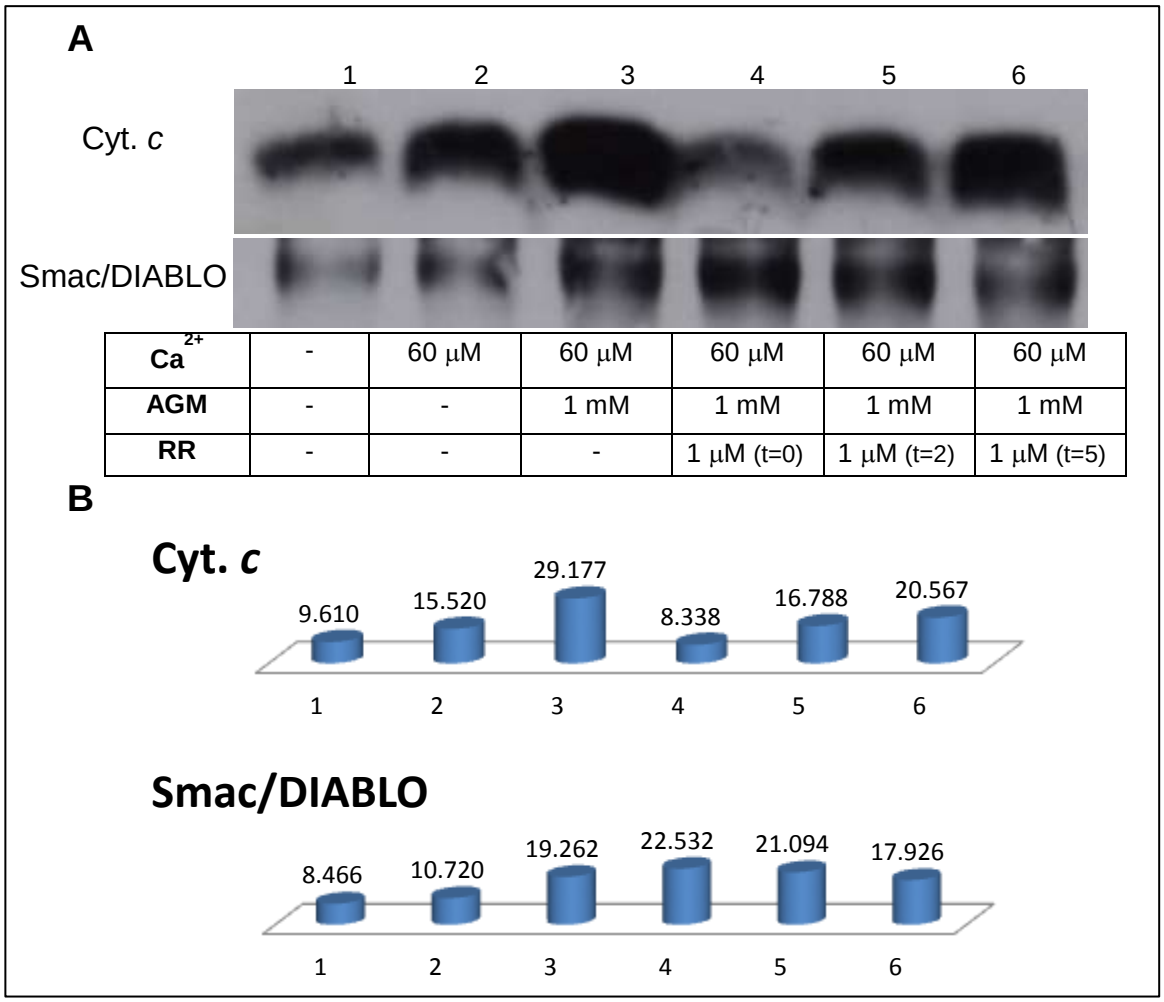

Fig. 17 Release of cytochrome c and Smac/DIABLO induced by agmatine in presence of Ca^{2+} and Ruthenium Red (A) and densitometric analysis (B).

RLM (1mg/ml) were incubated in standard medium under the same conditions as in Fig. 16 and the supernatant fraction was analyzed by SDS-Page and Western Blot, as described in Material and methods section. Ruthenium Red (RR) was added at different times: from the beginning (t=0), after 2 minutes (t=2) and after 5 minutes of incubation (t=5). Assays performed four times gave almost identical results. The values reported in Fig. 17B are expressed as percentage.

The data showed in Fig. 17A clearly evidence that the release of cyt. *c* induced by AGM (lane 3, 29%) is strongly decreased by the addition of RR from the first minute of incubation (t=0) (lane 4, 8%). The effect of RR diminishes by increasing the time of incubation: as evidenced, it is less effective after 2 minutes of incubation (lane 5,17%) and even less powerful after 5 minutes of incubation (lane 6, 21%). Smac/DIABLO release, instead, seems to be unaffected by the addition of RR at any time of incubation (lanes 4, 5 and 6, respectively 23%, 21%, and 18%) if compared to AGM alone (lane 3, 19%). As previously described, in mitochondria the presence of different pools of cyt. *c* has been detected. Given that 1mM AGM does not alter mitochondrial bioenergetics parameters, it is reasonable to think that the pool of cyt. *c* released is probably the loosly attached one, not involved in the electron transport chain. Thus, its mechanism of release will be almost immediate, as supported by our data, and for this reason RR was added at different times of incubation.

Discussion

As apparent from the preceding section, the study focused on the correlation between AGM and intrinsic apoptosis following AGM dichotomic effect on the MPT.

The importance of mitochondria in the apoptotic process, through at least three main mechanisms, is nowadays well-recognized: disruption of the electron transport chain with the consequent impairment of ATP synthesis; release of proteins able to trigger caspase activation; alteration of the cellular redox potential [Green and Reed, 1998]. In these scenarios, MPT represents a key step, whose induction alters the permeability of the organelle, allowing the release of pro-apoptotic proteins [van Gurp *et al.*, 2003].

I have presented data supporting AGM double effects on the induction of the MPT triggered by Ca^{2+} (Fig. 8), suggesting that AGM acts as a typical MPT inducer, or inhibitor, depending on the concentrations used (low concentrations, in the range of 10-100 µM, and high concentration, 1mM). The activity of an inducer or inhibitor of MPT is usually linked to the release and retention of pro-apoptotic proteins, respectively. Thus, my observation that both cyt. *c* (Fig. 9) and Smac/DIABLO (Fig. 11), but not AIF (Fig. 10) are released in the presence of Ca^{2+} and 1 mM AGM (a condition in which the MPTP is closed and mitochondrial impermeability is maintained) is unforeseen.

A possible explanation relates to the differential localization of the pro-apoptotic factors: cyt. *c* and Smac/DIABLO are intermembrane space proteins [Ott *et al.*, 2001; Maly, 2007], whereas AIF is a type I IM protein [Otera *et al*., 2005]. Thus, it is reasonable to hypothesize that AGM could trigger MOMP, a process that involves only the OM, and release only intermembrane space proteins (cyt. *c* and Smac/DIABLO), as observed. This could be related to other reports showing that several compounds, among which polyamines, exhibit a similar behavior, allowing the release of pro-apoptotic factors without MPT induction [Stefanelli *et al*., 2000; Yamada *et al*., 2009].

That observed differential release of pro-apoptotic factors by AGM, could thus occur independently of the MPT. To verify this possibility the release of pro-apoptotic proteins was further investigated in the presence of the powerful MPT inhibitor CsA (Figs. 12,13), with the expectation that, if only MOMP is involved, CsA should not inhibit the AGM-dependent release of pro-apoptotic proteins. Interestingly, while CsA enhanced the prevention of swelling exhibited by 1mM AGM (Fig. 12), it almost totally prevented also the release of cyt. *c* and Smac/DIABLO induced by AGM (Fig. 13). This latter data in clearly in disagreement with my previous hypothesis.

In front of these results, another consideration has to be taken into account: the Bcl-2 family proteins are important regulators of apoptosis and one of the pro-apoptotic members, Bax, is fundamental for MOMP induction. Moreover, the activity of this protein is inhibited by CsA, that prevents its activation and

translocation to mitochondria [Siu *et al*., 2008]. In order to shed light on AGM action, the possible involvement of Bax was then considered. Obtained data have provided evidence that Bax is present in each mitochondrial preparative and that it localizes in the pellet fraction (Fig. 14). Also its activation state was considered, given that, when inserted in the OM, a conformational change occurs, enabling Bax detection by a specific antibody. The reported results (Fig. 15) have indeed shown that a stronger activation of the protein is observable in the presence of both AGM and Ca^{2+}, which is inhibited by CsA, thus supporting Bax involvement in AGM action.

Several findings support that the interaction between Bax and VDAC results in the formation of pore openings in the OM and that the production of H_2O_2 causes the formation of channels, by interacting with membrane components and probably through the involvement of VDAC. It has also been suggested that Bax is fundamental for the release of cyt. *c* in a ROS-mediated and MPT-independent pathway [Petrosillo *et al*., 2003; Kumarswamy and Chandna, 2009]. These results acquire increasing importance in light of the observation that AGM can induce a dose-dependent production of H_2O_2 [Battaglia *et al*., 2007], probably following its oxidation by a copper-dependent amine oxidase present in matrix [Cardillo *et al*., 2009]. With this background, this work tested the involvement of VDAC to possibly disclose some mechanistic aspects of MOMP induction. The use of the VDAC inhibitor RR demonstrated that VDAC is involved in AGM-induced cyt. *c* release, whereas it is not part of the route exploited by Smac/DIABLO (Figs. 16, 17). Although studies are clearly necessary to eventually identify the components of the release pathways, the data obtained so far allow some considerations.

First of all, it is possible to hypothesize that, while preventing the MPT induced by Ca^{2+}, AGM is able to induce the release of the pro-apoptotic factors that localize in the mitochondrial intermembrane space. This action is ascribable to the selective permeabilization of the OM of mitochondria, probably through the MOMP induction, for which both the production of H_2O_2 (caused by AGM oxidation into the matrix) and Bax activation play a role.

With regard to the production of ROS, which itself seems sufficient to permeabilize mitochondrial membranes [Petrosillo *et al*., 2003], also the scavenging action of AGM has to be taken into account. Indeed, AGM at high concentrations, besides being oxidized, is also able to exhibit self-protection, as SPM, against the produced ROS. Thus, it is reasonable to hypothesize that the amount of ROS produced by the amine could be sufficient to trigger the MOMP, but not enough to open the MPTP. Moreover, H_2O_2, or other ROS derived from its metabolism, interacting with membrane components, can cause the formation of pores in the OM, probably mediated by VDAC and Bax. Cyt. *c* and Smac/DIABLO could then be released by mitochondria through these openings, without alterations of the IM. As mentioned before, cyt. *c* is one of the proteins involved in the intrinsic apoptotic pathway, being a component of the apoptosome that activate caspases and promotes cell death. However it is possible that the

release observed in these conditions, without MPT opening and thus in the absence of all the components of the intrinsic apoptotic machinery, could have a different physiological significance. Indeed, there are evidences supporting the notion that the redox state of cyt. *c* is fundamental for the apoptosome formation and the subsequent death signal cascade. Specifically, it has been reported that only oxidized cyt. *c* triggers the apoptosome [Hancock *et al*., 2001; Ripple *et al*., 2010]. Thus, by considering that, even if cyt. *c* is released from mitochondria in a oxidized state, it can be rapidly reduced by other factors, such as glutathione, the possibility exists that cyt. *c* does not trigger apoptosis under these conditions.

Part II

Analyzing agmatine action by using its analog α-methyl-agmatine

ROS production by agmatine

Battaglia and collaborators [2007] have demonstrated that AGM induces an oxidative stress in RLM, by producing H_2O_2 in a dose-dependent manner. This process is probably due to the oxidation of AGM by an amine oxidase whose activity was discovered in RLM [Cardillo *et al*., 2009]. To explain the inhibition of MPT exhibited by 1mM AGM –despite the huge amount of H_2O_2 produced under these conditions– it has been claimed that AGM at high concentrations exhibits antioxidant properties because the amount of AGM not yet oxidized, act as a ROS scavenger. This process thus results in a self-protecting event against the same ROS that AGM itself produces.

α-methyl-agmatine

The second part of the thesis, that is now presented, has focused on the AGM analog, α-methyl-agmatine (αMeAGM), (kindly provided by Professor Khomutov, Engelhardt Institute, Moscow, Russia).

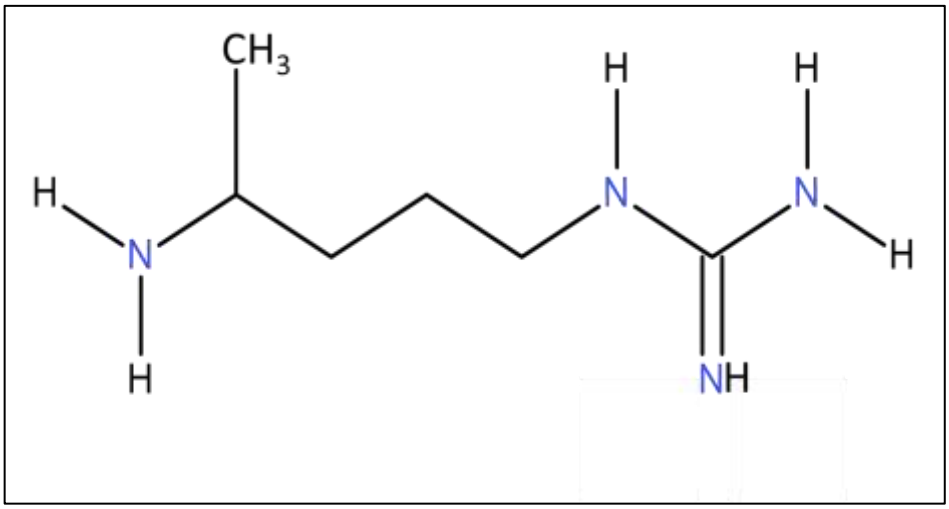

Fig. 18 α-methyl-agmatine.

This compound has been designed with the aim to have a molecule unable to be oxidized by amine oxidases, as a methyl group in α-position to amino group generally prevents oxidation [Khomutov AR, Personal Communication]. Thus, αMeAGM would be a useful tool to better examine the involvement of ROS in AGM-dependent pro-apoptotic factors release. The investigation was carried out by analyzing αMeAGM in the same experimental conditions employed for analyzing AGM behavior.

Results

α-methyl-agmatine uptake by RLM

The transport of the analog in RLM is fundamental to study its activity on the organelles. It is possible that, being structurally similar to AGM, both compounds utilize the same transporter. Thus, the aim of the following experiments is to characterize the transport of AGM in the presence of αMeAGM. It is to note that, unfortunately, it was not possible to measure the direct transport of αMeAGM, due to the unavailability of the radio-labelled compound. Thus, an indirect measurement was done with [^{14}C]AGM, as shown in the following figure.

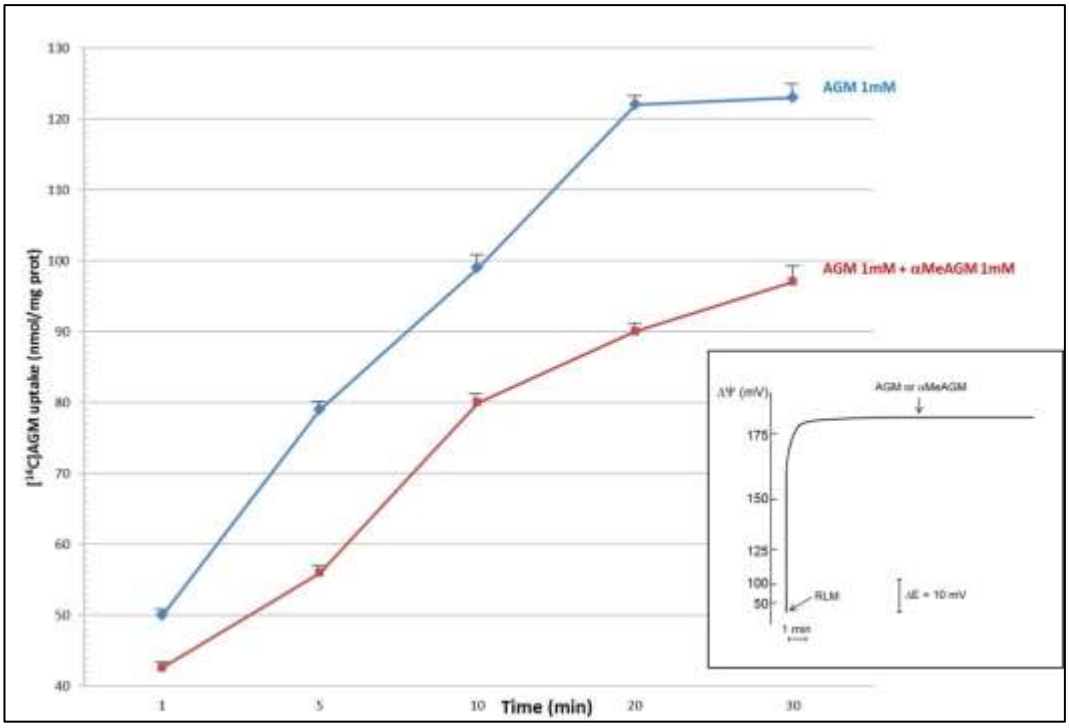

Fig. 19 Agmatine transport in presence of α-methyl-agmatine.
RLM (1mg/ml) were incubated in standard medium, as described in Materials and Methods section, with [^{14}C]AGM (50µCi/mmol). Values are the means ± SD of five experiments. Inset: effect of AGM and αMeAGM on ΔΨ.

AGM uptake by energized RLM, incubated in standard medium and measured with the radio-labeled molecule, is about 123 nmol/mg of protein after 30 minutes of incubation. In the presence of αMeAGM, a gradual inhibition of AGM transport is observable, (with a decreased transport of about 33 and 26 nmol/mg of protein at 20 and 30 minutes, respectively). These data support the hypothesis that the amine and its analog use the same transporter. Considering that AGM transport is electrophoretic, it is also to emphasize that both AGM and αMeAGM do not affect ΔΨ, as shown in the inset of Fig.19.

AGM uptake by energized RLM during the first 5 minutes of incubation is linear with time at all the concentrations tested (an example is given in the inset of Fig. 20). This linear trend allows to extrapolate, as previously reported [Dalla Via *et al*., 1996], the different aliquots of AGM that bind to mitochondrial membranes at zero-time, represented in Fig. 20.

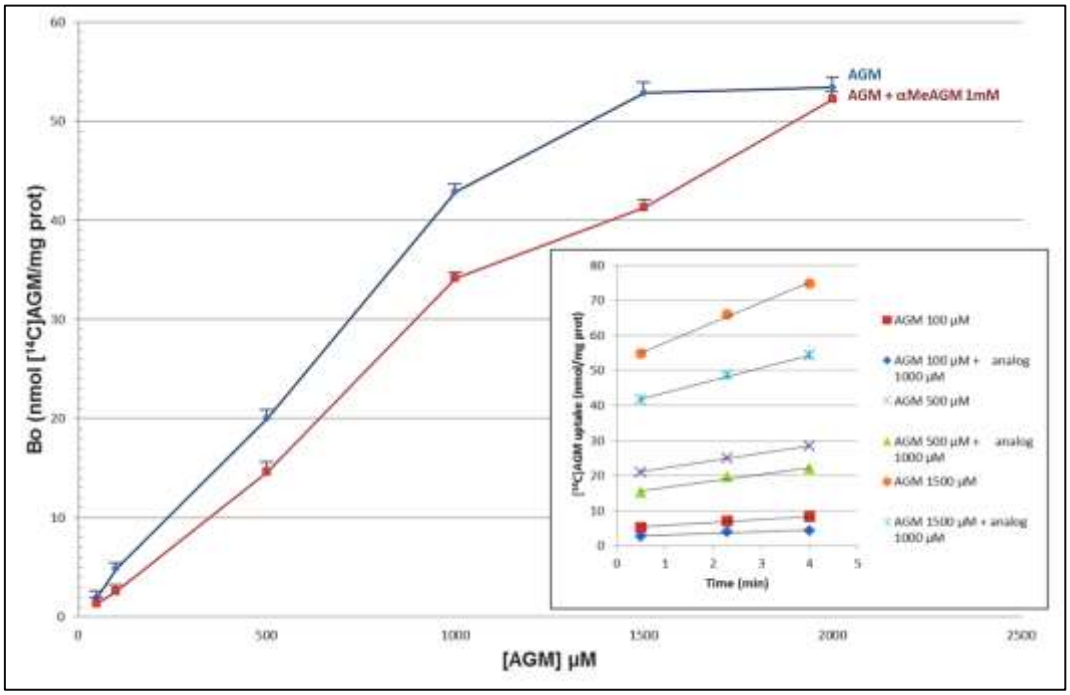

Fig. 20 Concentration-dependent agmatine binding in presence of α-methyl-agmatine.

RLM (1mg/ml) were incubated for 5 minutes in standard medium, as described in Materials and methods section, with different [^{14}C]AGM concentrations in the range of 50-2000 µM (50µCi/mmol). AGM bound at zero-time (B_o) has been plotted as a function of the exogenous AGM concentration [AGM]. Values are the means ± SD of five experiments. Inset: concentration-dependent SPM uptake by RLM.

In Fig. 20 it is shown that the aliquots of AGM bound at zero-time (B_0) decrease in the presence of the analog, in particular when AGM concentration is in the range between 100-1500 µM.

These parameters allow to apply the thermodynamic treatment of ligand-receptor interactions [Di Noto *et al.*, 1996]. Some preliminary and qualitative information about the type of process examined are reported in Table 3.

	B_{max} (nmol/mg prot)	B_{max1} (nmol/mg prot)	B_{max2} (nmol/mg prot)	$K_{1,1}$ (mg prot/nmol)	$K_{2,1}$ (mg prot/nmol)	β_1 (mg prot/nmol)
AGM	120.22(4)	0.047(2)	120.17(2)	$4.9(1)x10^{-2}$	$4.15(3)x10^{-4}$	93(4)
AGM + αMeAGM	120(1)	0.01(3)	119.99(4)	$2.0(1)x10^{-2}$	$3.70(5)x10^{-4}$	200(3)

Table 3. Agmatine binding parameters determined by curve fittings of Eqs. 10 and 11 reported in the Materials and methods section.

1mM αMeAGM was present in the medium.

(a) Standard deviations in the least significant digits are given in parentheses and were determined by the propagation formula on the basis of experimental and fitting error analyses.

In Table 3 the binding parameters of AGM in the absence or in the presence of the analog are reported. This analysis confirms the presence of two binding sites for AGM on mitochondrial membranes, observation in agreement with previously published data [Martinis *et al.*, 2012]. With regard to AGM alone, the total binding concentration is 120.22 nmol/mg of protein distributed between two sites (S_1 and S_2), in the percentages of 0.04 and 99.96, respectively, as demonstrated by the maximum amount of AGM bound to S_1 (B_{max1} = 0.047 nmol/mg of protein) and to S_2 (B_{max2} = 120.17 nmol/mg of protein). The association constants $K_{1,1}$ and $K_{2,1}$ of S_1 and S_2 sites, respectively, demonstrate that S_1 has a higher affinity than S_2. β_1 describes the possible influence of the parallel filling of S_2 on that of S_1 site. This parameter results to be very high, indicating that AGM binding on S_2 can influence its binding on S_1. The presence of αMeAGM causes a decrease of AGM binding on S_1 of about 79% (as B_{max1} in the presence of αMeAGM is 0.01 nmol/mg of protein with respect to 0.047 nmol/mg of protein with AGM alone). This inhibiting effect exerted by the analog on AGM binding is not present on the second site S_2: the total binding site concentration (B_{max}), and the one referring to the second site (B_{max2}), are almost identical and S_2 influence on S_1 is enhanced. Moreover the association constants are both decreased in the presence of αMeAGM and, in particular, the strongest effect is observable on $K_{1,1}$.

Production of hydrogen peroxide by α-methyl-agmatine

H_20_2 production by AGM has already been tested, as previously described, showing the capacity of the amine to produce a dose-dependent amount of this ROS [Battaglia *et al*., 2007]. A comparison between AGM and αMeAGM production of H_20_2 is shown in Fig. 21.

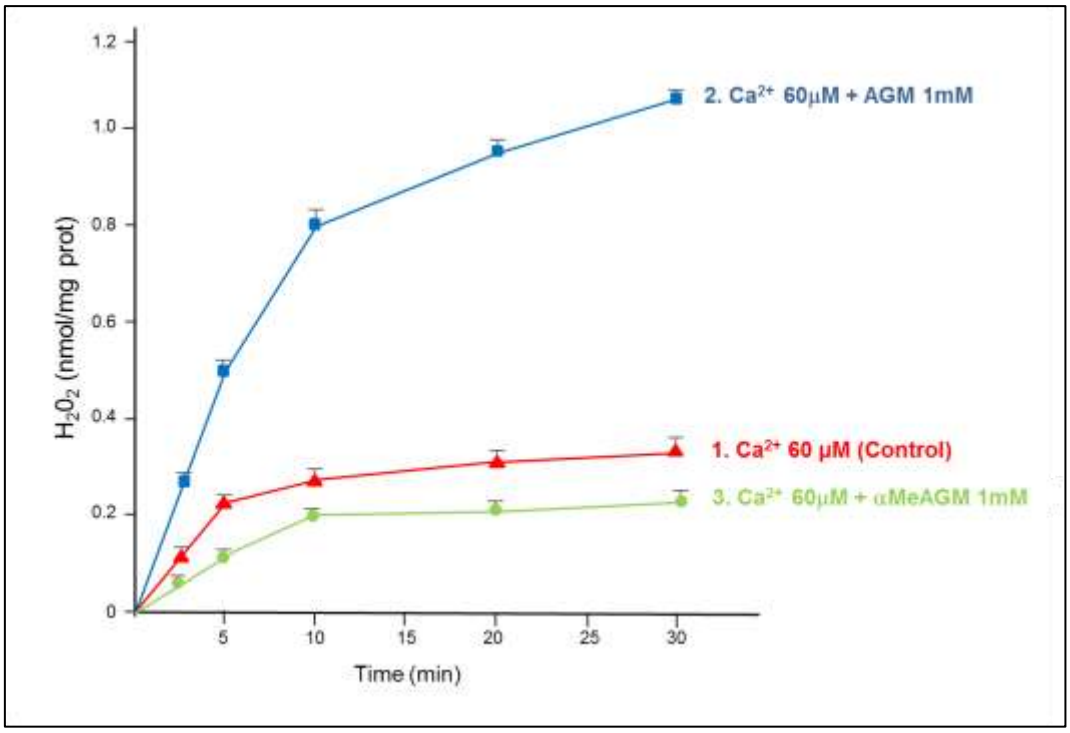

Fig. 21 Effect of αMeAGM on H_20_2 production.
RLM (0.5 mg/ml) were incubated in standard medium, as described in Materials and methods section. When present: Ca^{2+}, AGM and αMeAGM at the concentrations indicated at side of the traces. Values are the means ± SD of five experiments.

AGM, in the presence of Ca^{2+}, is able to produce about 1 nmol H_20_2/mg of protein (trace 2) if compared to Ca^{2+} alone (trace 1, about 0.3 nmol/mg of protein). In the same experimental conditions the presence of αMeAGM (trace 3) is comparable to the control trace, suggesting that the analog is not able to produce significant amounts of H_20_2. The same output was obtained also in the absence of Ca^{2+} (data not shown).

Effect of α-methyl-agmatine on pro-apoptotic factors release

The investigation on the behavior of αMeAGM, in order to compare its activity to AGM action, leads to the evaluation of its effect on the MPT, monitoring mitochondrial swelling.

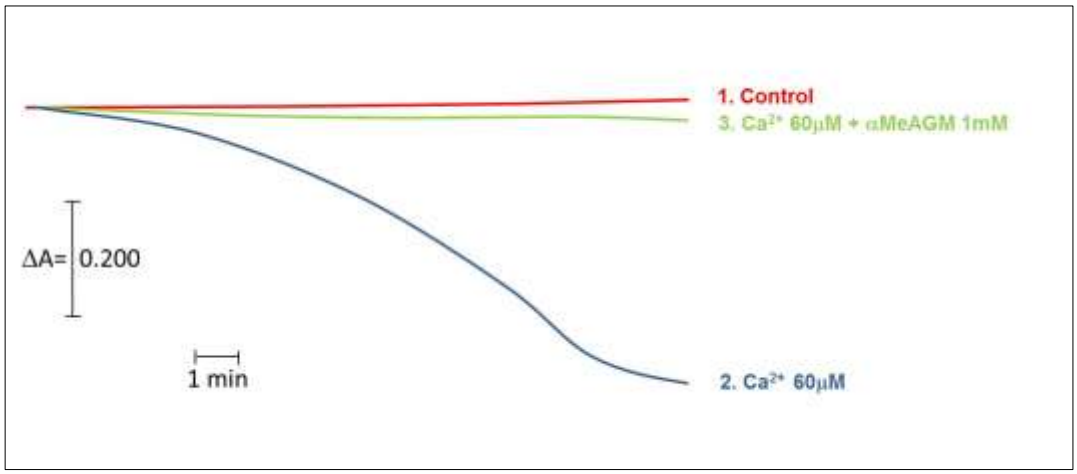

Fig. 22 Effect of αMeAGM on mitochondrial swelling induced by Ca^{2+}.
RLM (1mg/ml) were incubated in standard medium, as described in Materials and methods section. When present: Ca^{2+} and αMeAGM at the concentrations indicated at side of the traces. Downward deflections indicate mitochondrial swelling. Assays performed five times gave almost identical results.

Fig. 22 shows the effect of 1mM αMeAGM on mitochondrial swelling induced by Ca^{2+}. It is clear the inhibitory effect exerted by this compound (trace 3) if compared to Ca^{2+} alone (trace 2). In addition, the analog, at the concentration of 1mM, shows a stronger effect if compared to 1mM AGM (Fig. 8, previous section), being able to fully protect mitochondria against the MPT induced by Ca^{2+}. Thus the release of pro-apoptotic factors was analyzed, as shown in Fig. 23.

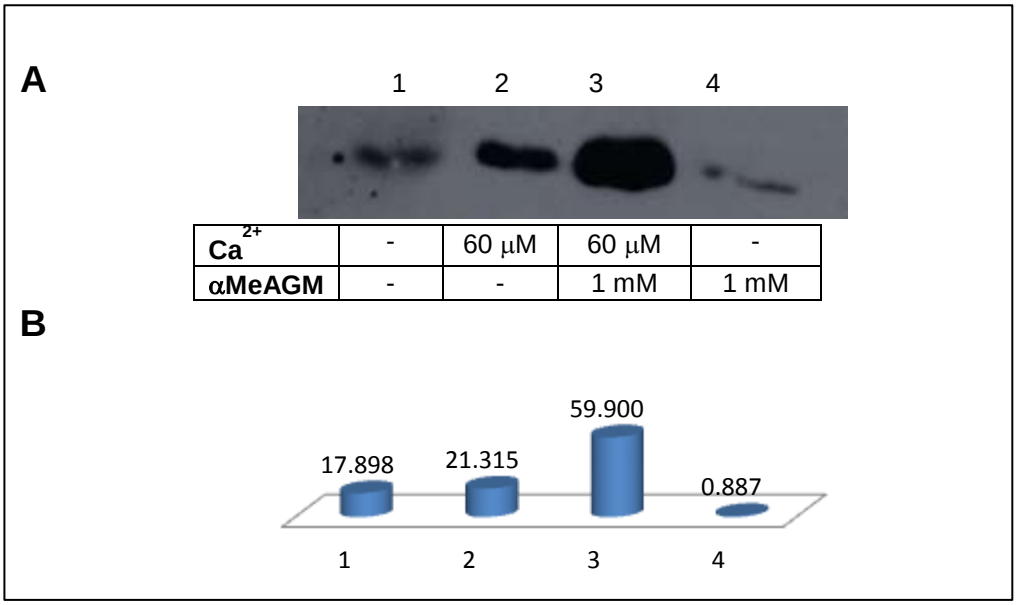

Fig. 23 Release of cytochrome c induced by αMeAGM in presence of Ca^{2+} (A) and densitometric analysis (B). RLM (1mg/ml) were incubated in standard medium under the same conditions as in Fig. 22 and the supernatant fraction was analyzed by SDS-Page and Western Blot, as described in Material and methods section. Assays performed four times gave almost identical results. The values reported in Fig. 23B are expressed as percentage.

αMeAMG shows a strong effect in inducing the release of cyt. *c* (lane 3, 60%), as shown in Fig. 23A, especially if compared to Ca^{2+} alone (lane 2, 21%). αMeAMG alone does not show any effect (lane 4, 0.9%).

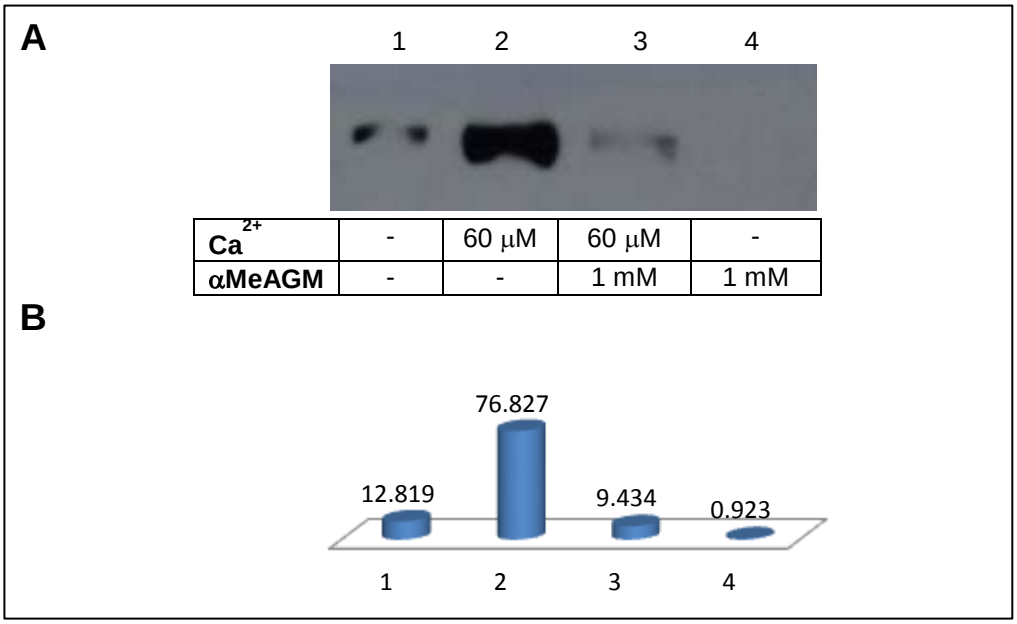

Fig. 24 Release of AIF induced by αMeAGM in presence of Ca^{2+} (A) and densitometric analysis (B). RLM (1mg/ml) were incubated in standard medium under the same conditions as in Fig. 22 and the supernatant fraction was analyzed by SDS-Page and Western Blot, as described in Material and methods section. Assays performed four times gave almost identical results. The values reported in Fig. 24B are expressed as percentage.

As previously observed for agmatine activity (Fig. 10, previous section), the release of AIF shown in Fig. 24A is observable only in the presence of Ca^{2+} (lane 2, 77%) whereas the effect of the analog, in the presence of Ca^{2+} (lane 3, 9%) is comparable with the control lane (lane 1, 13%). αMeAMG alone does not show any effect (lane 4, 0.9%).

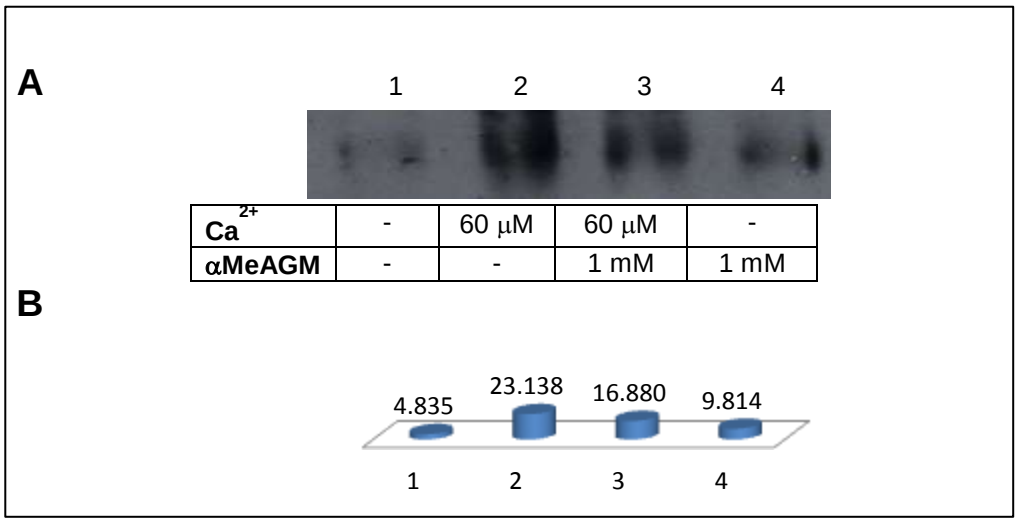

Fig. 25 Release of Smac/DIABLO induced by αMeAGM in presence of Ca^{2+} (A) and densitometric analysis (B). RLM (1mg/ml) were incubated in standard medium under the same conditions as in Fig. 22 and the supernatant fraction was analyzed by SDS-Page and Western Blot, as described in Material and methods section. Assays performed four times gave almost identical results. The values reported in Fig. 25B are expressed as percentage.

It has to be clarified, before the description of this experiment, that the release of Smac/DIABLO in presence of the analog shows two different trends. The one described by this picture (Fig. 25A), shows that the release of Smac/DIABLO by Ca^{2+} (lane 2, 23%) is slightly decreased by αMeAMG (lane 3, 17%). However, it is to take into account that the analog alone (lane 4, 10%) induces Smac/DIABLO efflux, if compared to the control line (trace 1, 5%). In several other experiments, instead, the presence of both Ca^{2+} and αMeAMG exhibit a synergic effect in inducing its release, if compared to Ca^{2+} alone, (an example is given at page 59). One possible explanation could be that the presence of the compound, besides inhibiting Ca^{2+} action (which is also supported by the swelling experiments), acts itself in inducing the pro-apoptotic factors release. Thus, the outputs obtained by Western Blot analyses are the result of both the inhibiting effect on Ca^{2+} action and the stimulating activity on pro-apoptotic factors release.

MPT-independence

As previously shown for the study of AGM behavior, the MPT-inhibitor CsA was tested to assess the MPT-independence of the differential release of pro-apoptotic factors observed in the presence of αMeAGM.

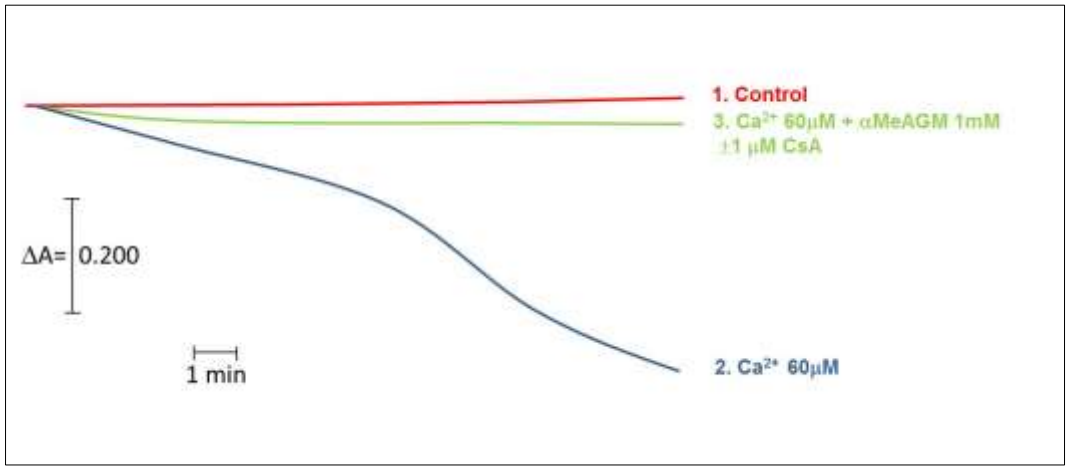

Fig. 26 Effect of αMeAGM and cyclosporin A on mitochondrial swelling induced by Ca^{2+}.
RLM (1mg/ml) were incubated in standard medium, as described in Materials and methods section. When present: Ca^{2+}, αMeAGM and CsA at the concentrations indicated at side of the traces. Downward deflections indicate mitochondrial swelling. Assays performed five times gave almost identical results.

Fig. 26 shows that, as expectable, CsA does not have any effect on αMeAGM prevention of swelling, as αMeAGM alone (trace 3) is able to fully prevent the effect of Ca^{2+} (trace 2).

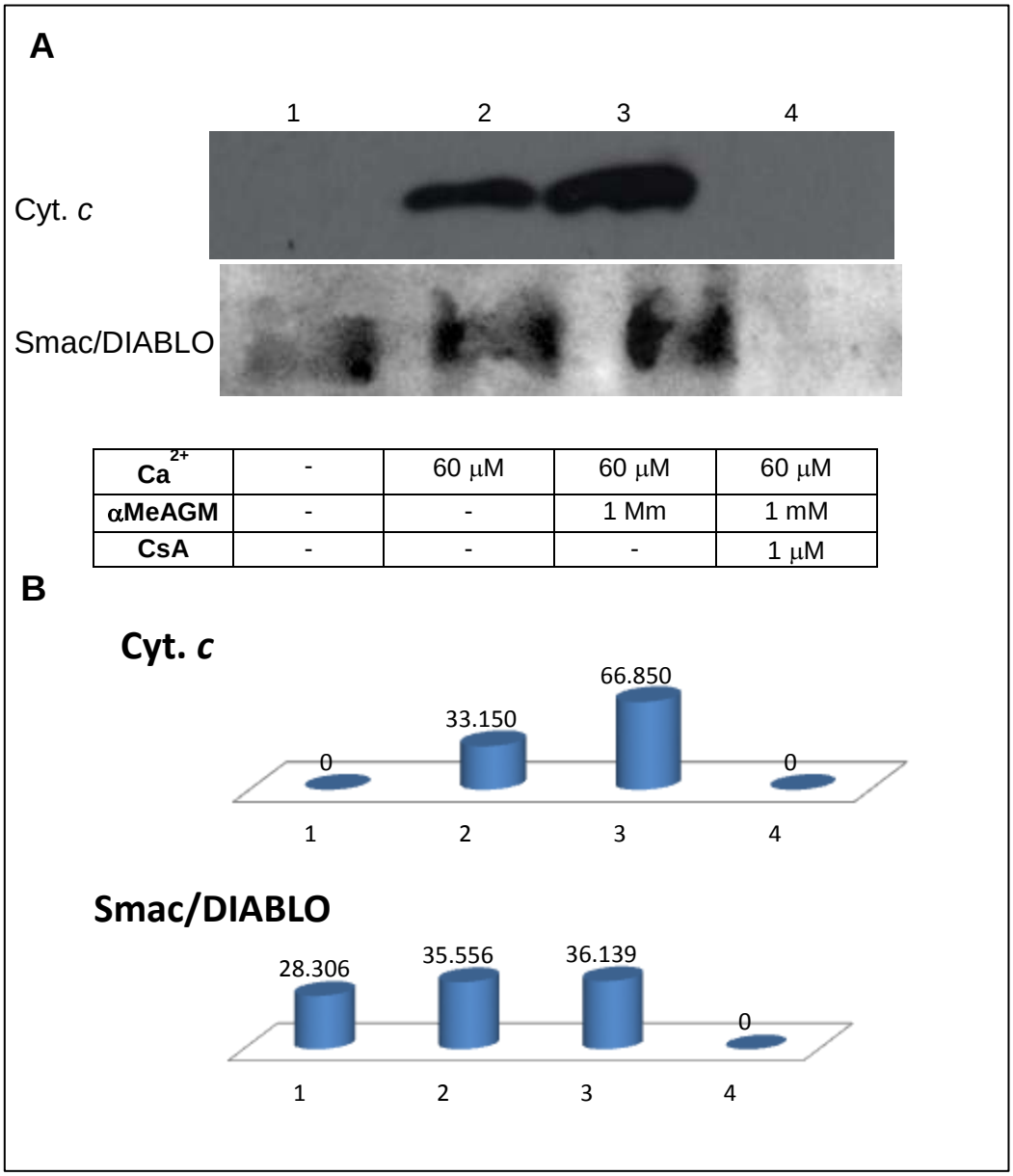

Fig. 27 Release of cytochrome c and Smac/DIABLO induced by αMeAGM in presence of Ca^{2+} and cyclosporin A (A) and densitometric analysis (B).

RLM (1mg/ml) were incubated in standard medium in the same conditions as in Fig. 26 and the supernatant fraction was analyzed by SDS-Page and Western Blot, as described in Material and methods section. Assays performed four times gave almost identical results. The values reported in Fig. 27B are expressed as percentage.

Fig. 27A shows the Western Blot conducted on the mitochondrial supernatant fractions, from samples obtained at the end of the incubations shown in Fig. 26. Concerning cyt. *c*, the addition of CsA totally prevents its release (lane 4, 0%) comparing to the effect of αMeAGM plus Ca^{2+} (lane 3, 67%). As previously observed, Ca^{2+} is able to release the protein (lane 2, 33%) with respect to control (lane 1, 0%). A similar behavior of CsA is evidenced also for the release of Smac/DIABLO, that is prevented (lane 4, 0%) if compared to the effect shown by αMeAGM plus Ca^{2+} (lane 3, 36%). These results demonstrated that αMeAGM and its analog share the same behavior on the release of pro-apoptotic factors.

Possible involvement of the Voltage-Dependent Anion Channel

The involvement of VDAC was also tested, by the use of its inhibitor RR, as described in the precedent section.

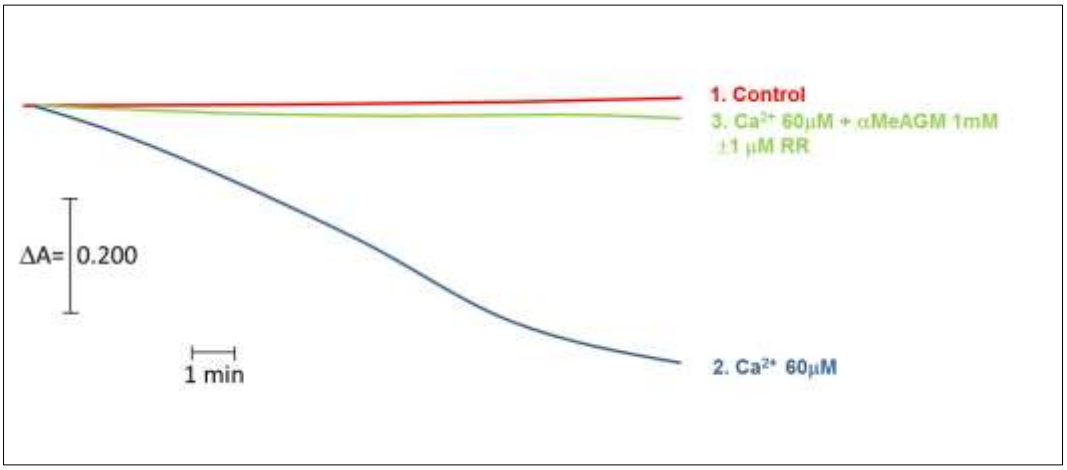

Fig. 28 Effect of αMeAGM and Ruthenium Red on mitochondrial swelling induced by Ca^{2+}.

RLM (1mg/ml) were incubated in standard medium, as described in Materials and methods section. When present: Ca^{2+}, αMeAGM and RR at the concentrations indicated at side of the traces. Downward deflections indicate mitochondrial swelling. Assays performed five times gave almost identical results.

Fig. 28 shows that, as expectable, RR does not have any effect on αMeAGM prevention of swelling, as αMeAGM alone (trace 3) is able to fully prevent the effect of Ca^{2+} (trace 2).

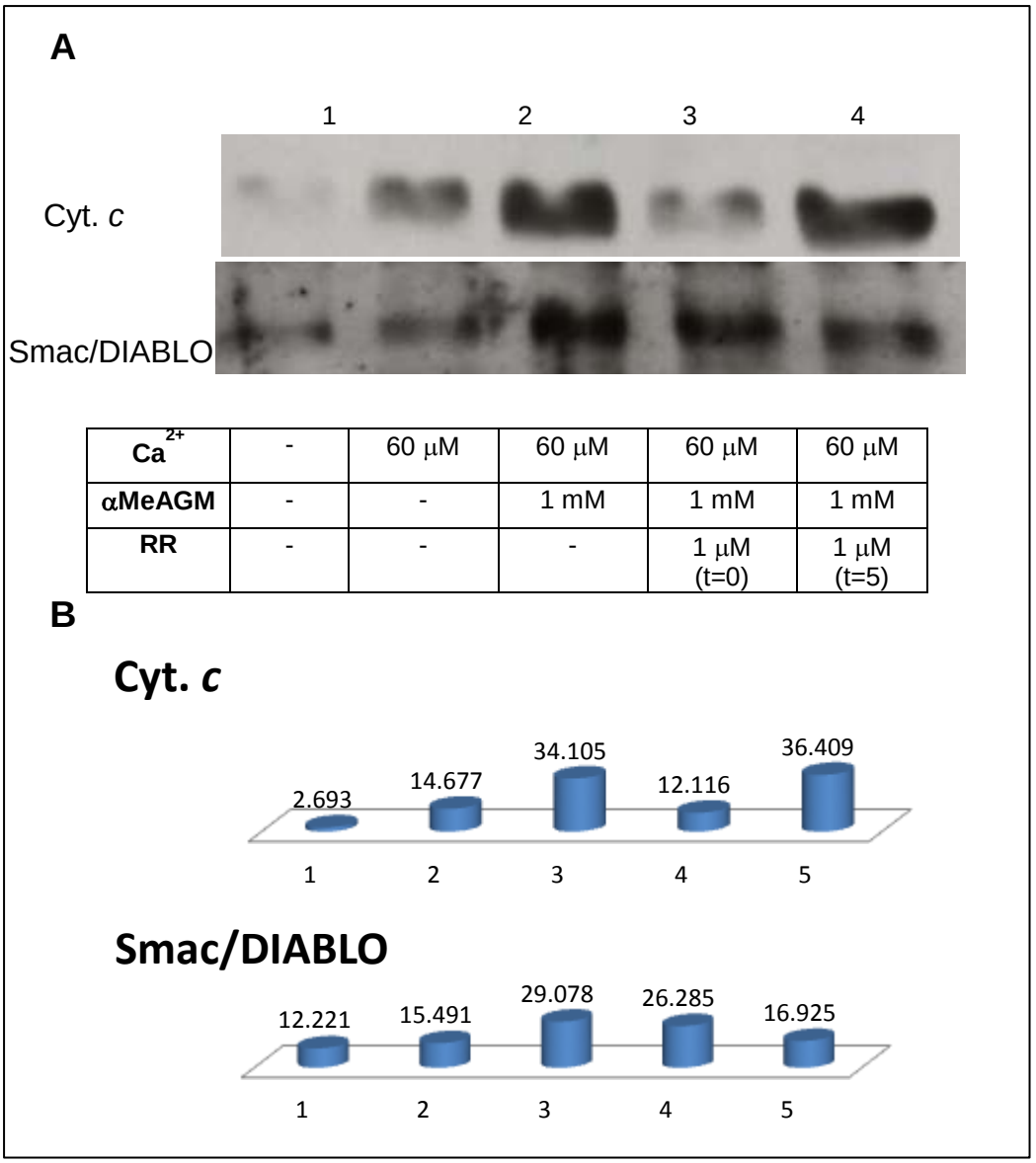

Ca^{2+}	-	60 μM	60 μM	60 μM	60 μM
αMeAGM	-	-	1 mM	1 mM	1 mM
RR	-	-	-	1 μM (t=0)	1 μM (t=5)

Fig. 29 Release of cytochrome c and Smac/DIABLO induced by αMeAGM in presence of Ca^{2+} and Ruthenium Red (A) and densitometric analysis (B).

RLM (1mg/ml) were incubated in standard medium in the same conditions as in Fig. 28 and the supernatant fraction was analyzed by SDS-Page and Western Blot, as described in Material and methods section. Ruthenium Red (RR) was added at different times: from the beginning (t=0) and after 5 minutes of incubation (t=5). Assays performed four times gave almost identical results. The values reported in Fig. 29B are expressed as percentage.

The data showed in Fig. 29A evidence a strong inhibition of RR, when added from the first minute of incubation (t=0) on the release of cyt. *c* (lane 4, 12%), if compared to the release of the protein induced by αMeAGM (lane 3, 34%). RR is less effective if added after 5 minutes of incubation (t=5), as evidenced by the output of lane 4, 36%. With regard to Smac/DIABLO release, RR seems to be ineffective if added from the first minute of incubation (lane 4 26%, if compared to αMeAGM-induced release (lane 3, 29%). A slight decrease is observable if RR is added after 5 minutes of incubation (lane 5, 17%).

Discussion

As presented, the investigation on the effects of AGM on the permeabilization of the OM was carried out by comparing the effects of αMeAGM, an AGM analog designed to be resistant to amine oxidases.

This approach is justified by considering that in RLM the oxidation of AGM produces H_2O_2 in a dose-dependent manner [Battaglia *et al.*, 2007], by the activity of a copper-dependent amine oxidase present in matrix [Cardillo *et al*., 2009], and that moreover H_2O_2 is one of the strongest factors responsible for MOMP induction [Petrosillo *et al.*, 2003].

The reported results suggest that both AGM and its analog share the same transport mechanism, in light of the data showing that, in the presence of αMeAGM, both AGM transport (Fig. 19) and binding (Fig. 20) are decreased. Moreover, the binding parameters of AGM alone (Table 3), fully comparable with other published data [Martinis *et al.*, 2012], confirm the presence of two binding sites (S_1 and S_2) on mitochondrial membranes for AGM. In the presence of αMeAGM, a noticeable decrease of AGM bound to S_1 is observable, whereas the amount of amine bound to S_2 remains almost unaffected. The effect of αMeAGM on S_1 resembles in part the behavior of the I_2 inhibitor idazoxan [Martinis *et al*., 2012]. Indeed, idazoxan binding to S_1 was found to decrease the amount of bound AGM (from 1.34 to 0.56 nmol/mg of protein), and also the correspondent association constant (from 4.9×10^{-2} to 2.3×10^{-2}). On the other hand, whereas idazoxan increased the maximum amount of amine bound to S_2, αMeAGM had no effect. Considering our previous hypothesis with regard to idazoxan action, whereby S_1 could act as a sensor of the amount of AGM present outside mitochondria and could thus modify the properties of S_2 transport site, it is possible to suggest that a different mechanistic action pertains to αMeAGM. Indeed, when idazoxan binds to S_1, this site detects a lower AGM concentration, and this can cause a modification of the binding and transport properties of S_2, to increase the transport of AGM. However, given the structural similarities of AGM and αMeAGM, in the presence of the analog it could also be possible that S_1 is unable to discriminate between the two compounds. αMeAGM binding to S_1 is therefore not achieved as a diminution of AGM concentration and consequently the transport properties of S_2 are not modified. Although the characterization of the transport mechanism of the analog is not yet fully clarified, these data support the contention that the internalization of both compounds into the mitochondrial matrix, occurs exploiting the same transporter, possibility that is of value for the study of αMeAGM effects on mitochondria.

Presented data have clearly underlined that αMeAGM binding to mitochondrial membranes, and its subsequent internalization, does not result in ROS production, because αMeAGM production of H_2O_2 is negligible compared to the amounts produced in the presence of AGM (Fig. 21). This observation sets a difference between the behavior of these two compounds. However, αMeAGM activity on the permeabilization of mitochondrial membranes closely resembles

AGM behavior, in light of the capacity of the analog to fully prevent Ca^{2+}-induced MPT (Fig. 22) and to induce the release of cyt. *c* and Smac/DIABLO (Figs. 23, 25 respectively), but not AIF (Fig 24), as was shown with AGM. Taken together, all these results seem to exclude that the production of H_2O_2 by AGM is key to its effects, thus supporting the possibility that the main mechanism driving AGM-induced permeabilization of mitochondrial membranes is through Bax activation.

The effects of CsA (Figs. 26 and 27) and of the VDAC inhibitor RR (Figs. 28 and 29) were also analyzed in the presence of αMeAGM. CsA fully prevented the release of cyt. *c* and Smac/DIABLO and RR inhibited the release of cyt. *c*, but not of Smac/DIABLO release.

Obtained data show that both molecules behaved in a similar way, probably inducing the MOMP.

Part III

Polyamines action on the permeabilization of mitochondrial membranes

Effect of polyamines on the MPT

Polyamines are related to AGM, given that both have arginine as precursor amino acid (Fig. 30). Moreover polyamine metabolism is regulated by AGM because the amine induces antizyme that leads to the inactivation of ornithine decarboxylase and the suppression of polyamine transport [Piletz *et al*., 2013].

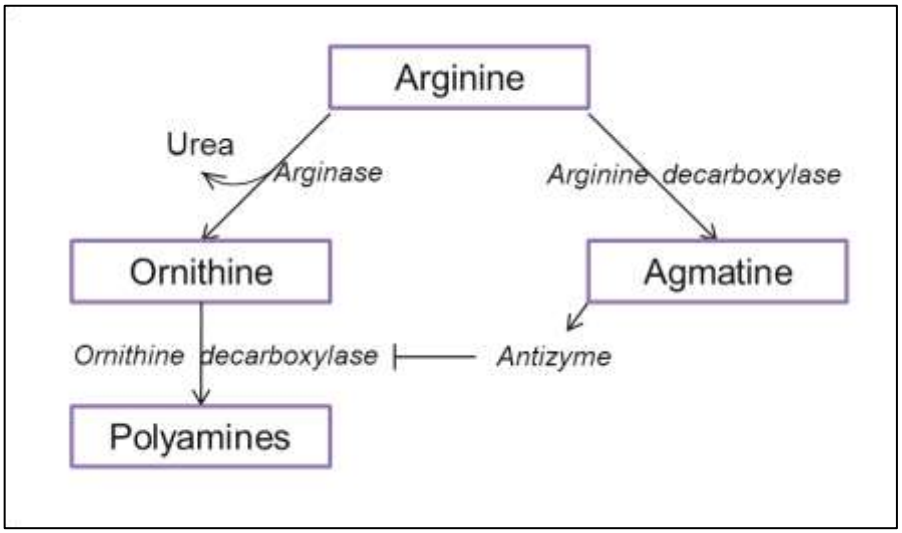

Fig. 30 Arginine is the precursor of both polyamines and agmatine biosynthesis.

In mitochondria, polyamines exhibit a protective effect against the MPT [Tassani *et al*., 1995], similar to that observed with 1 mM AGM [Battaglia *et al*., 2007]. The aim of the following study was thus to evaluate polyamine action on the release of pro-apoptotic factors and to make a comparison with the effects of AGM.

Results

Effect of polyamines on pro-apoptotic factors release

The evaluation of the effect of polyamines on the MPT is carried out by monitoring mitochondrial swelling.

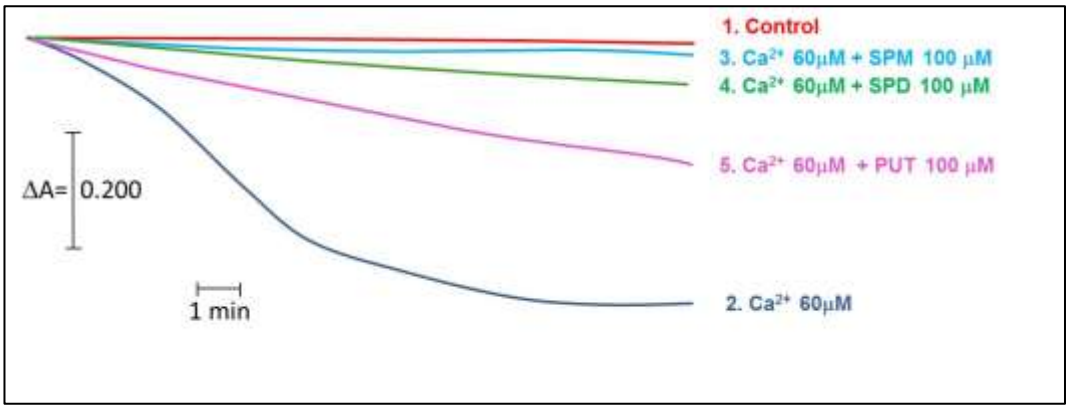

Fig. 31 Effect of polyamines on mitochondrial swelling induced by Ca^{2+}.
RLM (1mg/ml) were incubated in standard medium, as described in Materials and methods section. When present: Ca^{2+}, SPM, SPD, PUT and Mg^{2+} at the concentrations indicated at side of the traces. Downward deflections indicate mitochondrial swelling. Assays performed five times gave almost identical results.

The swelling experiment showed in Fig. 31 clearly demonstrates that all the polyamines (traces 3, 4 and 5) are able to prevent the effect exhibited by Ca^{2+} (trace 2). SPM demonstrates the most powerful action (trace 3) if compared to SPD (trace 4), and PUT (trace 5), which is the less effective. Thus the following experiments were made with the aim of investigate the release of pro-apoptotic factors, in the presence of all the polyamines.

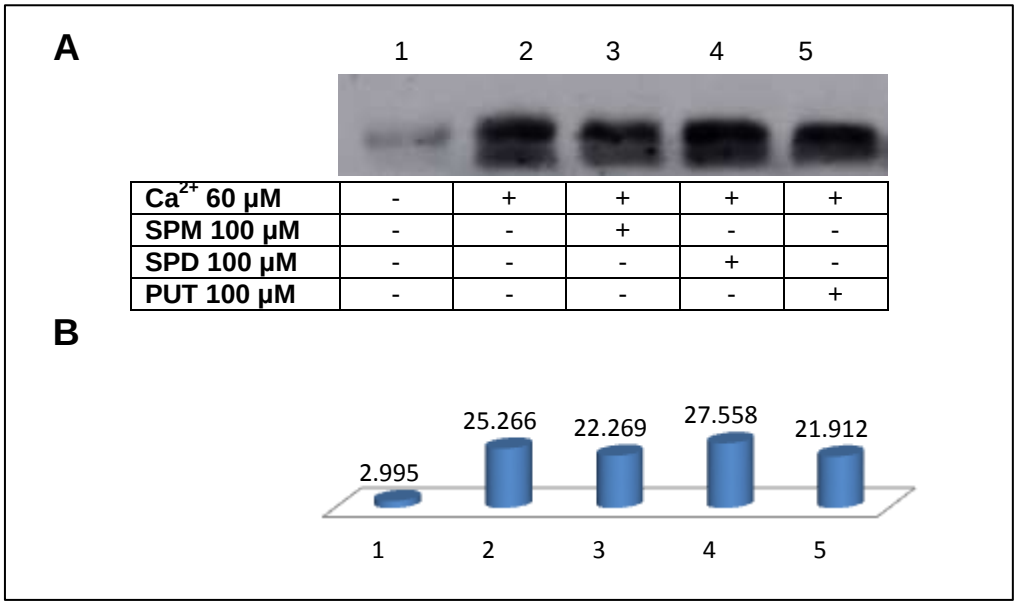

Fig. 32 Release of cytochrome c induced by polyamines in presence of Ca^{2+} (A) and densitometric analysis (B). RLM (1mg/ml) were incubated in standard medium in the same conditions as in Fig. 31 and the supernatant fraction was analyzed by SDS-Page and Western Blot, as described in Material and methods section. Assays performed four times gave almost identical results. The values reported in Fig. 32B are expressed as percentage.

Fig. 32A shows the Western Blot analyses conducted on the mitochondrial supernatant fraction. First of all, it clearly shows that Ca^{2+} alone (lane 2) or in the presence of polyamines (lanes 3, 4, 5), is able to release cyt. *c*, if compared to the control (lane 1). However, it is to underline that none of the polyamines show a synergic effect with Ca^{2+} (observed, instead, with AGM, Results presented in Part I, Figs. 9, 11). Indeed SPM-, SPD-, and PUT-induced release (lanes 3, 22%; 4, 28% and 5, 22%) does not differ considerably from Ca^{2+} one (trace 2, 25%). This can be explained by considering the inhibiting effect shown by these compounds on Ca^{2+} action (which is also supported by the swelling experiments). Thus, the outputs obtained are the result of both the inhibiting effect on Ca^{2+} action and the stimulating activity on pro-apoptotic factors release exhibited by polyamines. Probably the release observed is due only to the action of polyamines, rather than a sum of their action and Ca^{2+} effect. Very preliminary data support this hypothesis, showing that the polyamines alone, in particular SPM, are able to release some pro-apoptotic factors in the absence of Ca^{2+} (an example is given in the following figure).

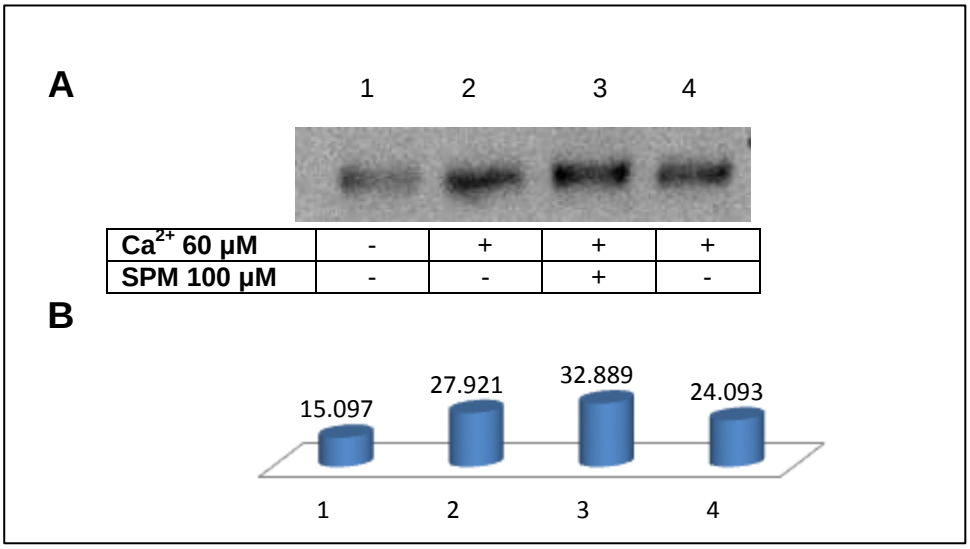

Fig. 33 Release of cytochrome c induced by spermine in presence of Ca^{2+} (A) and densitometric analysis (B). RLM (1mg/ml) were incubated in standard medium and analyzed by SDS-Page and Western Blot, as described in Material and methods section. Preliminary data. The values reported in Fig. 33B are expressed as percentage.

The preliminary experiment presented in Fig. 33 shows the induced release of cyt. *c* in the presence of Ca^{2+} alone (lane 2, 28%) or with SPM (lane 3, 33%). The presence of SPM alone causes a noticeable release (lane 4, 24%).

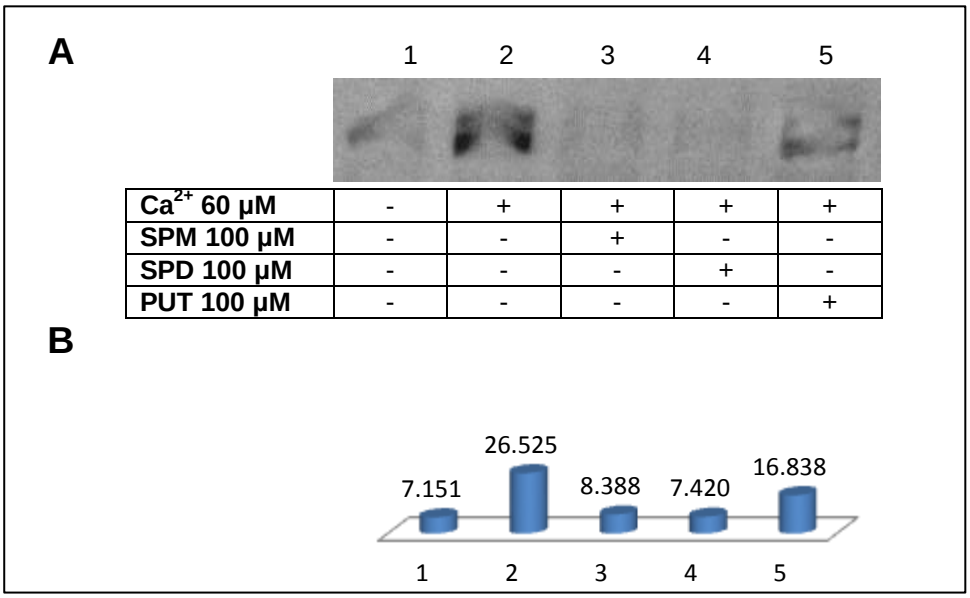

Fig. 34 Release of AIF induced by polyamines in presence of Ca^{2+} (A) and densitometric analysis (B). RLM (1mg/ml) were incubated in standard medium under the same conditions as in Fig. 31 and analyzed by SDS-Page and Western Blot, as described in Material and methods section. Assays performed four times gave almost identical results. The values reported in Fig. 34B are expressed as percentage.

A strong release of AIF, shown in Fig. 34A, is observable only in the presence of Ca^{2+} (lane 2, 27%), whereas both SPM and SPD lanes in the presence of Ca^{2+} (lanes 3, 8% and 4, 7%) are comparable with the control lane (lane 1, 7%). A slight release is observable with PUT (lane 5, 17%) and it can be explained by considering that this polyamine is not able to fully prevent the MPT (Fig. 31).

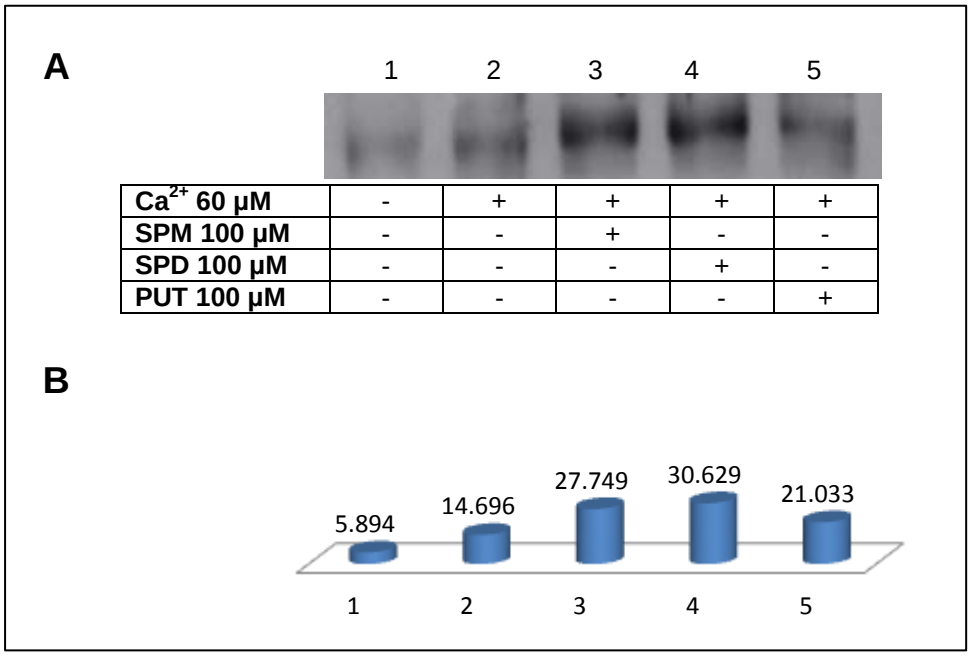

Fig. 35 Release of Smac/DIABLO induced by polyamines in presence of Ca^{2+} (A) and densitometric analysis (B). RLM (1mg/ml) were incubated in standard medium in the same conditions as in Fig. 31 and the supernatant fraction was analyzed by SDS-Page and Western Blot, as described in Material and methods section. Assays performed four times gave almost identical results. The values reported in Fig. 35B are expressed as percentage.

The release of Smac/DIABLO presented in Fig. 35A evidences that Ca^{2+} effect (lane 2, 15%) is increased by SPM (lane 3, 28%), SPD (lane 4, 31%) and PUT (lane 5, 21%).

MPT-independence

As showed in the previous sections, to assess that the differential release of pro-apoptotic factors is independent from MPT, the MPT inhibitor CsA was tested. By taking into account that the interpretations of the results of PUT could be compromised by its not complete prevention against the MPT, only SPM and SPD were considered.

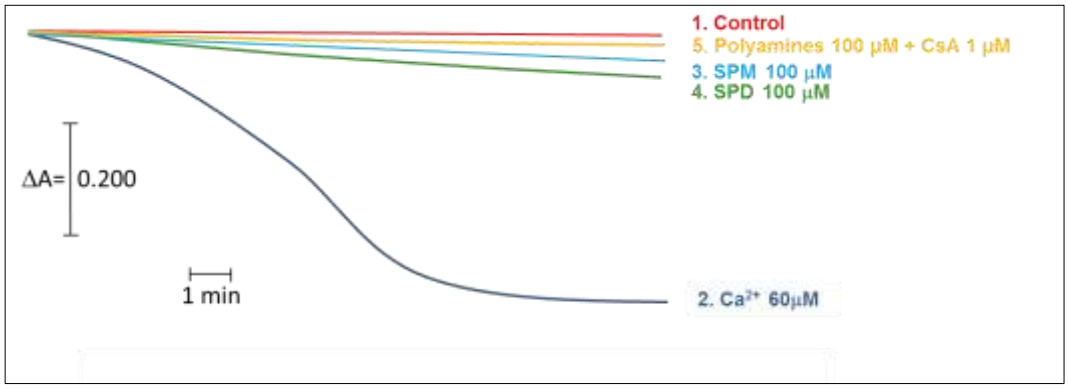

Fig. 36 Effect of spermine, spermidine and cyclosporin A on mitochondrial swelling induced by Ca^{2+}.

RLM (1mg/ml) were incubated in standard medium, as described in Materials and methods section. When present: Ca^{2+}, SPM, SPD and CsA at the concentrations indicated at side of the traces. Downward deflections indicate mitochondrial swelling. Assays performed five times gave almost identical results.

Fig. 36 shows that, as expectable, CsA (trace 5) does not have any effect on SPM (trace 3) and SPD (trace 4) prevention of swelling, as these compounds alone are already able to fully prevent the effect of Ca^{2+} (trace 2).

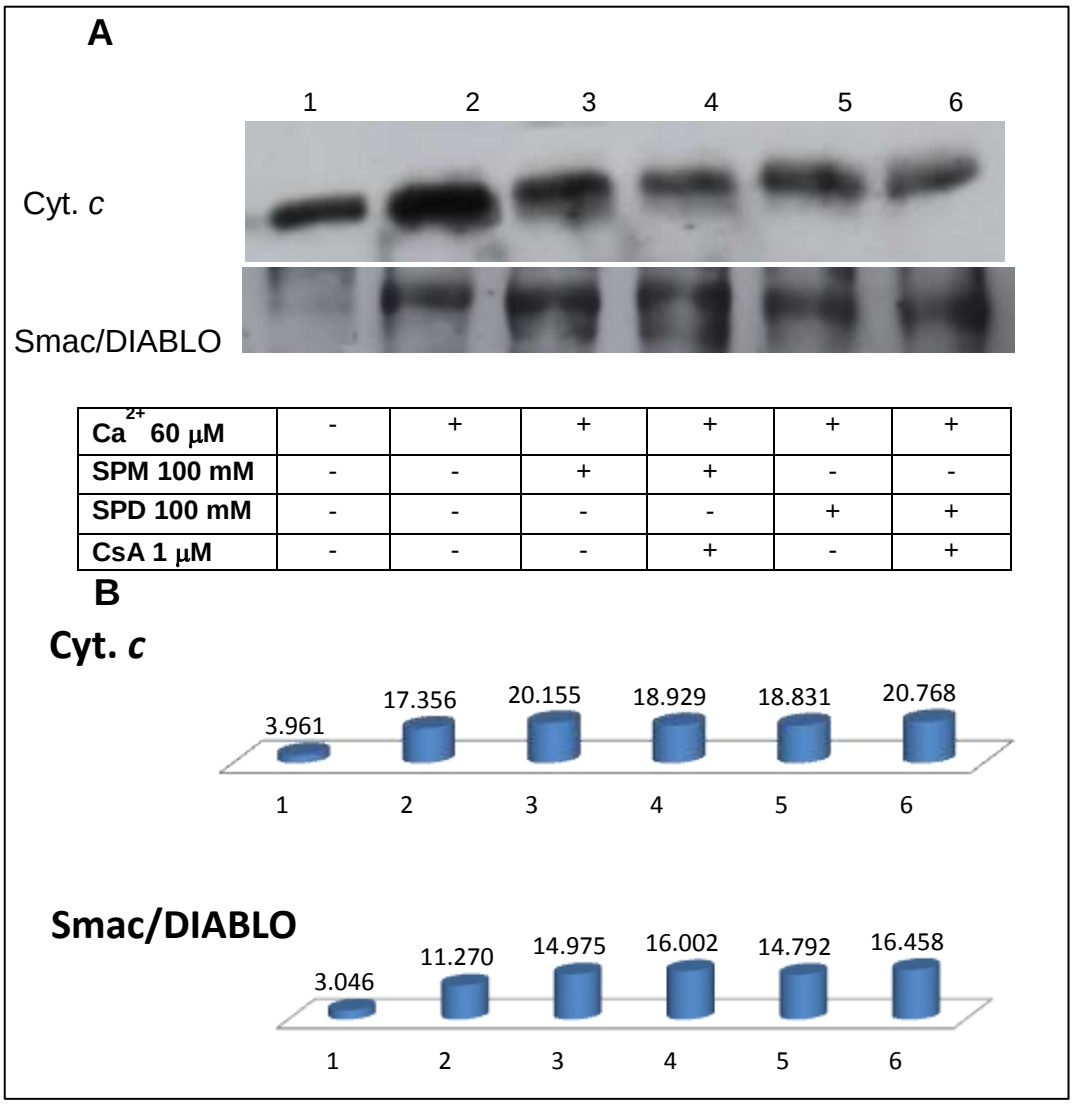

Ca^{2+} 60 μM	-	+	+	+	+	+
SPM 100 mM	-	-	+	+	-	-
SPD 100 mM	-	-	-	-	+	+
CsA 1 μM	-	-	-	+	-	+

Fig. 37 Release of cytochrome c and Smac/DIABLO induced by spermine and spermidine in presence of Ca^{2+} and cyclosporin A (A) and densitometric analysis (B).

RLM (1mg/ml) were incubated in standard medium in the same conditions as in Fig. 36 and the supernatant fraction was analyzed by SDS-Page and Western Blot, as described in Material and methods section. Assays performed four times gave almost identical results. The values reported in Fig. 37B are expressed as percentage.

In Fig. 37A, with regard to cyt. *c* release, it is shown that the presence of Ca^{2+} induces a considerable loss of the protein from mitochondria (lane 2, 17%) if compared to the control (lane 1, 4%). The presence of both Ca^{2+} and SPM (lane 3, 20%) does not enhance considerably Ca^{2+} action (lane 2, 17%) and the addition of CsA does not prevent the release of the protein (lane 4, 19%). Moreover, SPD (lane 5, 19%) neither enhances Ca^{2+} action (lane 2, 17%) nor is inhibited by the addition of CsA (lane 6, 21%). Concerning the release of Smac/DIABLO induced by SPM (lane 3, 15%), the addition of CsA does not prevent its release (lane 4, 16%). The same output is observable also for SPD action, in which the addition of CsA (lane 6, 16%) does not alter its activity (lane 5, 15%).

Possible involvement of the Voltage-Dependent Anion Channel

In light of these different effects of polyamines, with respect to AGM, the involvement of VDAC was also tested, by the use of its inhibitor RR.

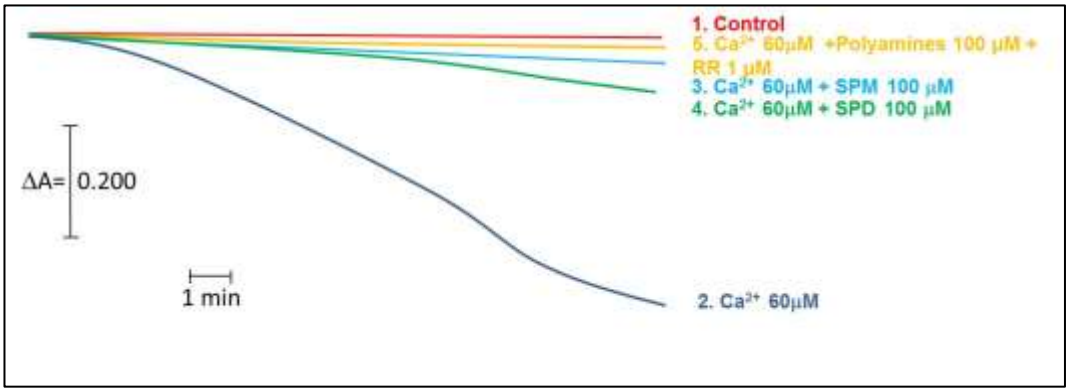

Fig. 38 Effect of polyamines and Ruthenium Red on mitochondrial swelling induced by Ca^{2+}.

RLM (1mg/ml) were incubated in standard medium, as described in Materials and methods section. When present: Ca^{2+}, SPM, SPD and RR at the concentrations indicated at side of the traces. Downward deflections indicate mitochondrial swelling. Assays performed five times gave almost identical results.

Fig. 38 shows that, as expectable, RR (trace 5) does not have evaluable effects on SPM (trace 3) and SPD (trace 4) prevention of swelling, as polyamines alone fully prevent the effect of Ca^{2+}(trace 2).

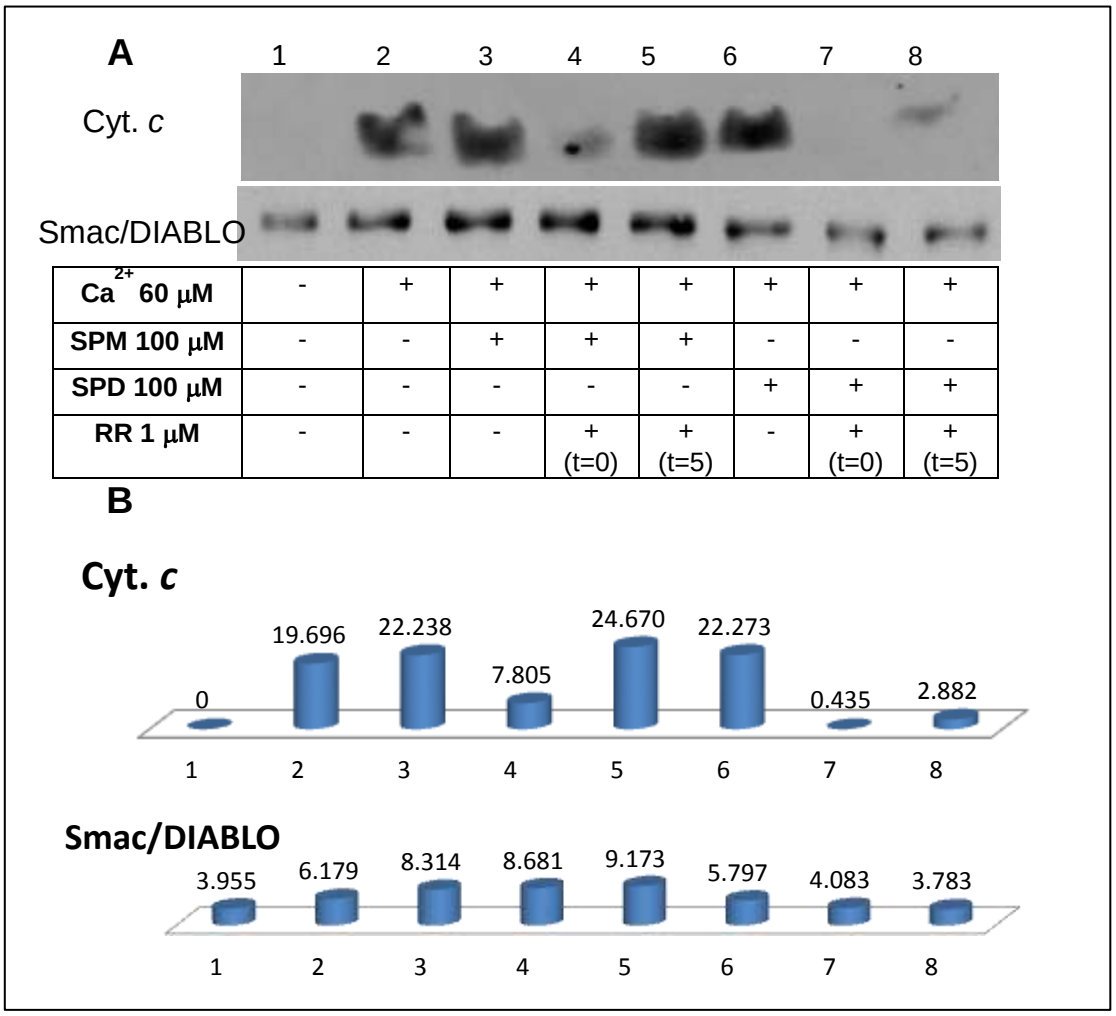

Ca^{2+} 60 μM	-	+	+	+	+	+	+	+
SPM 100 μM	-	-	+	+	+	-	-	-
SPD 100 μM	-	-	-	-	-	+	+	+
RR 1 μM	-	-	-	+ (t=0)	+ (t=5)	-	+ (t=0)	+ (t=5)

Fig. 39 Release of cytochrome c and Smac/DIABLO induced by αMeAGM in presence of Ca^{2+} and Ruthenium Red (A) and densitometric analysis (B).

RLM (1mg/ml) were incubated in standard medium in the same conditions as in Fig. 38 and the supernatant fraction was analyzed by SDS-Page and Western Blot, as described in Material and methods section. Ruthenium Red (RR) was added at different times: from the beginning (t=0) and after five minutes of incubation (t=5). Assays performed four times gave almost identical results. The values reported in Fig. 39B are expressed as percentage.

Results shown in Fig. 39A evidence a strong inhibition of RR, when added from the first minute of incubation (t=0) on the release of cyt. *c* induced by SPM and SPD (lanes 4, 8% and 7, 0.4%, respectively), if compared to the release of the protein induced by the compounds (lanes 3, 22% and 6, 22%, respectively). RR is less effective in inhibiting cyt. *c* release induced by SPM, if added after 5 minutes of incubation (t=5), as evidenced by the output of lane 5 (25%), whereas a strong inhibition is observed on SPD induced release (lane 8, 3%) even in this incubating conditions. With regard to Smac/DIABLO release, RR seems to be ineffective on SPM effect, when added from the first minute of incubation (lane 4, 9%) or after 5 minutes (lane 5, 9%), if compared to the polyamine-induced release (lane 3, 8%). A negligible effect on SPD-induced release (lane 6, 6%) is observable if RR is added at both times of incubation (lanes 7, 4% and 8, 4%).

Discussion

According to the notion that polyamines and AGM show similar structural and activity features, the previous section evaluated the behavior of polyamines under the same conditions used for both AGM and αMeAGM study.

Among the variety of effects ascribable to polyamines action in mitochondria [for a review see Toninello *et al*., 2004], MPT is undoubtedly one main target, which is strictly related to the release of pro-apoptotic proteins from mitochondria. Polyamines are generally considered inhibitors of the MPT (SPM is one of the most powerful physiological ones) [Toninello *et al*., 1984; Tassani *et al*., 1995] and, indeed, results presented in the previous section support this aspect (Fig 31). However, the Western Blot analyses on mitochondrial supernatant fractions (Figs. 32, 34, 35) have also shown the release of both cyt. *c* and Smac/DIABLO, but not of AIF, in the presence of Ca^{2+} and polyamines. At difference from the synergic effect exhibited by Ca^{2+} and AGM (Figs. 9 and 11, respectively, Part I), polyamines and Ca^{2+} together release as much pro-apoptotic factors as Ca^{2+} alone. A possible explanation, as above emphasized, should take into account the inhibiting effect shown by polyamines on Ca^{2+}-induced MPT. Polyamines, in particular SPM, while inhibiting the induction of MPT by Ca^{2+}, are able to stimulate themselves the release of pro-apoptotic factors, thus not resulting in a synergic effect with Ca^{2+}. Indeed, preliminary data (Fig. 33) show that SPM alone (in the absence of Ca^{2+}) is able to release the pro-apoptotic factors, thus supporting this hypothesis.

It has to be underlined that the latter effect exerted by polyamines alone is not very surprising considering that they also stimulate the uptake of phosphate [Toninello *et al*., 1984], which, together with Ca^{2+}, is one of the main MPT inducers. It thus seems that polyamines, while enhancing its uptake, are also able to exert a protective effect on mitochondrial swelling and it is possible that the combination of the protective and toxic effects of polyamine results in MOMP, but not in MPT induction.

Another difference between AGM and polyamines relates to the action of CsA. As expected, CsA does not modify the inhibition of swelling exerted by SPM and SPD (which fully prevent the MPT) (Fig. 36), but it cannot inhibit the release of cyt. *c* and Smac/DIABLO induced by these polyamines in the presence of Ca^{2+} (Fig. 37). These results demonstrate the MPT-independence of the observed phenomenon and also suggest that the mechanism of action of polyamines is different from that of AGM.

In cells, polyamines are also a source of cytotoxic metabolites and, as reported by Agostinelli and collaborators [2004], the oxidative deamination of polyamines by amine oxidase (*i.e*., monoamine oxidases, diamine oxidases, polyamine oxidases and copper-containing amine oxidases) generates H_2O_2 and aldehyde(s). It is therefore possible that, at the cellular level, the damaging action of polyamines is ascribable to their oxidation products. However, having Cardillo and collaborators [2009] detected also in mitochondria the activity of a copper-

dependent amine oxidase (capable to oxidize polyamines and diamines), one can speculate that the small amount of ROS produced by polyamine oxidation could be sufficient to trigger the MOMP. Indeed, as previously underlined, it has been observed a ROS-mediated and MPT-independent release of cyt. *c* and that the ROS-induced permeabilization of the OM is likely to be mediated by VDAC [Petrosillo et al., 2003; Kumarswamy and Chandna, 2009]. For this reason, the involvement of VDAC was tested (Fig. 38-39), and the obtained results showed that, as already observed for AGM, VDAC is probably involved in the pathway of release of cyt. *c*, excluding, at the same time, its role in Smac/DIABLO release.

These data further highlight that AGM, although related to polyamines, displays typical features. A further confirmation arises from data obtained by the use of liposomes carrying electrostatically attached cyt. *c*, where the only variable is the electric charge [Stefanelli C, Department of Pharmacy and Biotechnology, University of Bologna, Personal Communication]. In this study, AGM (divalent) potential in inducing the release of cyt. *c* is lower than that of SPM (tetravalent) and SPD (trivalent). This is in contrast with the experiments presented in the previous sections where AGM action in releasing cyt. *c* is higher than polyamines one.

Part IV

Polyamines efflux from mitochondria

Polyamines cycling in mitochondria

The mechanism of influx of polyamines have been characterized in RLM [Toninello *et al.*, 1992a; 1992b], but there is a lack of knowledge about their efflux pathway. Indeed, despite the presence of several previous studies [Toninello *et al.*, 1985; 1986; 1988], this pathway is far from being completely understood. It is reasonable to think that a cycling-mechanism, similar to Ca^{2+} one, could be a crucial point in order to explain the previous shown observed effects.

Results

Spermine efflux

SPM is accumulated in RLM by an electrophoretic mechanism, dependent on a high transmembrane potential [Toninello *et al.*, 1985]. Thus the addition of uncouplers is able to cause the efflux of the polyamine, a mechanism that could account for deenergizing, or even pathological, conditions. However, in a more physiological environment, due to the importance of maintaining an equilibrium in the polyamine content, another pathway it feasible, able to operate with a high membrane potential.

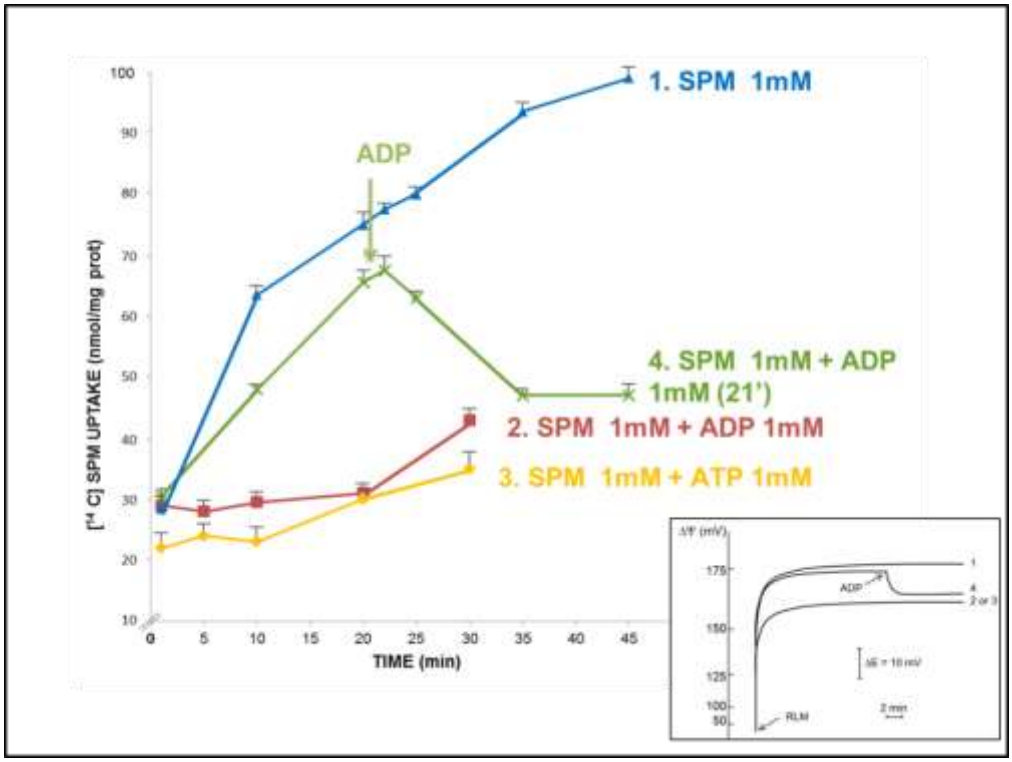

Fig. 40 Spermine uptake by RLM in the presence of adenine nucleotides. Mitochondria were incubated in standard medium supplemented with [^{14}C]SPM 50μCi/mmol. Values are the means ± SD of four experiments. Inset: effect of SPM and ADP (incubated under the same conditions as in Fig. 40) on $\Delta\Psi$.

Fig. 40 shows that the amount of SPM transported by RLM (trace 1) is consistently decreased by the presence of both ADP (trace 2) or ATP (trace 3) in the medium of incubation. Trace 4 also evidences that a considerable efflux of SPM is observable, if ADP is added after 21 minutes. Thus the efflux of SPM seems to be linked to the presence of these adenine nucleotides. However, it has to be admitted that the addition of ADP causes a slight decrease of $\Delta\Psi$, due to the fact that a portion of the electrochemical gradient is used to synthesize ATP and this effect is shown also in the presence of SPM (Inset, trace 4).

Thus an objection could be that SPM efflux is caused by this decrease.

Membrane potential-independence

In order to exclude that the decrease of $\Delta\Psi$ is responsible for the above observed SPM efflux, the effects of nigericin (Fig. 41) and mersalyl (Fig. 42) were tested. The first is a ionophore that induces an exchange of endogenous K^+ with exogenous H^+, leading to a complete collapse of ΔpH and a consequent argument of $\Delta\Psi$ to the maximum value of 220 mV [Graven *et al*., 1966]. Mersalyl, instead, is an inhibitor of phosphate transport and, as a consequence, its addition causes also a decrease of $\Delta\Psi$ [Tyler, 1968].

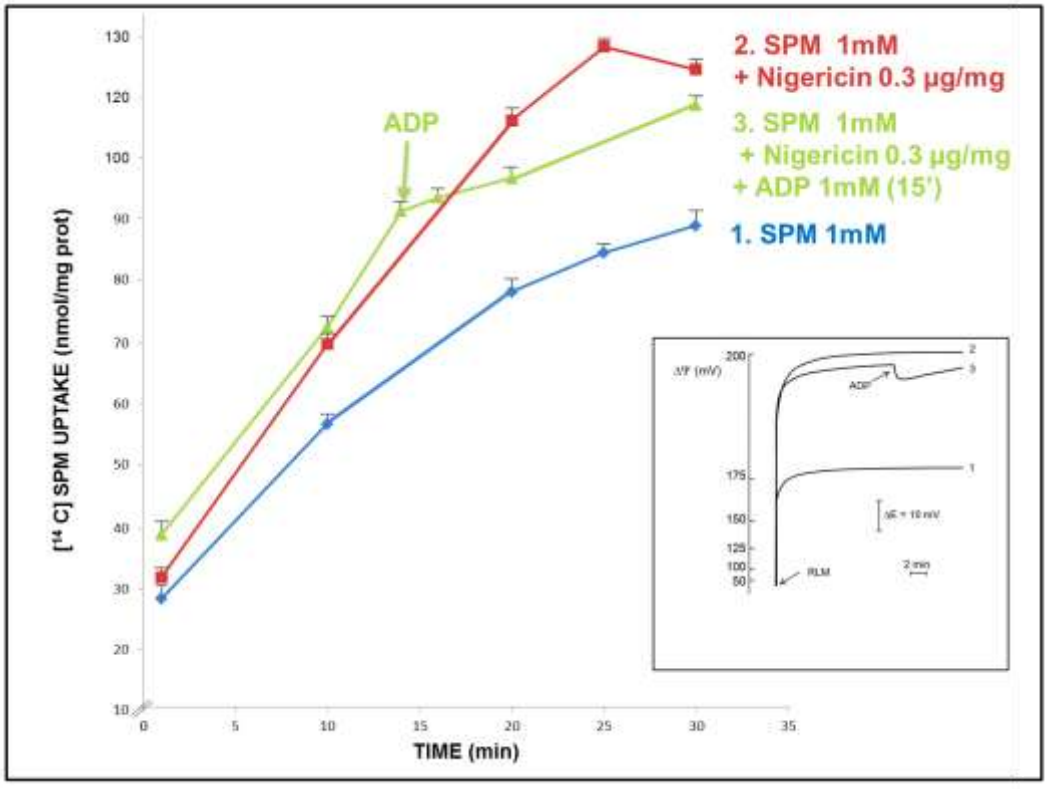

Fig. 41 Spermine uptake by RLM in the presence of ADP and/or nigericin. Mitochondria were incubated in standard medium supplemented with [^{14}C]SPM 50µCi/mmol. Values are the means ± SD of four experiments. Inset: effect of SPM, ADP, and nigericin (incubated under the same conditions as in Fig. 41) on $\Delta\Psi$.

SPM transport (trace 1) is increased in the presence of nigericin (trace 2), as a result of $\Delta\Psi$ enhancement (Inset, trace 2). The addition of ADP in the same experimental condition decreases the rate of entrance of SPM (trace 3), suggesting that even with the maintenance of a high $\Delta\Psi$, a SPM efflux pathway is operating. Indeed, in these conditions, as shown in the inset, the decrease of $\Delta\Psi$ caused by oxidative phosphorylation is negligible. It is to note that, in this experimental condition, the addition of ADP at the 15th minute of incubation, instead of the 21st as the other experiments, is made with the purpose to better appreciate the effect.

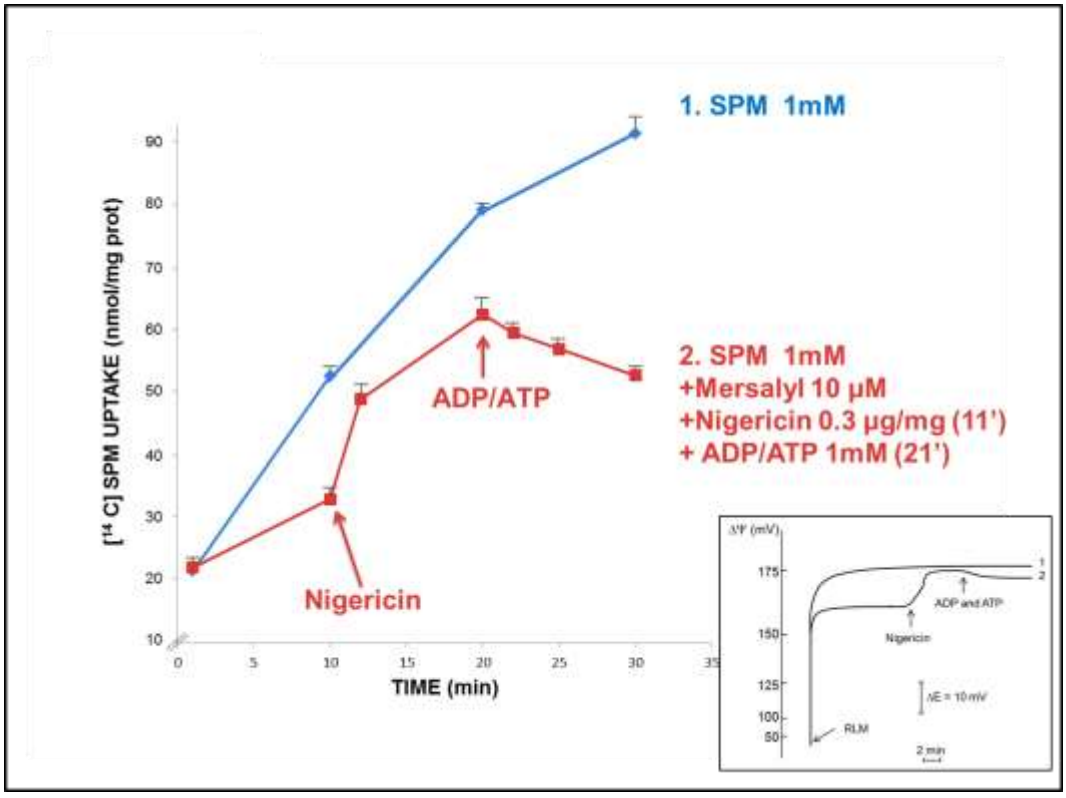

Fig. 42 Spermine uptake by RLM in the presence of mersalyl and/or adenine nucleotides and/or nigericin. Mitochondria were incubated in standard medium supplemented with [^{14}C]SPM 50µCi/mmol. Values are the means ± SD of four experiments. Inset: effect of SPM, mersalyl, nigericin, and adenine nucleotides, (incubated under the same conditions as in Fig. 42) on $\Delta\Psi$.

The experiment represented in Fig. 42 further support the previous findings. The presence of mersalyl in the medium of incubation excludes the possibility of ATP formation, as the uptake of phosphate is blocked. This condition causes also the decrease of $\Delta\Psi$ (Inset, trace 2), as previously described, and thus SPM transport is lowered. The subsequent addition of nigericin (11th minute) increases SPM transport, as expected, due to the enhancement of $\Delta\Psi$ caused by the ionophore. Finally, the addition of both ADP and ATP (21st minute), causes SPM efflux.

Correlation with adenine nucleotide translocator

The hypothesized correlation between SPM efflux and the fluxes of ADP and ATP was further studied by the use of the ATP-synthase inhibitor oligomycin (Fig. 43) and the AdNT inhibitor bongkrekic acid (BKA) (Fig. 44).

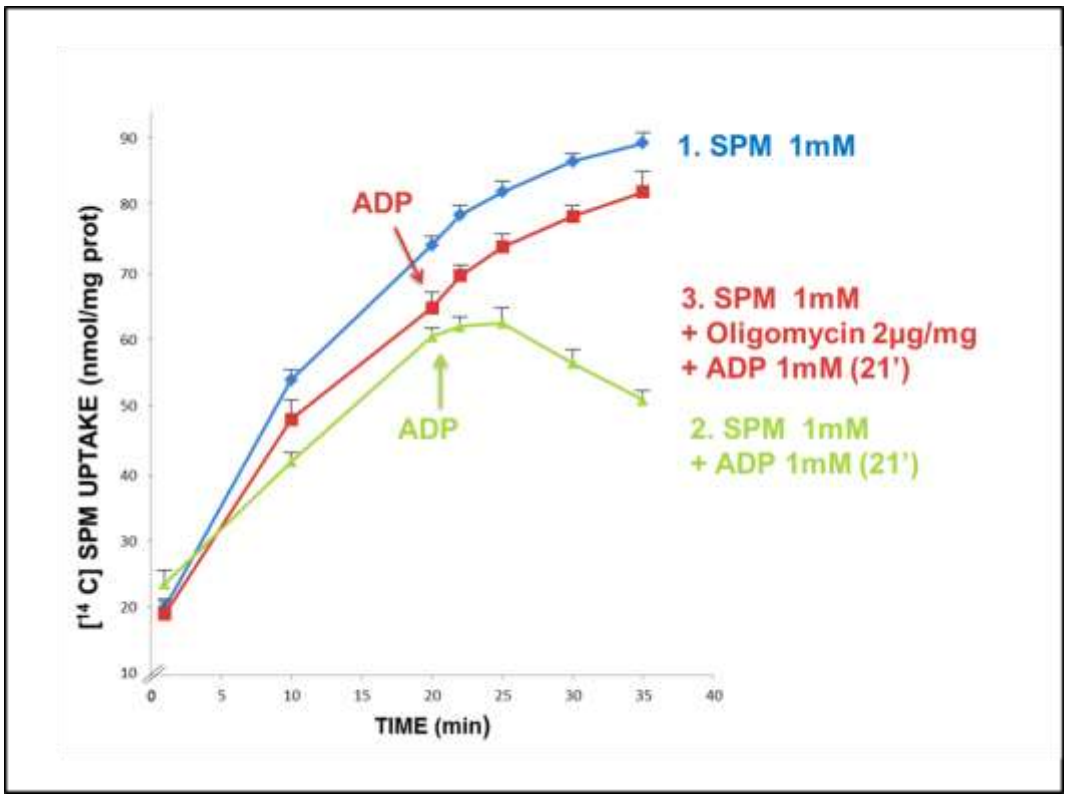

Fig. 43 Spermine uptake by RLM in the presence of ADP and/or oligomycin. Mitochondria were incubated in standard medium supplemented with [^{14}C]SPM 50μCi/mmol. Values are the means ± SD of four experiments.

In Fig. 43 the effect of oligomycin is shown. Trace 2 represents the efflux of SPM after the addition of ADP (21st minute). If oligomycin is present in the medium, the subsequent addition of ADP does not provoke any effect in the uptake of the polyamine. Thus, this process seems to be related to ATP synthesis or ADP/ATP exchange. The involvement of the adenine nucleotide translocator was investigated by the use of BKA, as shown by Fig. 44.

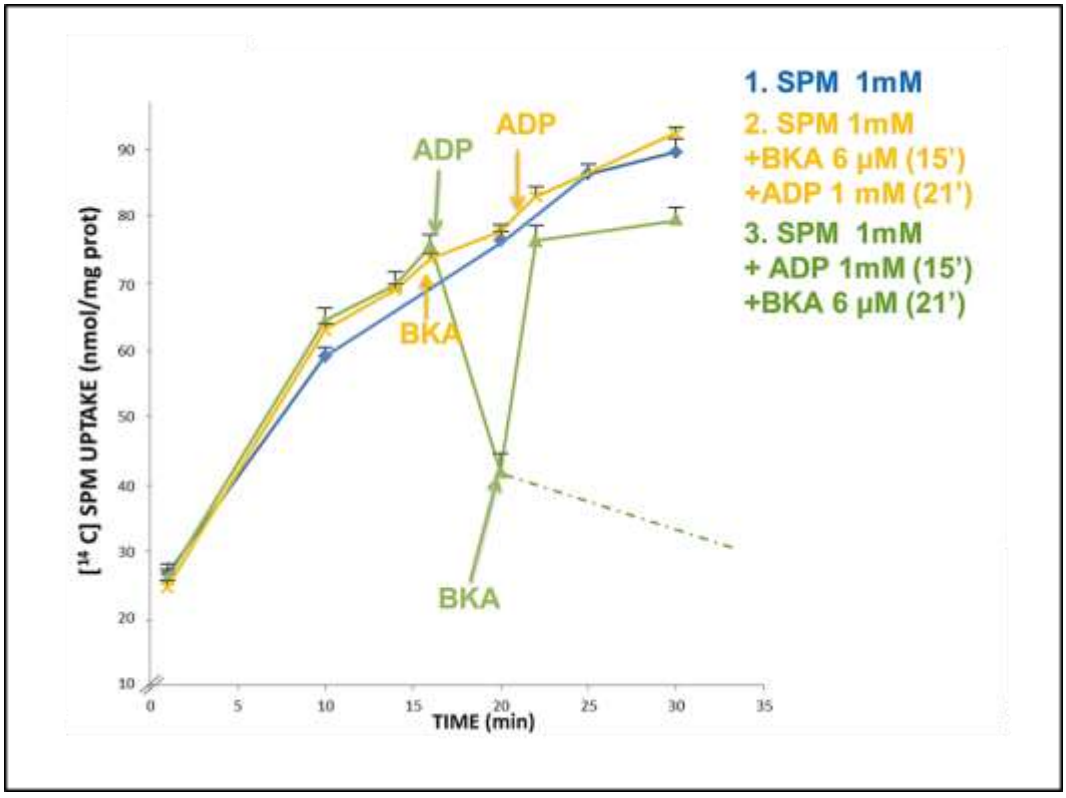

Fig. 44 Spermine uptake by RLM in the presence of adenine nucleotides and/or BKA. Mitochondria were incubated in standard medium supplemented with [^{14}C]SPM 50μCi/mmol. Values are the means ± SD of four experiments.

SPM transport as a control is represented by trace 1. As evidenced by trace 2, if BKA is added after 15 minutes, SPM accumulation is not affected, as well as after the addition of ADP (21st minute). A possible explanation is that even if ATP is endogenously synthesized, it cannot exit from mitochondria because of BKA block on the translocator. In these conditions SPM continues to accumulate. A different output is observable by adding first ADP (15th minute), causing SPM exit from mitochondria, and then BKA (21st minute), that clearly inhibits its efflux, restoring SPM uptake (trace 3). These data suggest that SPM, ADP and ATP fluxes are linked.

Discussion

The issue of polyamine cycling across mitochondrial membranes was investigated in this paragraph.

As described in the Introduction, polyamines exhibit a large number of functions in cells as well as in mitochondria. The requirement of a polyamine transporter is legitimized by the fact that high quantities of these compounds have been found in mitochondria, even if the organelles do not possess a biosynthetic pathway. Moreover, their activity in preventing or inducing apoptosis, is dependent on their concentration, modulated also by the proposed mitochondrial cycling. Unfortunately, despite the presence of several previous studies their efflux pathway is not completely characterized [Toninello *et al.*, 1985; 1986; 1988]. As Toninello and collaborators demonstrated [1985], deenergized mitochondria by the addition of uncouplers or electron transport chain inhibitors, release SPM. In this conditions the driving force able to transport and retain in matrix the polyamine, $\Delta\Psi$, is collapsed, by which it has been proposed that SPM exits in exchange with protons, reuptaken by the collapse of the electrochemical gradient. This mechanism of efflux could account for deenergizing, or even pathological, conditions, but a different case, maybe operating in physiological environments, is considered in this section.

I have presented data supporting the involvement of the AdNT in the mechanism of efflux of SPM. First of all, the presence of either ADP or ATP in the medium considerably decreased the amount of SPM transported by mitochondria. Moreover, the addition of ADP after 21st minutes of incubation, when a substantial quantity of the polyamine was internalized, caused an evident efflux of SPM (Fig. 40). During ATP synthesis, a slight decrease of $\Delta\Psi$ is observable, due to the fact that a portion of the electrochemical gradient is used to synthesize ATP. Being SPM transport electrophoretic, an objection could be that the decrease of $\Delta\Psi$ causes SPM efflux. However, the decrease observed is unlikely involved in SPM efflux because of its extent (of about 10 mV), which maintains membrane potential in a physiological condition.

Moreover, the use of nigericin, a ionophore able to increase $\Delta\Psi$ at its maximum level, (Fig. 41) seems to exclude again the possibility of a mere effect on $\Delta\Psi$. The inset of Fig. 41 shows that the decrease of $\Delta\Psi$ caused by ADP addition, is minimized in the presence of nigericin, whereas the rate of influx of the polyamine is decreased even with the addition of nigericin, supporting the presence of an efflux pathway, which balances the influx.

A further confirmation is demonstrated in the concomitant presence of mersalyl (inhibitor of phosphate transporter) and nigericin (Fig. 42), where the addition of both ATP and ADP, with the consequent exchange of ADP/ATP across the membrane, induced SPM efflux, suggesting that, in this case, the process is not driven by a decrease in $\Delta\Psi$. In this experimental conditions both the nucleotides are necessarily added, because the presence of phosphate in the matrix is at

minimum (due to mersalyl action) by which ATP is not synthesized. These data exclude the involvement of the decrease of $\Delta\Psi$ in SPM efflux and arise the hypothesis about the correlation between the fluxes of SPM and the adenine nucleotides.

At this point, the investigation better analyzed this hypothesis by the use of the H^+-ATP-synthase inhibitor, oligomycin, and the adenine nucleotide translocator inhibitor, BKA (Figs. 43 and 44, respectively). Oligomycin and BKA fully prevented SPM outflow, supporting the correlation between SPM effluxes and ADP/ATP exchange.

Taking into account all these data, some considerations can be made. First of all, as it is well-known, the ATP/ADP exchange is electrogenic, with a net efflux of a negative charge. Moreover, the tetravalent SPM, by interacting with the alkaline matrix, is most probably partially deprotonated, by which it is supposable that SPM carries three positive charges. It is also to consider that during SPM efflux also phosphate is released, as supported by a recent paper of our group [Grancara *et al.*, 2013]. Indeed, as we suggested, in the presence of both SPM and mersalyl (blocker of phosphate uptake), the efflux of phosphate is observed, suggesting a new pathway or a change in the carrier function for its efflux. Thus, it is possible to propose an electroneutral efflux of SPM during ATP/ADP exchange, in parallel with the efflux of phosphate, as a bivalent anion.

The efflux pathway of SPM, at present, is yet unknown as it cannot utilize the uptake transporter [Toninello *et al.*, 1992a]. However, the direct involvement of the AdNT in this process, also if it seems too speculative, is not to be completely discarded. In fact, the function of the AdNT, according to Brustovetsky and Klingenberg [1996] can change from a specific channel for ADP/ATP exchange, to a large unselective channel. This possibility could take place also in the presence of SPM. It has been previously reported that SPM is able to interact with some proteins such as just the AdNT [Krämer *et al*., 1986], ATP synthase [Solaini and Tadolini, 1984], and phosphate carrier [Toninello *et al*., 1986], by modifying their activity and/or function. Finally, all these proteins, due to the above mentioned changes and considering the observed effects of oligomycin, BKA and mersalyl, may be involved in SPM efflux. Experiments are in progress in our laboratory for obtaining results to further support this hypothesis.

Conclusions

The work carried out for my PhD thesis focused primarily on the action of biologically active amines –agmatine and polyamines, such as spermine and spermidine– on isolated mitochondria. Accumulated data allow to draw the following conclusions.

(I) Both agmatine and polyamines are able to induce the release of mitochondrial pro-apoptotic factors, such as cyt. *c* and Smac/DIABLO, but not AIF.

(II) All tested amines can also induce MOMP, the likely responsible for cyt. *c* and Smac/DIABLO release from the intermembrane space, but not of AIF, a protein integral to the IM.

(III) The action of agmatine and polyamines on MOMP exploits distinct mechanisms: while that by polyamines appears CsA-insensitive and mediated by ROS, agmatine action is CsA-sensitive and probably Bax-dependent.

(IV) VDAC was found to be part of the efflux pathway of cyt. *c*, but not of the route exploited by SMAC/DIABLO.

(V) Spermine efflux from mitochondria is linked to the fluxes of ADP/ATP and phosphate, supporting the presence of a cycling mechanism for polyamines in mitochondria.

In conclusion, MOMP could thus be regarded as a phenomenon linked to both intrinsic and extrinsic apoptosis, given that it is mediated by extra- (Bcl-2 family proteins) and intra-mitochondrial signals (polyamines and ROS). In this view, biologically active amines represent a useful tool to delineate the structural and functional features of both MOMP and MPT.

References

Abramoff MD, Magalhães PJ, Ram SJ (2004) Image processing with ImageJ. Biophotonics international. 11:36-42.

Agostinelli E, Arancia G, Dalla Vedova L, Belli F, Marra M, Salvi M, Toninello A (2004) The biological functions of polyamine oxidation products by amine oxidases: perspectives of clinical applications. Amino Acids. 27:347-58.

Agostinelli E, Marques MP, Calheiros R, Gil FP, Tempera G, Viceconte N, Battaglia V, Grancara S, Toninello A (2010) Polyamines: fundamental characters in chemistry and biology. Amino Acids. 38:393-403.

Affolter H, Sigel E (1979) A simple system for the measurement of ion activities with solvent polymeric membrane electrodes. Anal Biochem. 97:315-9.

Anup R, Madesh M, Balasubramanian KA (1999) Enterocyte mitochondrial dysfunction due to oxidative stress. Indian J Biochem Biophys. 36:266-71.

Arnoult D, Parone P, Martinou JC, Antonsson B, Estaquier J, Ameisen JC (2002) Mitochondrial release of apoptosis-inducing factor occurs downstream of cytochrome c release in response to several proapoptotic stimuli. J Cell Biol. 159:923-9.

Babal P, Ruchko M, Olson J. W, Gillespie MN (2000) Interactions between agmatine and polyamine uptake pathways in rat pulmonary artery endothelial cells. Gen Pharmacol. 34:255-61.

Battaglia V, Rossi CA, Colombatto S, Grillo MA, Toninello (2007) Different behavior of agmatine in liver mitochondria: inducer of oxidative stress or scavenger of reactive oxygen species? Biochim Biophys Acta. 1768:1147-53.

Bleicken S, Landeta O, Landajuela A, Basañez G, García-Sáez AJ (2013) Proapoptotic Bax and Bak form stable protein-permeable pores of tunable size. J Biol Chem. 288:33241-52.

Brenner C, Moulin M (2012) Physiological roles of the permeability transition pore. Circ Res. 111:1237-47.

Brustovetsky N, Klingenberg M (1996) Mitochondrial ADP/ATP carrier can be reversibly converted into a large channel by Ca^{2+}. Biochemistry. 35:8483-8.

Cabella C, Gardini G, Corpillo D, Testore G, Bedino S, Solinas SP, Cravanzola C, Vargiu C, Grillo MA, Colombatto S (2001) Transport and metabolism of agmatine in rat hepatocyte cultures. Eur J Biochem. 268:940-7.

Carafoli E, Tiozzo R, Lugli G, Crovetti F, Kratzing C (1974) The release of calcium from heart mitochondria by sodium. J Mol Cell Cardiol. 6:361-71.

Cardillo S, Iuliis AD, Battaglia V, Toninello A, Stevanato R, Vianello F (2009) Novel copper amine oxidase activity from rat liver mitochondria matrix. Arch Biochem Biophys. 485:97-101.

Casero RA Jr, Marton LJ (2007) Targeting polyamine metabolism and function in cancer and other hyperproliferative diseases. Nat Rev Drug Discov. 6:373-90.

Costantini P, Jacotot E, Decaudin D, Kroemer G (2000) Mitochondrion as a novel target of anticancer chemotherapy. J Natl Cancer Inst. 92:1042-53.

Dalla Via L, Di Noto V, Siliprandi D, Toninello A (1996) Spermine binding to liver mitochondria. Biochim Biophys Acta. 1284:247-52.

Dalla Via L, Di Noto V, Toninello A (1999) Binding of spermidine and putrescine to energized liver mitochondria. Arch Biochem Biophys. 365:231-8.

Dalla Via L, Garcia-Argaez AN, Martinez-Vazquez M, Grancara S, Martinis P, Toninello A (2014) Mitochondrial permeability transition as target of anticancer drugs. Curr Pharm Des. 20: 223-244.

De Stefani D, Raffaello A, Teardo E, Szabò I, Rizzuto R (2011) A forty-kilodalton protein of the inner membrane is the mitochondrial calcium uniporter. Nature. 476:336-40.

DeLuca HF, Engstrom GW (1961) Calcium uptake by rat kidney mitochondria. Proc Natl Acad Sci U S A. 47:1744-50.

Del Valle AE, Paz JC, Sanchez-Jimenez F, Medina MI (2000) Agmatine uptake by cultured hamster kidney cells. Biochem Biophys Res Commun. 280:307-11.

Di Noto V, Dalla Via L, Toninello A, Vidali M (1996) Thermodynamic treatment of ligand–receptor interactions. Macromol Theory Simul 5:165-181.

Di Noto V, Dalla Via L, Zatta P (2002) Review of binding methods and detection of Al(III) binding events in trypsin and DL-DPPC liposomes by a general thermodynamic model. Coord Chem Rev 228:343-63.

Fiskum G, Lehninger AL (1979) Regulated release of Ca^{2+} from respiring mitochondria by $ca^{2+}/2H^{+}$ antiport. J Biol Chem. 254:6236-9.

Gardini G, Cabella C, Cravanzola C, Vargiu C, Belliardo S, Testore G, Solinas SP, Toninello A, Grillo MA, Colombatto (2001) Agmatine induces apoptosis in rat hepatocyte cultures. J Hepatol. 35:482-9.

Gardini G, Cravanzola C, Autelli R, Testore G, Cesa R, Morando L, Solinas SP, Muzio G, Grillo MA, Colombatto S (2003) Agmatine inhibits the proliferation of rat hepatoma cells by modulation of polyamine metabolism. J Hepatol. 39:793-9.

Giorgio V, von Stockum S, Antoniel M, Fabbro A, Fogolari F, Forte M, Glick GD, Petronilli V, Zoratti M, Szabó I, Lippe G, Bernardi P (2013) Dimers of

mitochondrial ATP synthase form the permeability transition pore. Proc Natl Acad Sci U S A. 110:5887-92.

Grancara S, Battaglia V, Martinis P, Viceconte N, Agostinelli E, Toninello A, Deana R (2011) Mitochondrial oxidative stress induced by Ca^{2+} and monoamines: different behaviour of liver and brain mitochondria in undergoing permeability transition. Amino Acids. 42:751-9.

Grancara* S, Martinis* P, Manente S, García-Argáez AN, Tempera G, Bragadin M, Dalla Via L, Agostinelli E, Toninello A (2013) Bidirectional fluxes of spermine across the mitochondrial membrane. Amino Acids. [Epub ahead of print]

Graven SN, Estrada-O S, Lardy HA (1966) Alkali metal cation release and respiratory inhibition induced by nigericin in rat liver mitochondria. Proc Natl Acad Sci U S A. 56: 654-58.

Green DR, Kroemer G (2004) The pathophysiology of mitochondrial cell death. Science. 305:626-9.

Green DR, Reed JC (1998) Mitochondria and apoptosis. Science. 281:1309-12.

Grijalba MT, Vercesi AE, Schreier S. (1999) Ca^{2+}-induced increased lipid packing and domain formation in submitochondrial particles. A possible early step in the mechanism of Ca^{2+}-stimulated generation of reactive oxygen species by the respiratory chain. Biochemistry. 38:13279-87.

Gogvadze V, Orrenius S, Zhivotovsky B (2006) Multiple pathways of cytochrome c release from mitochondria in apoptosis. Biochim Biophys Acta. 1757:639-47.

Gornall AG, Bardawill CJ, David MM (1949) Determination of serum proteins by means of the biuret reaction. J Biol Chem. 177:751-66.

Grundemann D, Hahne C, Berkels R, Schomig E (2003) Agmatine is efficiently transported by non-neuronal monoamine transporters extraneuronal monoamine transporter (EMT) and organic cation transporter 2 (OCT2). J Pharmacol Exp Ther. 304:810-7.

Haenisch B, Bönisch H, Cichon S, Allam JP, Novak N, Molderings GJ (2011) Effects of exogenous agmatine in human leukemia HMC-1 and HL-60 cells on proliferation, polyamine metabolism and cell cycle. Leuk Res. 35:1248-53.

Halestrap AP (2005) Biochemistry: a pore way to die. Nature. 434:578-9.

Halestrap AP (2009) What is the mitochondrial permeability transition pore? J Mol Cell Cardiol. 46:821-31.

Halestrap AP, Connern CP, Griffiths EJ, Kerr PM (1997) Cyclosporin A binding to mitochondrial cyclophilin inhibits the permeability transition pore and protects hearts from ischaemia/reperfusion injury. Mol Cell Biochem. 174:167-72.

Halestrap AP, Woodfield KY, Connern CP (1993) Oxidative stress, thiol reagents, and membrane potential modulate the mitochondrial permeability transition by affecting nucleotide binding to the adenine nucleotide translocase. J Biol Chem. 272:3346-54.

Hancock JT, Desikan R, Neill SJ (2001) Does the redox status of cytochrome C act as a fail-safe mechanism in the regulation of programmed cell death? Free Radic Biol Med. 31:697-703.

Hong S, Kim CY, Lee JE, Seong GJ (2009) Agmatine protects cultured retinal ganglion cells from tumor necrosis factor-alpha-induced apoptosis. Life Sci. 84:28-32.

Hoshino K, Momiyama E, Yoshida K, Nishimura K, Sakai S, Toida T, Kashiwagi K, Igarashi K (2005) Polyamine transport by mammalian cells and mitochondria: role of antizyme and glycosaminoglycans. J Biol Chem. 280:42801-8.

Israelson A, Zaid H, Abu-Hamad S, Nahon E, Shoshan-Barmatz V (2008) Mapping the ruthenium red-binding site of the voltage-dependent anion channel-1. Cell Calcium. 43:196-204.

Jensen BD, Gunter KK, Gunter TE (1986) The efficiencies of the component steps of oxidative phosphorylation. II. Experimental determination of the efficiencies in mitochondria and examination of the equivalence of membrane potential and pH gradient in phosphorylation. Arch Biochem Biophys. 248:305-23.

Kamo N, Muratsugu M, Hongoh R, Kobatake Y (1979) Membrane potential of mitochondria measured with an electrode sensitive to tetraphenyl phosphonium and relationship between proton electrochemical potential and phosphorylation potential in steady state J Membr Biol. 49:105-21.

Keynan O, Mirovsky Y, Dekel S, Gilad VH, Gilad GM (2010) Safety and efficacy of dietary agmatine sulfate in lumbar disc-associated radiculopathy. An open-label, dose-escalating study followed by a randomized, double-blind, placebo-controlled trial. Pain Med. 11:356-68.

Kossel A (1910) Über das Agmatin. Zeitschrift für Physiologische Chemie. 66: 257-61.

Kowaltowski AJ, Castilho RF, Vercesi AE (2001) Mitochondrial permeability transition and oxidative stress. FEBS Lett. 495:12-5.

Krämer R, Mayr U, Heberger C, Tsompanidou S (1986) Activation of the ADP/ATP carrier from mitochondria by cationic effectors. Biochim Biophys Acta. 855:201-10.

Kumarswamy R, Chandna S (2009) Putative partners in Bax mediated cytochrome-c release: ANT, CypD, VDAC or none of them? Mitochondrion. 9:1-8.

Laemmli UK (1970) Cleavage of structural proteins during the assembly of the head of bacteriophage T4. Nature. 227:680-5.

Lapidus RG, Sokolove PM (1993) Spermine inhibition of the permeability transition of isolated rat liver mitochondria: an investigation of mechanism. Arch Biochem Biophys. 306:246-53.

Leung AW, Halestrap AP (2008) Recent progress in elucidating the molecular mechanism of the mitochondrial permeability transition pore. Biochim Biophys Acta. 1777:946-52.

Loschen G, Flohè L, Chance B (1971) Respiratory chain linked H_2O_2 production in pigeon heart mitochondria. FEBS Lett. 18:261-4.

Lötscher HR, Winterhalter KH, Carafoli E, Richter C (1980) The energy-state of mitochondria during the transport of Ca^{2+}. Eur J Biochem. 110:211-6.

Martinis P, Battaglia V, Grancara S, Dalla Via L, Di Noto V, Saccoccio S, Agostinelli E, Bragadin M, Grillo MA, Toninello A (2012) Further characterization of agmatine binding to mitochondrial membranes: involvement of imidazoline I_2 receptor. Amino Acids. 42:761-8.

Maly DJ (2007) Exploring the intermembrane space. ACS Chem Biol. 2:213-6.

Murphy MP (2009) How mitochondria produce reactive oxygen species. Biochem J. 417:1-13.

Molderings GJ, Bonisch H, Gothert M, Bruss M (2001) Agmatine and putrescine uptake in the human glioma cell line SK-MG-1. Naunyn-Schmiedeberg's Arch Pharmacol. 363:671-9.

Moreno-Sánchez R, Hernández-Esquivel L, Rivero-Segura NA, Marín-Hernández A, Neuzil J, Ralph SJ, Rodríguez-Enríquez S (2013) Reactive oxygen species are generated by the respiratory complex II: evidence for lack of contribution of the reverse electron flow in complex I. FEBS J. 280:927-38.

Nowotarski SL, Woster PM, Casero RA Jr (2013) Polyamines and cancer: implications for chemotherapy and chemoprevention. Expert Rev Mol Med. 15:e3.

Osellame LD, Blacker TS, Duchen MR (2012) Cellular and molecular mechanisms of mitochondrial function. Best Pract Res Clin Endocrinol Metab. 26:711-23.

Otera H, Ohsakaya S, Nagaura Z, Ishihara N, Mihara K (2005) Export of mitochondrial AIF in response to proapoptotic stimuli depends on processing at the intermembrane space. EMBO J. 24:1375-86.

Ott M, Robertson JD, Gogvadze V, Zhivotovsky B, Orrenius S (2001) Cytochrome c release from mitochondria proceeds by a two-step process. Proc Natl Acad Sci U S A. 99:1259-63.

Palade GE (1952) The fine structure of mitochondria. Anat Rec. 114:427-51.

Palmieri F, Klingenberg M (1979) Direct methods for measuring metabolite transport and distribution in mitochondria. Methods Enzymol. 56:279-301.

Pegg AE, Casero RA Jr (2011) Current status of the polyamine research field. Methods Mol Biol. 720:3-35.

Petrosillo G, Ruggiero FM, Paradies G (2003) Role of reactive oxygen species and cardiolipin in the release of cytochrome c from mitochondria. FASEB J. 17:2202-8.

Piletz JE, Aricioglu F, Cheng JT, Fairbanks CA, Gilad VH, Haenisch B, Halaris A, Hong S, Lee JE, Li J, Liu P, Molderings GJ, Rodrigues AL, Satriano J, Seong GJ, Wilcox G, Wu N, Gilad GM (2013) Agmatine: clinical applications after 100 years in translation. Drug Discov Today. 18:880-93.

Raddatz R, Savic SL, Bakthavachalam V, Lesnick J, Jasper JR, McGrath CR, Parini A, Lanier SM (2000) Imidazoline-binding domains on monoamine oxidase B and subpopulations of enzyme. J Pharmacol Exp Ther. 292:1135-45.

Renault TT, Manon S (2011) Bax: Addressed to kill. Biochimie. 93:1379-91.

Ripple MO, Abajian M, Springett R (2010) Cytochrome c is rapidly reduced in the cytosol after mitochondrial outer membrane permeabilization. Apoptosis. 15:563-73.

Rossner M, Yamada KM (2004) What's in a picture? The temptation of image manipulation. J Cell Biol. 166:11-5.

Salvi M, Battaglia V, Mancon M, Colombatto S, Cravanzola C, Calheiros R, Marques MP, Grillo MA, Toninello A (2006) Agmatine is transported into liver mitochondria by a specific electrophoretic mechanism. Biochem J. 396:337-45.

Sava IG, Battaglia V, Rossi CA, Salvi M, Toninello A (2006) Free radical scavenging action of the natural polyamine spermine in rat liver mitochondria. Free Radic Biol Med. 41:1272-81.

Scheffler IE. (2001) Mitochondria make a come back. Adv Drug Deliv Rev. 49:3-26.

Schneider WC, Hogeboom HG (1950) Intracellular distribution of enzymes: V. Further studies on the distribution of cytochrome c in rat liver homogenate. J Biol Chem. 183:123-8.

Scorrano L (2013) Keeping mitochondria in shape: a matter of life and death. Eur J Clin Invest. 43:886-93.

Siemen D, Ziemer M (2013) What is the nature of the mitochondrial permeability transition pore and what is it not? IUBMB Life. 65:255-62.

Siu WP, Pun PB, Latchoumycandane C, Boelsterli UA (2008) Bax-mediated mitochondrial outer membrane permeabilization (MOMP), distinct from the mitochondrial permeability transition, is a key mechanism in diclofenac-induced hepatocyte injury: Multiple protective roles of cyclosporin A. Toxicol Appl Pharmacol. 227:451-61.

Solaini G, Tadolini B. (1984) Spermine binding to submitochondrial particles and activation of adenosine triphosphatase. Biochem J. 218:495-9.

Stefanelli C, Stanic' I, Zini M, Bonavita F, Flamigni F, Zambonin L, Landi L, Pignatti C, Guarnieri C, Caldarera CM (2000) Polyamines directly induce release of cytochrome c from heart mitochondria. Biochem J. 347:875-80.

Susin SA, Zamzami M, Kroemer G (1998) Mitochondria as regulators of apoptosis: doubt no more. Biochim Biophys Acta. 194:1276-81.

Tait SW, Green DR (2010) Mitochondria and cell death: outer membrane permeabilization and beyond. Nat Rev Mol Cell Biol. 11:621-32.

Tait SW, Green DR (2012) Mitochondria and cell signalling. J Cell Sci. 125:807-15.

Tassani V, Biban C, Toninello A, Siliprandi D (1995) Inhibition of mitochondrial permeability transition by polyamines and magnesium: importance of the number and distribution of electric charges. Biochem Biophys Res Commun. 207:661-7.

Toninello A (2001) Interaction of polyamines with mammalian mitochondria. Curr Top Biochem Res. 4:37-48.

Toninello A, Dalla Via L, Siliprandi D, Garlid KD (1992a) Evidence that spermine, spermidine, and putrescine are transported electrophoretically in mitochondria by a specific polyamine uniporter. J Biol Chem. 267:18393-7.

Toninello A, Dalla Via L, Testa S, Siliprandi D (1992b) Electrophoretic polyamine transport in rat liver mitochondria. Amino Acids. 2:69-76.

Toninello A, Dalla Via L, Testa S, Siliprandi D, Siliprandi N (1990) Transport and action of spermine in rat heart mitochondria. Cardioscience. 1:287-94.

Toninello A, Di Lisa F, Siliprandi D, Siliprandi N (1984) “Protective and restorative effects of spermine in the membrane potential of rat liver mitochondria” in Advances in Polyamines in Biomedical Science. Caldarera CM and Bachrach U editors. 31-67.

Toninello A, Di Lisa F, Siliprandi D, Siliprandi N (1985) Uptake of spermine by rat liver mitochondria and its influence on the transport of phosphate. Biochim Biophys Acta. 815:399-404.

Toninello A, Di Lisa F, Siliprandi D, Siliprandi N (1986) Action of spermine on phosphate transport in liver mitochondria. Arch Biochem Biophys. 245:363-8.

Toninello A, Miotto G, Siliprandi D, Siliprandi N, Garlid KD (1988) On the mechanism of spermine transport in liver mitochondria. J Biol Chem. 263:19407-11.

Toninello A, Salvi M, Mondovì B (2004) Interaction of biologically active amines with mitochondria and their role in the mitochondrial-mediated pathway of apoptosis. Curr Med Chem. 11:2349-74.

Tyler DD (1968) The inhibition of phosphate entry into rat liver mitochondria by organic mercurials and by formaldehyde. Biochem J. 107:121-3.

Vahsen N, Candé C, Brière JJ, Bénit P, Joza N, Larochette N, Mastroberardino PG, Pequignot MO, Casares N, Lazar V, Feraud O, Debili N, Wissing S, Engelhardt S, Madeo F, Piacentini M, Penninger JM, Schägger H, Rustin P, Kroemer G (2004) AIF deficiency compromises oxidative phosphorylation. EMBO J. 23:4679-89.

Van Gurp M, Festjens N, van Loo G, Saelens X, Vandenabeele P (2003) Mitochondrial intermembrane proteins in cell death. Biochem Biophys Res Commun. 304:487-97.

Wallace HM, Fraser AV (2004) Inhibitors of polyamine metabolism: review article. Amino acids. 26:353-65.

Vercesi AE, Kowaltowski AJ, Grijalba MT, Meinicke AR, Castilho RF (1997) The role of reactive oxygen species in mitochondrial permeability transition. Biosci Rep. 17:43-52.

Westphal D, Dewson G, Czabotar PE, Kluck RM (2011) Molecular biology of Bax and Bak activation and action. Biochim Biophys Acta. 1813:521-31.

Yamada A, Yamamoto T, Yamazaki N, Yamashita K, Kataoka M, Nagata T Terada H, Shinohara Y (2009) Differential permeabilization effects of Ca^{2+} and valinomycin on the inner and outer mitochondrial membranes as revealed by proteomics analysis of proteins released from mitochondria. Mol Cell Proteomics. 8:1265-77.